TECHNISCHE
UNIVERSITÄT
WIEN
Vienna | Austria

Diploma Thesis

Indolo[3,2,1-*jk*]carbazole Based Materials for OLED Applications

conducted at the

Institute of Applied Synthetic Chemistry

at the **TU Wien**

under the supervision of

Univ.Prof. Dipl.-Ing. Dr.techn. Johannes **Fröhlich**

advised by

Dipl.-Ing. Dr.techn. Paul **Kautny**, BSc

Senior Lecturer Dipl.-Ing. Dr.techn. Ernst **Horkel**

by

Thomas **Schwartz**, BSc

Matr.Nr.: 1025996

Vienna, May 19, 2017

Abstract

The interest in organic electronics as an alternative to conventional inorganic semiconductors has been rising over the past few decades. One of the most important applications are organic light emitting diodes (OLEDs), which are already used in a variety of displays, such as flat panel TVs or in mobile devices, and might be of further interest for large area lighting applications.

In an OLED molecules are electrically excited. Those excited states are then transferred to a fluorescent or phosphorescent emitter, which in turn converts them into light. Iridium based metal complexes as phosphorescent emitters have gained a lot of attention, since they allow for up to 100% internal efficiency by using both singlet and triplet excited states.

These emitters have to be widely dispersed in a host material in order to reach high efficiencies and reduce the energy loss through thermal radiation. Ongoing research focuses on the development of such host materials for the use in blue OLEDs.

Since blue light lies on the high-energy end of the visible spectrum, the molecular design of host materials must aim for high triplet energies to guarantee pure blue emission. One promising new substance class for host materials are substances based on the indolo[3,2,1-*jk*]carbazole (ICz) scaffold. First ICz based materials have already been synthesized in the Fröhlich group and showed promising properties. Particularly consistent high triplet energies of around 2.8 eV and good thermal stabilities were observed.

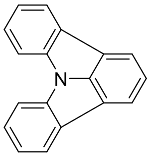

Structure of indolo[3,2,1-*jk*]carbazole.

The goal of this thesis was to modify the design of existing ICz based host materials to further increase the device efficiency. Additionally, new bipolar materials incorporating the ICz donor as possible blue emitters or host materials were investigated. Furthermore, the scope of the Pd catalyzed C-H activation reaction as a key step in the preparation of the ICz scaffold was expanded to a variety of substrates.

Kurzfassung

Das Interesse am Feld der organischen Elektronik als Alternative zu herkömmlichen anorganischen Halbleitern hat über die letzten Jahrzehnte stetig zugenommen. Eine der wichtigsten Anwendungen sind organische Leuchtdioden (OLEDs), welche bereits in Flachbildschirmen oder in mobilen Geräten Anwendung finden und in Zukunft für großflächige Beleuchtung interessant werden könnten.

In einer OLED werden Moleküle elektrisch angeregt. Diese angeregten Zustände werden dann auf einen fluoreszenten oder phosphoreszenten Emitter übertragen, welcher sie anschließend in Licht umwandelt. Phosphoreszente Iridiumkomplexe haben besonders viel Aufmerksamkeit erhalten, da sie bis zu 100 % interne Effizienz erlauben, indem sie sowohl Singulett- als auch Triplettzustände nutzen.

Diese Emitter müssen in einem Hostmaterial dispergiert werden um eine hohe Effizienz zu gewährleisten und um thermische Verluste zu reduzieren. Aktuelle Forschung beschäftigt sich mit der Entwicklung solcher Hostmaterialien für die Verwendung in blauen OLEDs.

Da blaues Licht am energiereichen Ende des sichtbaren Spektrums liegt, müssen Hostmaterialien hohe Triplettenergien aufweisen, um eine tiefblaue Emission zu gewährleisten.

Eine vielversprechende Substanzklasse sind Materialien, die auf Indolo[3,2,1-*jk*]carbazol (ICz) basieren. Erste ICz-Materialien wurden bereits in der Forschungsgruppe Fröhlich synthetisiert und zeigten vielversprechende Eigenschaften. Insbesondere hohe Triplettenergien im Bereich von 2,8 eV und gute thermische Stabilitäten wurden beobachtet.

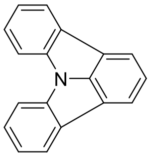

Struktur von Indolo[3,2,1-*jk*]carbazol.

Ziel dieser Arbeit war es, das Design bestehender ICz-Materialien zu verbessern, um deren Effizienz weiter zu erhöhen. Zusätzlich wurden bipolare Substanzen als mögliche blaue Emitter oder Hostmaterialien untersucht. Weiters wurde die Pd-katalysierte C-H Aktivierung, als wichtiger Schritt in der Synthese des ICz-Gerüsts, auf eine Vielfalt an Substraten ausgeweitet.

Danksagung

Besonderer Dank gilt Prof. Johannes Fröhlich für die Möglichkeit schon meine Bachelorarbeit und auch diese Arbeit in seiner Arbeitsgruppe durchführen zu können.

Bei Paul Kautny bedanke ich mich für die herzliche Betreuung, das Beantworten vieler Fragen und dafür, mein Interesse an diesem Thema weiter gefördert zu haben.

Ernst Horkel danke ich für die Unterstützung in synthetischen, als auch vielen administrativen Belangen und für die Durchführung quantenmechanischer Rechnungen, auf deren Basis die Zielsubstanzen für diese Arbeit ausgewählt wurden.

Dank gilt auch dem Rest der Forschungsgruppe, insbesondere meinen Laborkollegen Florian Glöcklhofer und Thomas Kader, welche stets sehr hilfsbereit waren und mit denen ich immer neue Ideen austauschen konnte.

Weiters danke ich Berthold Stöger für die Bestimmung von Kristallstrukturen, sowie für den Zutritt zu Geräten aus seiner Arbeitsgruppe.

Dank gilt natürlich auch meiner Familie, insbesondere meinen Eltern Ernst und Alexandra Schwartz, welche mich immer unterstützt haben. Sie haben mir mein Studium und somit das Verfassen dieser Arbeit erst wirklich ermöglicht.

General remarks

Labeling of substances

Identification of substances is achieved by strict sequential numbering. Substances previously reported in literature receive Arabic numbers, whereas substances unknown to literature are labeled with Roman numbers.

References to literature citations

References to literature are given within the text by superscript Arabic numbers in square brackets.

Nomenclature

The nomenclature of chemical compounds not described in literature is based on the rules of Chemical Abstracts. Other compounds, reagents and solvents may be described by simplified terms, trivial or trade names.

Abbreviations

Besides common abbreviations in the English language and chemical element symbols the below listed short forms are used.

ΔE_{ST}	singlet-triplet energy splitting
ACN	acetonitrile
aq.	aqueous
BmPyPb	1,3-bis(3,5-dipyrid-3-yl-phenyl)benzene
Cz	9*H*-carbazole
CBP	4,4’-bis(9-carbazolyl)biphenyl
dba	dibenzylideneacetone
DCM	dichloromethane
DMA	dimethylacetamide
DMF	dimethylformamide
DMSO	dimethylsulfoxide
DMT	2,5-dimethoxytetrahydrofuran
dppf	1,1’-bis(diphenylphosphino) ferrocene
EA	ethylacetate
E_T	triplet energy
eq.	equivalents
EQE	external quantum efficiency
FIrpic	bis[2-(4,6-difluorophenyl) pyridinato-C^2,*N*](picolinato) iridium(III)
GC	gas chromatography
HOMO	highest occupied molecular orbital
HR-MS	high resolution mass spectrometry
ICz	indolo[3,2,1-*jk*]carbazole
ITO	indium tin oxide
IPB	4,4,5,5-tetramethyl-2-(1-methylethoxy)-1,3,2-dioxaborolane
LUMO	lowest unoccupied molecular orbital
MS	mass spectrometry
NBS	*N*-bromosuccinimide
NHC-lig.	1,3-bis(2,6-diisopropylphenyl)-1*H*-imidazol-3-ium chloride
NMR	nuclear magnetic resonance
OLED	organic light emitting diode
PCz	9-phenyl-9*H*-carbazole
PhOLED	phosphorescent OLED
rf	reflux
rt	room temperature
S_NAr	nucleophilic aromatic substitution
TAPC	4,4’-cyclohexylidenebis[*N*,*N*-bis(4-methylphenyl)benzenamine]
THF	tetrahydrofuran
TLC	thin layer chromatography
Tz	1,3,5-triazine

Table of contents

A Formula scheme

A.1 Synthesis of basic building blocks

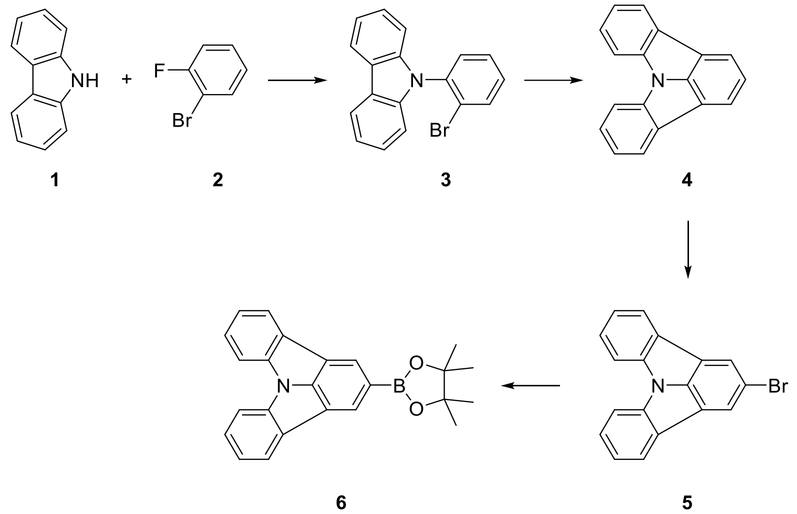

A.2 Synthesis of CzICz derivatives

A.2.1 Synthesis of 5CzICz

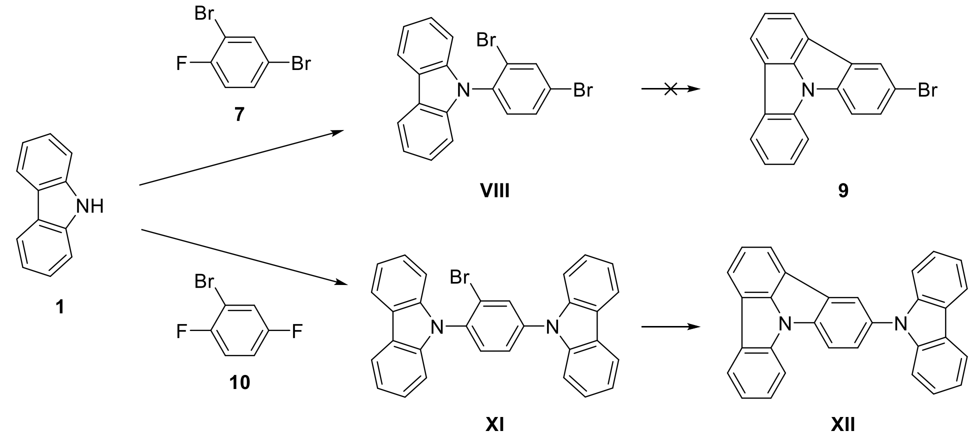

A.2.2 Synthesis of Cz$_2$ICz

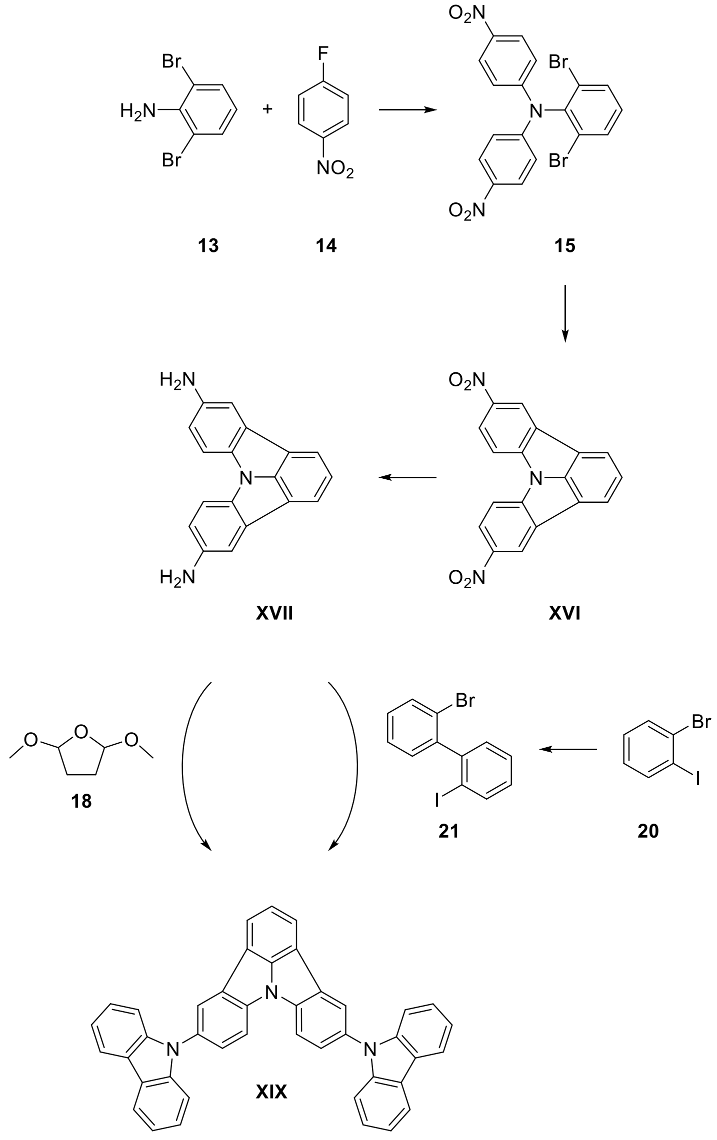

A.2.3 Synthesis of Cz_3ICz

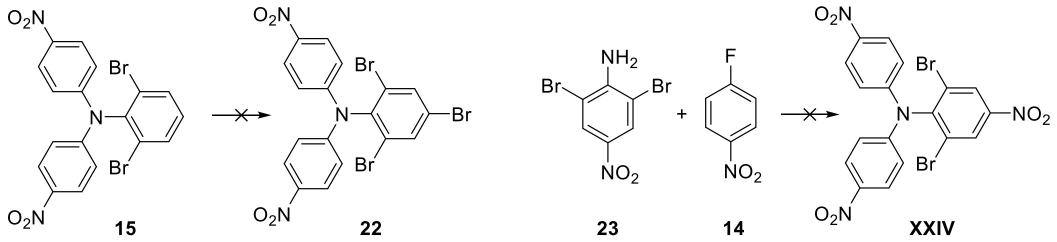

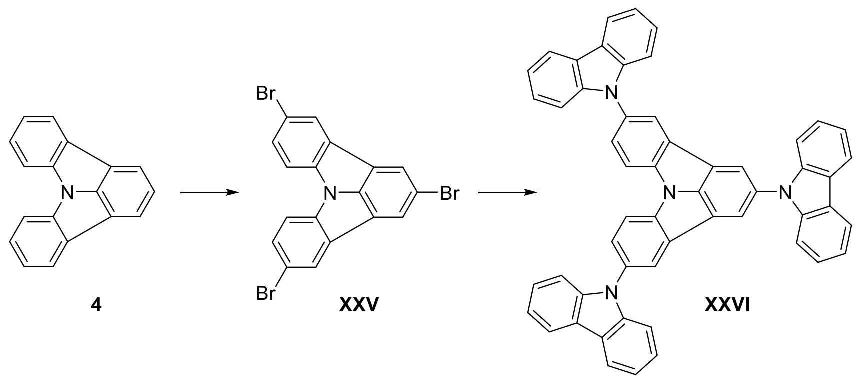

A.3 Synthesis of ICzPCz and ICzICz

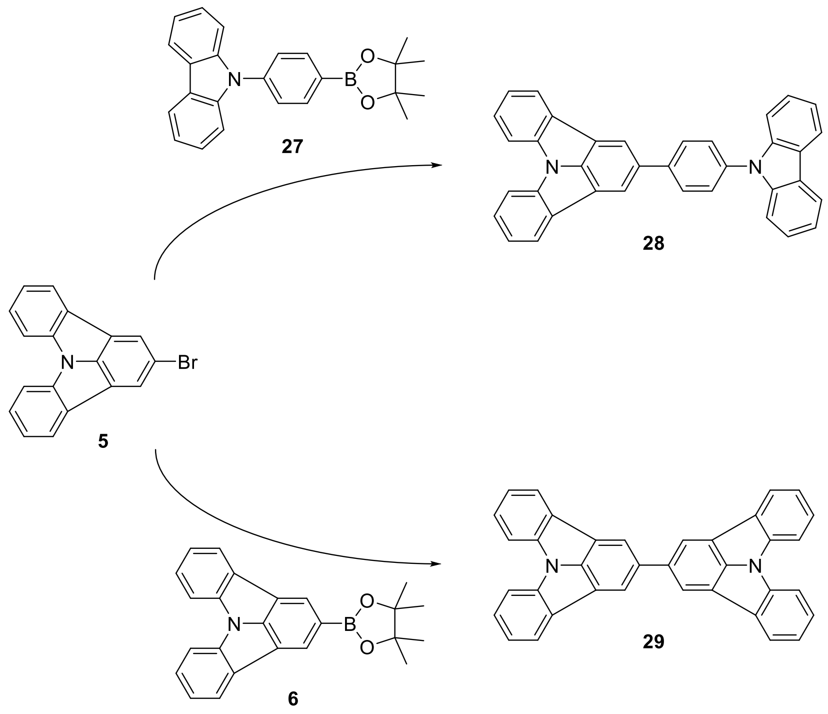

A.4 Synthesis of bipolar materials

A.4.1 Synthesis of the triazines

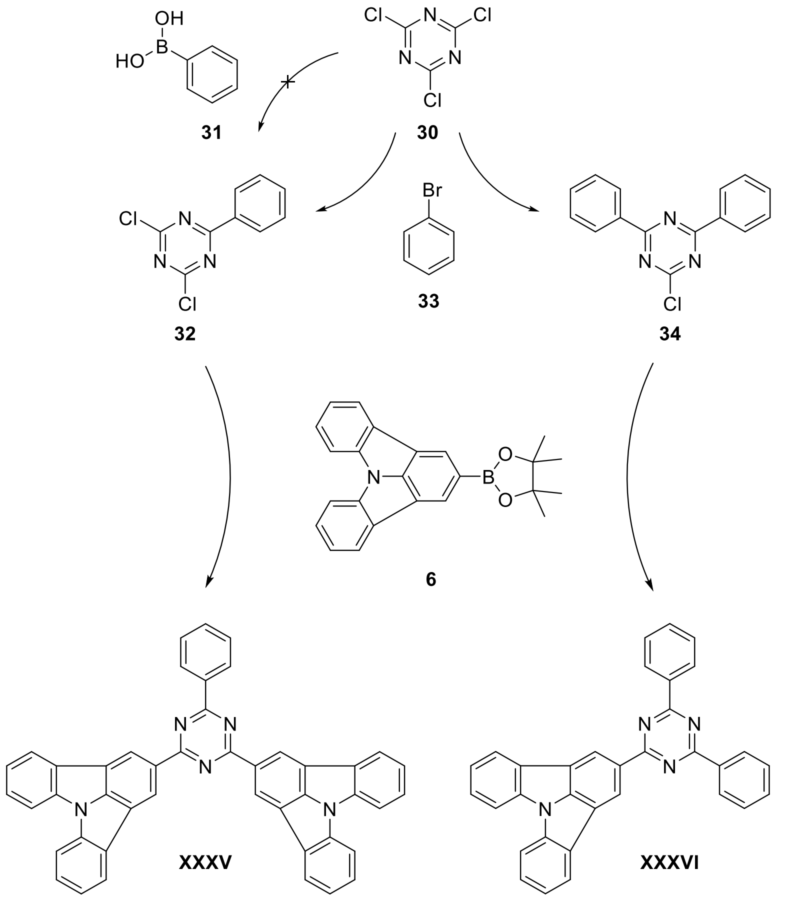

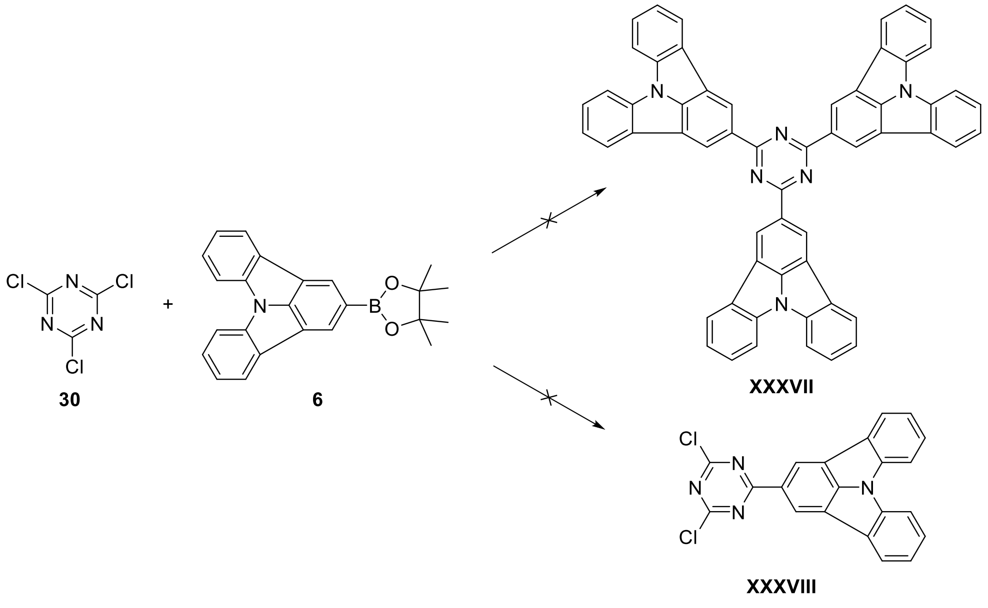

A.4.2 Synthesis towards carbonyl compounds

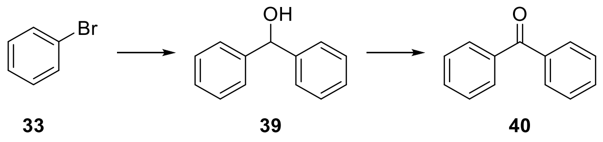

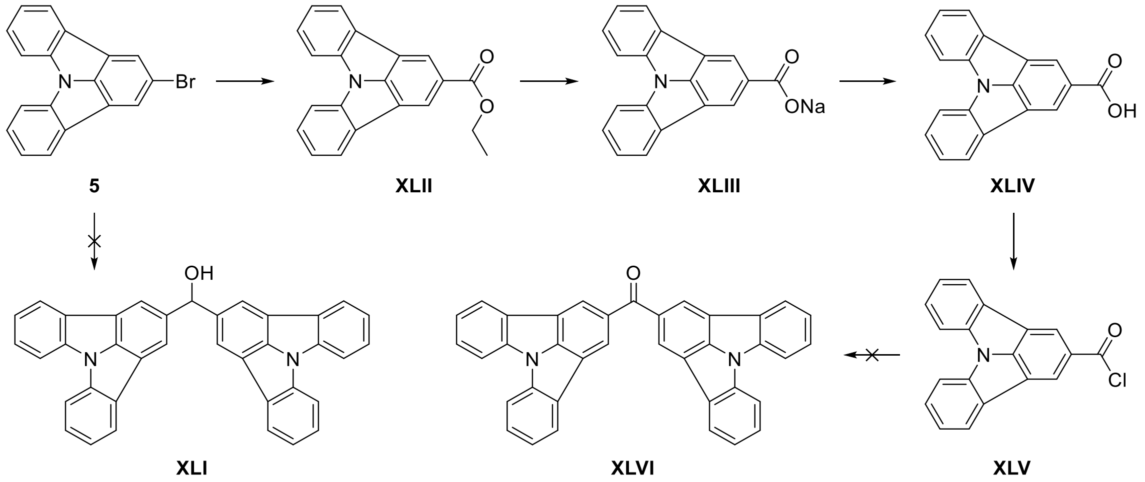

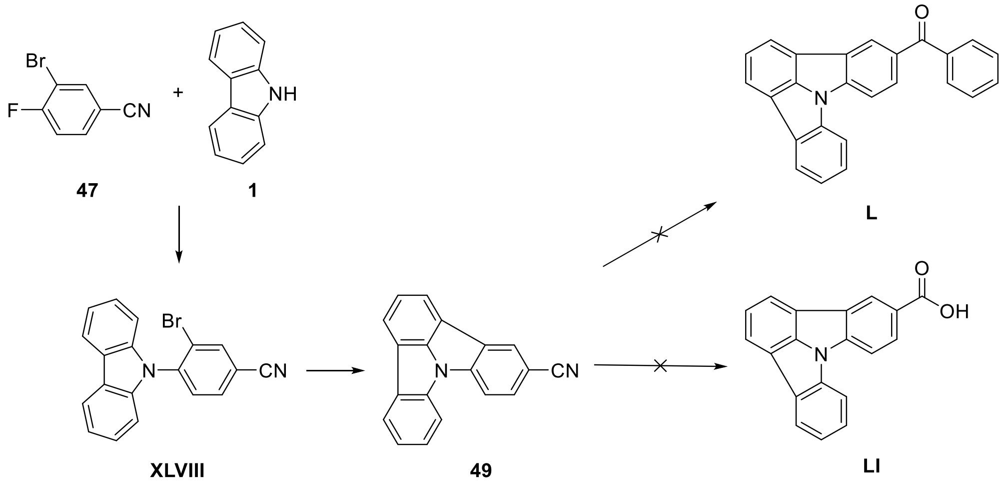

A.5 Synthesis of the highly annulated ring system LIV

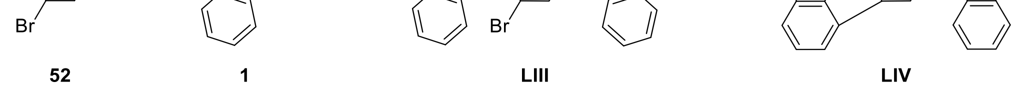

B General part

B.1 Organic electronics

The field of organic electronics is concerned with the investigation of small molecules and polymers. Applications for those substances range from organic light emitting diodes (OLEDs), to thin-film transistors and organic photovoltaic cells. Organic semiconductors are inherently different from their inorganic counterparts in many ways (e.g. mechanical properties, thermal stability). While inorganic semiconductors are hard and brittle, organic materials are soft, which enables their use in flexible devices. Furthermore, organic materials can be deposited on a variety of cheap substrates, which include glass, plastic or metal foils. Device fabrication can also be adapted to use simpler processing techniques, such as direct printing with stamps or ink-jets. This could further decrease fabrication cost and enable the use of large-area substrates.[1]

B.2 Organic light emitting diodes

A lot of research has been conducted to investigate the properties of organic materials as emitters for OLEDs since the electroluminescent properties of anthracene crystals were first described by Pope *et al.* in the 1960s.[2]

In comparison to current display technologies, OLEDs show several advantages, such as a better contrast ratio, a wider viewing angle and a lower power consumption. Some devices using OLED technology are already commercially available, including smartphones, digital cameras, and ultra-high definition TVs. Due to their high efficiency, OLEDs will also be used for lighting applications and might be able to replace incandescent bulbs and fluorescent tubes in the near future.[3]

First OLED devices were made up of one single layer sandwiched between two electrodes. Further improvements led to layered device structures with increased efficiencies. Such a multilayer OLED architecture can be seen in Figure B.1, but devices can have even more layers to reach higher efficiencies.

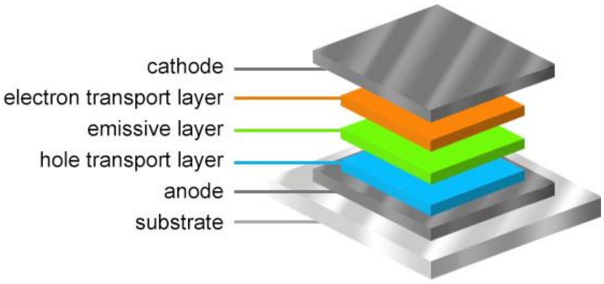

Figure B.1: Multilayer OLED architecture.

Due to the vertical device setup, one of both sides needs to be transparent. This is typically achieved by using indium tin oxide (ITO) as anode material in combination with a glass or plastic substrate. As cathode material metals such as aluminum or silver are used. The emissive layer generally consists of a light emitting material embedded in a host material, which will be described in more detail in chapter B.2.3.

The working principle of an OLED relies on the excitation of the emitter molecules, followed by their relaxation back into the ground state, accompanied by the emission of photons. Upon applying voltage to the device, electrons are injected from the cathode into the LUMO of the electron transport layer while electron holes are injected from the anode into the HOMO of the hole transport layer. In the electric field the charge carriers migrate to the emissive layer by hopping from one molecule to another. Once an electron and a hole meet in the emissive layer, they recombine, forming an exciton, an excited molecular state. Due to the quantum mechanical nature of this process, one quarter of those excitons are in a singlet state, while the remainder is in a triplet state. Those excitons can then either be transferred to another molecule or relax into the ground state by different mechanisms.[4,5]

The first generation of OLEDs relied on fluorescent emitters, which can only convert singlet excitons into photons by fluorescence, while the radiative decay of triplet excitons (phosphorescence) is spin-forbidden (Figure B.2). Hence, three quarters of excited states are lost through non-radiative processes, limiting the internal quantum efficiency to 25%.[6]

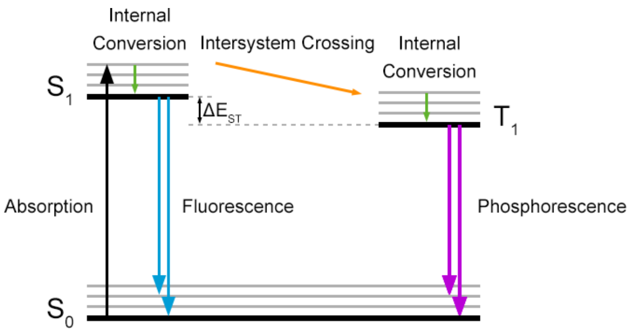

Figure B.2: Jablonski diagram showing possible pathways for exciton relaxation.

B.2.1 Phosphorescent organic light emitting diodes

One way to use the previously mentioned triplet excitons is the incorporation of a phosphorescent emitter instead of a purely fluorescent emitter. Since transitions from a triplet to a singlet state are generally spin-forbidden by selection rules, particular materials with a high spin-orbit coupling have to be used. Typical and well established examples are the iridium complexes shown in Scheme B.1.[5]

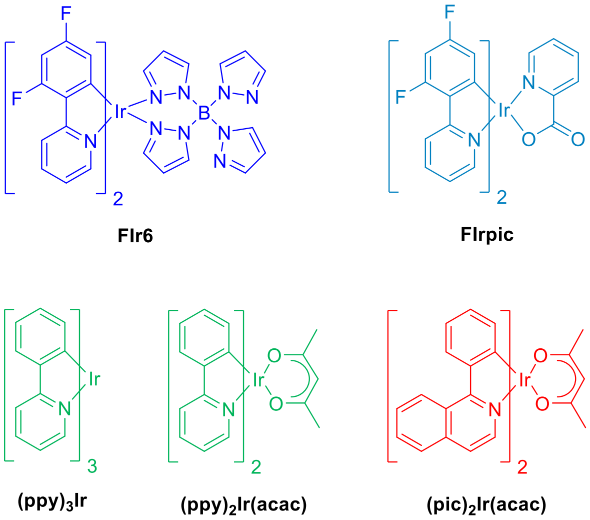

Scheme B.1: Molecular structures of iridium based triplet emitters.[5]

These phosphorescent emitters convert the singlet excitons into triplet excitons by intersystem crossing. The excited triplet states can then relax into the ground state by emitting a photon *via* phosphorescence. Since all singlet excitons are converted, no relaxation from the S_1 state occurs and thus, fluorescence is suppressed.

The big advantage of phosphorescent OLEDs (PhOLEDs) is the increased internal quantum efficiency of up to 100% by converting all generated excitons into photons.[7] One drawback is the requirement of expensive phosphorescent coordination complexes.

B.2.2 Thermally activated delayed fluorescence

The concept of thermally activated delayed fluorescence (TADF) eradicates the need for a phosphorescent emitter to harvest triplet excitons. Instead, it works the other way around: thermal energy is used to repopulate singlet excited states S_1 from triplet states T_1 *via* reverse intersystem crossing (Figure B.3). Those singlet states then undergo relaxation by fluorescence and thereby emit a photon. Since reverse intersystem crossing occurs at a substantially larger timescale than regular fluorescence, the emission from converted excitons is *delayed*. Due to the fact that photons are exclusively emitted by relaxation from singlet states, TADF spectra are only slightly red-shifted compared to regular fluorescence spectra of the same substance.[4,8]

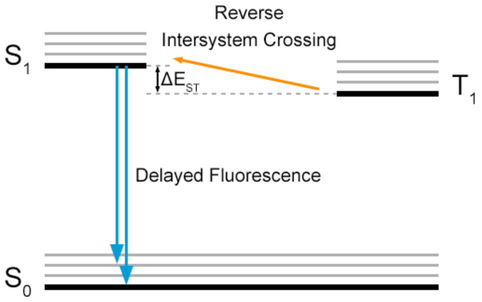

Figure B.3: Jablonski diagram for the pathway of TADF.

For an efficient TADF the emitter materials must possess the following properties:

- the energy splitting between the two excited states (ΔE_{ST}) should be as low as possible to enhance reverse intersystem crossing,
- the fluorescent radiative decay rate (k_r) must be sufficiently high to compete with non-radiative mechanisms.

Since those two properties are generally conflicting with each other, particular molecular designs have to be used. The combination of an electron donor and an acceptor unit, interrupted through steric hindrance, has shown to be a successful approach through the generation of an intramolecular charge transfer S_1 state. The confinement of HOMO and LUMO energy levels to the donor and acceptor, respectively, leads to a spatial separation of the frontier molecular orbitals and therefore yields a low ΔE_{ST}, while maintaining reasonably high values for k_r.[4,9] The ΔE_{ST} of TADF emitters typically lies below 0.2 eV, although the phenomenon has also been observed for materials with a ΔE_{ST} of 0.43 eV.[6]

The biggest challenge is the development of blue TADF emitters, because high triplet energies (E_T) are required. To obtain substances with a high E_T, weak donors have to be employed in such bipolar materials.

B.2.3 Host materials

Host materials are used in the emissive layer to embed the emitter (guest) molecules, which reduces processes competitive to photoemission, such as concentration quenching, which are caused by interactions between excited emitter molecules, especially at high current densities. Host materials are particularly important for PhOLEDs and TADF devices, because long lifetimes of the excited state further increase these undesired processes, due to higher exciton concentrations.[5]

There are certain requirements for those materials to reach high device efficiencies:

- host materials need to have a higher E_T than the guest to confine the excited states on the emitter and prevent energy back transfer,
- the HOMO and LUMO energy levels should match those of neighboring layers to reduce the electron and hole injection barriers, therefore lowering the driving voltage,
- good transport properties for both charge carriers are required and should be similar to each other to have a well-defined exciton formation zone in the emissive layer,
- good thermal and morphological stability (high glass transition temperature) are essential to form morphologically stable amorphous films.[5]

One well-established host material, which has been widely used in many studies, is 4,4'-bis(9-carbazolyl)biphenyl (CBP, Scheme B.2). Its triplet energy of 2.56 eV is, however, rather low compared to the blue emitters FIrpic (E_T = 2.65 eV) and FIr6 (E_T = 2.73 eV), which require a host material with a significantly higher triplet energy for an efficient PhOLED device.[5,10,11] The glass transition temperature of 62 °C is also rather low and can lead to crystallization or deformation during device operation, causing shorter lifetimes.[12,13]

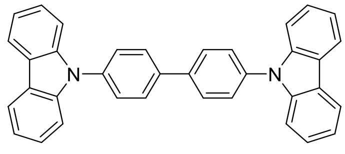

CBP

Scheme B.2: Structure of CBP.

Based on the molecular structure of CBP, Kautny *et al.* developed new host materials with an increased degree of planarization of the triarylamine fragments (Scheme B.3). Application of the fully planarized indolocarbazole led to higher triplet energies, glass transition temperatures (above 110 °C) and thermal stabilities compared to CBP.[14]

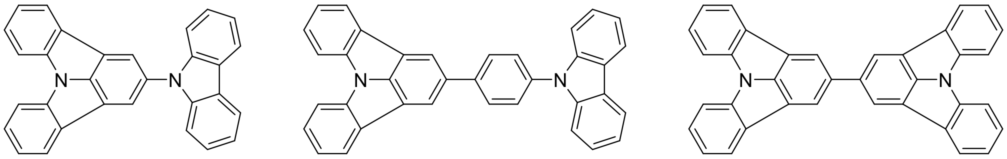

2CzICz **ICzPCz** **ICzICz**

Scheme B.3: Substances investigated by Kautny *et al.* as promising host materials.

The optical bandgap was also lowered from 3.52 eV for CBP to 3.14-3.21 eV for the planarized derivatives, leading to higher power efficiencies as a result of lower driving voltages. Interestingly, the three substances showed E_Ts of 2.82-2.84 eV, which might be due to a local excited triplet state on the ICz moiety. However, the increased planarization also leads to aggregation of molecules through π-stacking, which in turn facilitates the formation of excimers, excited states of aggregates consisting of two or more molecules. This undesired intermolecular interaction reduces the external quantum efficiency of the OLED device due to the low E_T of the excimers. Out of the three substances, **2CzICz** showed the lowest tendency for excimer formation and was therefore used as a starting point for the design of novel host materials in this thesis.[14]

B.3 Goal of the thesis

The goal of this thesis was to utilize the high E_T accompanying the indolo[3,2,1-*jk*]carbazole scaffold in order to prepare new materials for the use in blue OLEDs. This includes the synthesis of candidate substances for blue TADF emitters, as well as new host materials, which are applicable in combination with blue phosphorescent emitters.

Based on the good performance of **2CzICz** in previously manufactured prototype devices, the effects of different degrees and patterns of substitution should be investigated in order to decrease the intermolecular interaction in the thin film and thus increase the device performance. Additionally, the other two planarized CBP derivatives (**ICzPCz** and **ICzICz**) should be synthesized to gain a deeper understanding of the excimer formation in host materials.

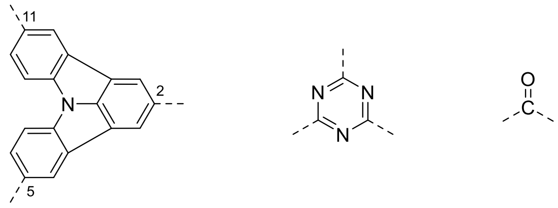

Scheme B.4: Substitution positions 2, 5 and 11 on **ICz** and acceptor units for bipolar materials.

Furthermore, synthetical strategies towards novel bipolar materials based on either carbonyl compounds or 1,3,5-triazines as acceptor units should be explored. Those substances could be applicable either as TADF emitters or as host materials for PhOLEDs, depending on their ΔE_{ST}s.

C Specific part

C.1 Introduction

In order to synthesize new host materials for OLEDs and possible new TADF emitters, ICz was used as the major building block. ICz based materials were already investigated in the Fröhlich research group and showed promising properties.[14,15] There are several different ways to synthesize ICz from substituted 9*H*-carbazoles (Scheme C.1), which will be discussed in this chapter.

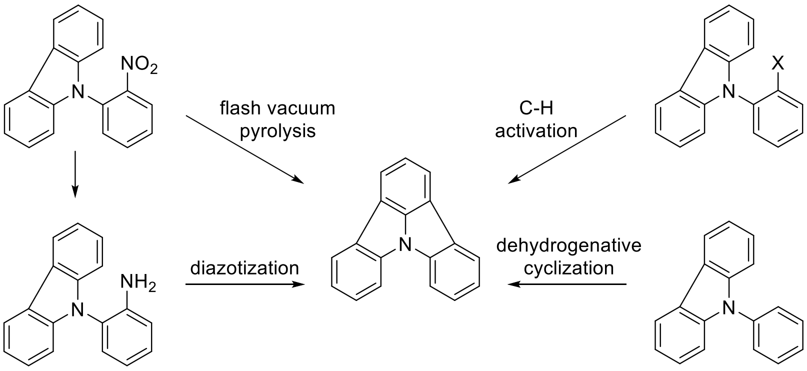

Scheme C.1: Overview for possible ring closing reactions leading to ICz; X=Cl, Br.

The first synthesis of ICz was reported by Dunlop and Tucker in 1939.[16] The diazonium salt, formed from 2-(9*H*-carbazol-9-yl)benzenamine, can decompose into an aryl radical, which can in turn undergo intramolecular cyclization with the carbazole moiety, giving ICz (Scheme C.1). The high reported yield, however, could not be reproduced in the Fröhlich research group and the synthesis is accompanied by the formation of side products. It is therefore not as feasible as the alternative reactions subsequently discussed.

Another approach was described by Wharton *et al*. and uses flash vacuum pyrolysis of the nitro substituted phenylcarbazole to yield ICz.[17] When heated to high temperatures (875 °C), the nitro group is cleaved, giving the aforementioned aryl radical, which in turn forms the ICz. This reaction, however, requires a tube furnace, which is not a common equipment in a synthetic laboratory. Due to the high temperatures required, the reaction also features a lower functional group tolerance than other methodologies.

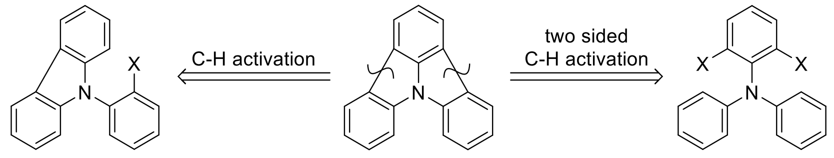

Scheme C.2: Retrosynthetic strategy towards ICz using C-H activation; X=Br, Cl.

An intramolecular C-H activation reaction is another alternative to synthesize ICz (Scheme C.2). Lv *et al.* reported yields of up to 83% for a $Pd(OAc)_2$ catalyzed cyclization of bromophenylcarbazoles.[18] Based on these results, further optimization of this reaction was carried out by Kautny *et al*.[15] Allyl[1,3-bis(2,6-diisopropylphenyl)imidazol-2-ylidene]chloropalladium(II), a palladium catalyst with an N-heterocyclic carbene ligand, widened the substrate scope to chlorinated starting materials and increased yields to over 90% for one-sided reactions. The two-sided reaction, however, was only carried out using the chlorinated substrate so far.

Bintinger showed, that the one-sided reaction can also be carried out with a catalyst formed *in situ* from $Pd(OAc)_2$ and the precursor salt for the N-heterocyclic carbene ligand (NHC-lig.), instead of the aforementioned palladium complex, which has to be prepared separately.[19] The formation of the ICz moiety for all target substances of this thesis was achieved using this methodology starting from either *ortho*-bromophenylcarbazoles or *ortho*-dibromotriarylamines.

Dehydrogenative cyclization using palladium catalysis is a very atom efficient alternative to regular C-H activation. In this reaction, two aromatic C-H bonds are cleaved, leading to a new aryl-aryl bond. The ring closing reaction from 9-phenyl-9*H*-carbazole to ICz was recently investigated by Jones *et al*.[20] In this reaction, the catalyst undergoes two insertions into aromatic C-H bonds and is then regenerated by an external oxidant. However, this reaction shows low yields for most substrates and was therefore not investigated in the course of this thesis.

C.2 Synthesis of basic building blocks

In order to synthesize more complex molecules containing the ICz scaffold, some precursors were synthesized according to Bintinger and Kautny, as depicted in Scheme C.3.[19,21]

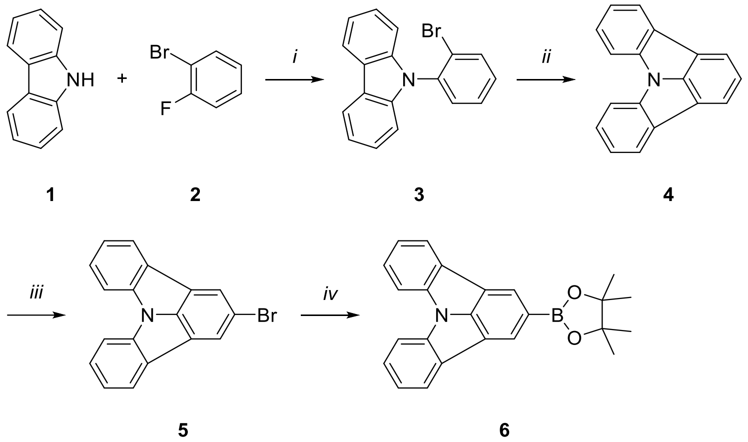

Scheme C.3: Synthesis of ICz building blocks. *i*: DMSO, Cs_2CO_3, 130 °C. *ii*: DMA, K_2CO_3, $Pd(OAc)_2$, NHC-lig., 130 °C. *iii*: $CHCl_3$:AcOH 1:1, NBS, 55 °C. *iv*: THF, -80 °C, 1. *n*-BuLi, 2. IPB → rt.

In the first step, **1** and **2** underwent a S_NAr reaction in DMSO in the presence of Cs_2CO_3. After filtration and refluxing in EtOH, precursor **3** was obtained in 87% yield. Subsequent C-H activation using NHC-lig. and $Pd(OAc)_2$ in DMA with K_2CO_3 as a base gave the building block ICz (**4**) in quantitative yield after filtration over silica. Bromination of **4** in AcOH:$CHCl_3$ (1:1) at 55 °C gave product **5** in 42% yield. Due to the low selectivity of this reaction, bromination also occurred in the 5-position of **4** or on both positions (2 and 5) at the same time. Those byproducts showed similar low solubilities and therefore had to be separated in a tedious workup by repeated refluxing in ACN and recrystallization from toluene. Therefore, lower yields were obtained than one would expect for such a straightforward reaction. Lithiation of **5** in THF at -80 °C and subsequent quenching with IPB gave the pinacol boronic ester **6** in 73% yield. In further reactions both **5** and **6** could be used in Suzuki coupling reactions.

C.3 Synthesis of CzICz derivatives

Based on the good performance of **2CzICz** as a host material in PhOLED devices (see chapter B.2.3), new host materials based on this particular scaffold (Scheme C.4) were synthesized with the goal to further reduce the excimer formation in the solid film. To decrease intermolecular interactions in the solid phase, a few modifications of the molecular structure were carried out:

- reduction of the molecular symmetry (**5CzICz**),
- increased steric hindrance through higher substitution (**Cz$_2$ICz**, **Cz$_3$ICz**).

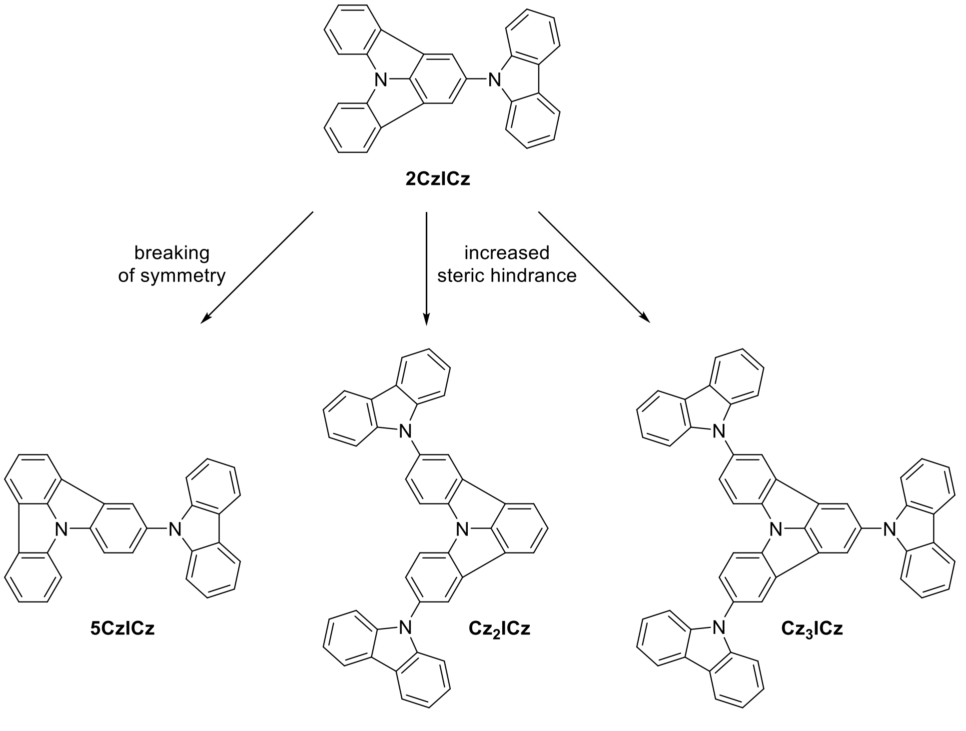

Scheme C.4: Structure of the new CzICz derivatives.

Those modifications should retain the high E_T of approximately 2.8 eV, decrease the intermolecular interactions and therefore lead to higher device efficiencies. The increased molecular weight of **Cz$_2$ICz** and **Cz$_3$ICz** could also have a high impact on properties like the glass transition temperature and thermal stability.

C.3.1 Synthesis of 5CzICz

The first synthetic approach towards **5CzICz** (**XII**) required the preparation of key intermediate **9** (Scheme C.5). Furthermore, **9** would also be a valuable starting material to other 5-substituted ICz compounds. Preparation of **9** should be carried out by C-H activation, analogously to the unsubstituted ICz. Subsequent Ullmann condensation reaction with 9*H*-carbazole would then lead to the desired product.

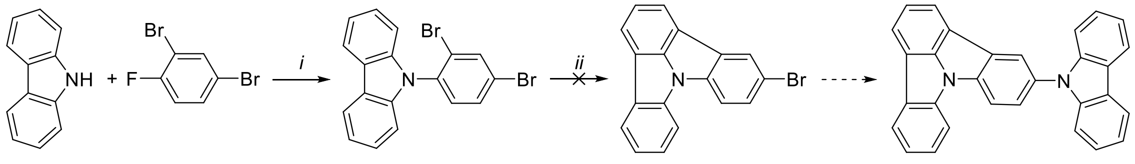

1 **7** **VIII** **9** **XII**

Scheme C.5: Synthesis towards the **5CzICz** (**XII**) using S$_N$Ar, C-H activation and Ullmann condensation. *i*: DMSO, Cs_2CO_3, 130 °C. *ii*: DMA, K_2CO_3, $Pd(OAc)_2$, NHC-lig., 130 °C.

The S$_N$Ar between **1** and **7** was carried out in DMSO in the presence of Cs_2CO_3. Precipitation of the product with water and subsequent crystallization from ACN gave **VIII** in 40% yield. The ring closing reaction by C-H activation was carried out using NHC-lig. and $Pd(OAc)_2$ as catalyst in DMA with K_2CO_3 as a base. After column chromatography, the formation of **9** could not be verified.

Based on the work of Cakmak *et al.*, a selective bromination of ICz on one of the less activated rings was attempted, as an alternative approach towards **9** (Scheme C.6).[22]

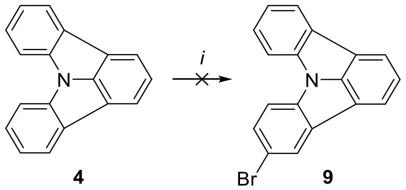

4 **9**

Scheme C.6: Attempt of selective bromination of ICz **4** in the 5-position using Br_2 in DCM. *i*: DCM, Br_2, -18 °C

A solution of **4** in DCM and one equivalent of Br_2 in DCM were cooled to -18 °C. Upon slow addition of the bromine solution, a white precipitate formed immediately. After filtration and characterization of the precipitate, it was identified as the 2,5,11-tribromo-ICz instead of **9**. The remaining solution almost exclusively contained the unsubstituted ICz.

Due to the lack of a feasible pathway towards **9**, an alternative route was chosen. In this approach, both 9*H*-carbazole moieties were introduced in the first reaction step eliminating the need for a subsequent Ullmann condensation to obtain **XXII** (Scheme C.7).

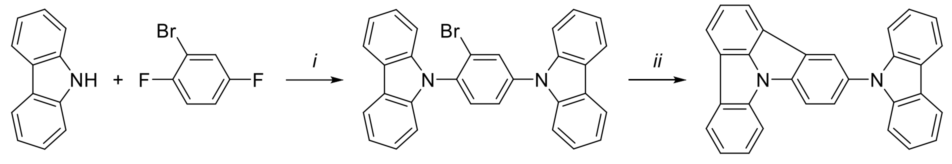

1 **10** **XI** **XII**

Scheme C.7: Synthesis towards **5CzICz** (**XII**) using S_NAr and C-H activation. *i*: DMSO, Cs_2CO_3, 130 °C. *ii*: DMA, K_2CO_3, $Pd(OAc)_2$, NHC-lig., 130 °C.

The S_NAr reaction between **1** and **10** was carried out in DMSO in the presence of Cs_2CO_3. The crude product was precipitated by the addition of water and after column chromatography, **XI** was obtained in 46% yield. C-H activation of **XI** with NHC-lig. and $Pd(OAc)_2$ gave the desired **5CzICz** (**XII**) in 79% yield after column chromatography.

C.3.2 Synthesis of Cz_2ICz

For the functionalization of ICz in the positions 5 and 11, a different approach than bromination had to be used due to the fact, that regioselectivity prefers the 2-position. Instead, the triarylamine **15** was synthesized, which already featured the desired substitution pattern before the ring closing step (Scheme C.8). The two nitro groups of **15** can later be reduced in order to introduce the desired carbazole moieties.

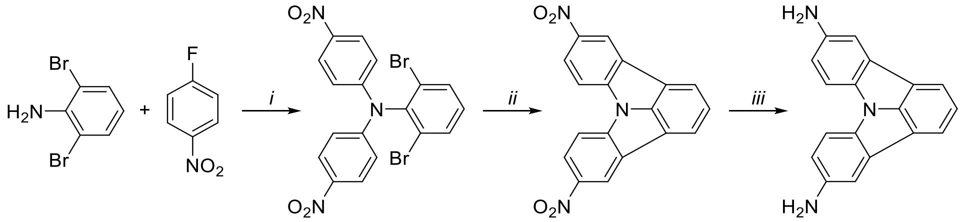

13 **14** **15** **XVI** **XVII**

Scheme C.8: General strategy to synthesize the **Cz_2ICz** precursor **XVI**. *i*: DMSO, Cs_2CO_3, 130 °C. *ii*: DMA, K_2CO_3, $Pd(OAc)_2$, NHC-lig., 130 °C. *iii*: DMSO/H_2O 10:1, $SnCl_2{\cdot}2H_2O$, 80 °C.

The S_NAr reaction between benzenamine **13** and fluorobenzene **14** was carried out as a modification of the protocol by Kautny *et al.*[23] Refluxing the crude product in EtOH gave the triarylamine **15** in 76% yield. C-H activation employing the already described reaction conditions gave the dinitro-compound **XVI** in 93% yield after filtration of the reaction mixture.

Reduction of the two nitro groups proved to be challenging, mainly due to the low solubility of **XVI**. The first attempt followed a modified protocol by Khan *et al.*[24] Reduction of **XVI** was successfully carried out in the ionic liquid [bmim][PF_6] using water, zinc and NH_4Cl. However, the product (**XVII**) could not be separated from the ionic liquid, making this reaction unfeasible. Another attempt followed a modified procedure by Rai *et al.*[25] **XVI** was sonicated in [C_2mim][OTf] in the presence of 10 eq. $SnCl_2 \cdot 2H_2O$ under argon atmosphere. After 15 min, no conversion was observed. Finally, the reduction was successfully carried out using $SnCl_2 \cdot 2H_2O$ in DMSO/H_2O (10:1) and gave **XVII** in 60% yield.

The first attempt to introduce the two 9*H*-carbazole moieties into **XVII** employed an extended Clauson-Kaas reaction by refluxing **XVII** with an excess of DMT (**18**) in AcOH (Scheme C.9). In the first step, the amino groups are converted into pyrrole rings. These pyrroles then undergo further condensation with DMT, giving indole and subsequently 9*H*-carbazole moieties.

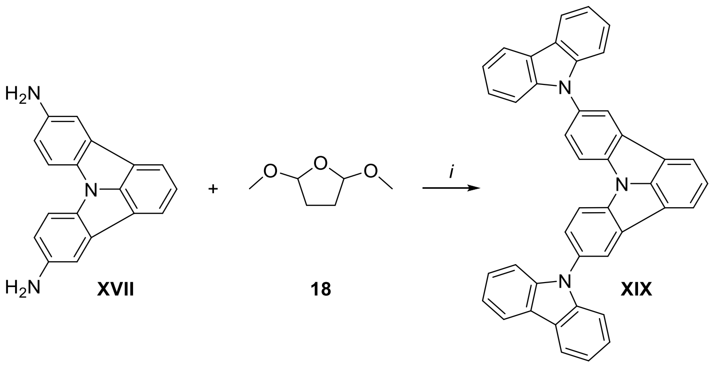

Scheme C.9: Formation of the 9*H*-carbazole units of **XIX** using DMT (**18**). *i*: AcOH, rf.

Unfortunately, the reaction does not stop at the carbazole level and also leads to higher condensation products with even larger annulated ring systems. The lack of selectivity causes the reaction mixture to contain similar quantities of intermediates and overcondensated products. The complex composition of the crude reaction mixture therefore only contains a small fraction of the desired product, leading to the low yield of 4% of **XIX** after column chromatography.

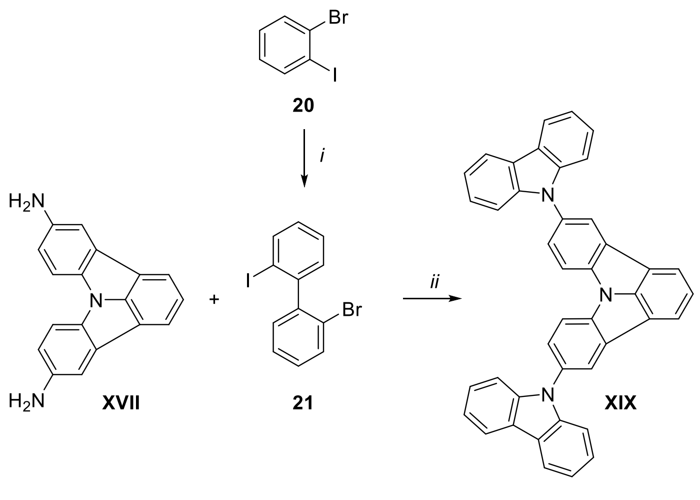

Scheme C.10: Formation of the 9*H*-carbazole units using Buchwald-Hartwig amination. *i*: THF, *n*-BuLi, -80 °C → rt. *ii*: toluene, $Pd_2(dba)_3$, dppf, NaO*t*Bu, rf.

An alternative route to obtain **Cz₂ICz** (**XIX**) utilized a Buchwald-Hartwig amination to form the two 9*H*-carbazole units (Scheme C.10). Biphenyl **21** can undergo two amination reactions with an amino group, forming a 9*H*-carbazole substituent. This reaction takes place on both amino groups of **XVII**, giving the desired product **XIX**. The biphenyl **21** was synthesized according to Leroux and Schlosser by lithiation of half an equivalent of bromoiodobenzene **20**, followed by warming to rt.[26] Crystallization from EtOH gave **21** in quantitative yield. The Buchwald-Hartwig amination was carried out using $Pd_2(dba)_3$ with dppf as a catalyst in toluene with NaO*t*Bu as a base. After column chromatography, **XIX** was obtained in 78% yield.

C.3.3 Synthesis of Cz_3ICz

Compared to the previously described **Cz_2ICz** a third functionality had to be added to the ICz scaffold in the synthesis of **Cz_3ICz**. The first attempt started from the previously prepared triarylamine **15** to give **22** after bromination (Scheme C.11). Compound **22** could undergo reactions analogous to **15**, forming 2-bromoindolo[3,2,1-*jk*]carbazole-5,11-diamine after C-H activation and reduction. Condensation reaction with DMT followed by Ullmann condensation with 9*H*-carbazole could then lead to **XXVI**. Furthermore, a differentiation between the 2 and the 5/11-position would be possible due to the different substituents, which could be used in the preparation of a variety of new products.

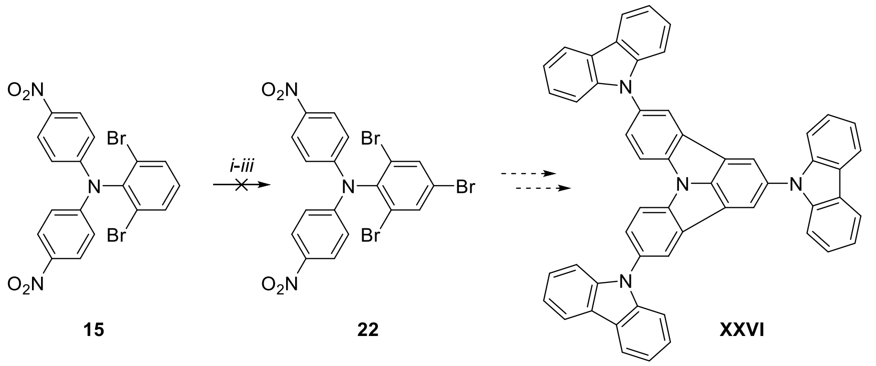

Scheme C.11: Strategy towards **Cz_3ICz** (**XXVI**) *via* the nitro compound **22**. *i*: AcOH:$CHCl_3$ (1:1), NBS, 45 °C → 60 °C *ii*: DMF, NBS, 80 °C. *iii*: DCM, Br_2, -5 °C → rt.

The first bromination reaction was carried out analogously to the bromination of ICz. **15** was suspended in AcOH:$CHCl_3$ (1:1) with 1.05 equivalents of NBS and heated to 45 °C for 4 h. Since no conversion was observed, the reaction mixture was further heated to 60 °C for another 5 h. After filtration, only the starting material was isolated. Also in the solvent, no trace of the product could be detected.

Alternatively, the bromination was carried out as a modification of the protocol by Huang *et al*. for the *para*-bromination of 4-nitro-*N,N*-diphenylbenzenamine.[27] **15** was suspended in DMF and NBS suspended in DMF was added dropwise. After stirring for 24 h at rt, no conversion was observed. The mixture was therefore heated to 80 °C and the reactants dissolved. A second equivalent of NBS was added and stirring overnight at 80 °C led to darkening of the solution. However, no product could be detected.

Another attempt to brominate **15** was carried out as a modification of the protocol by Wu *et al*. for the *para*-bromination of 4-nitro-*N*-(4-nitrophenyl)-*N*-phenylbenzenamine.[28] **15** was dissolved in DCM and cooled to -5 °C. One equivalent of bromine dissolved in DCM was slowly added and the reaction mixture was allowed to warm to rt overnight. Since no conversion was observed, another 5 equivalents of bromine were added and the reaction mixture was stirred at rt over the weekend. However, no product formation was observed.

A different approach aimed to obtain **XXIV** by a S_NAr of the substituted aniline **23** and **14** (Scheme C.12). Triarylamine **XXIV** could then undergo a two-sided C-H activation reaction, giving the 2,5,11-trinitro-ICz. Reduction of the nitro groups followed by Buchwald-Hartwig amination with 2-bromo-2'-iodo-1,1'-biphenyl (**21**) could then yield the desired **XXVI**.

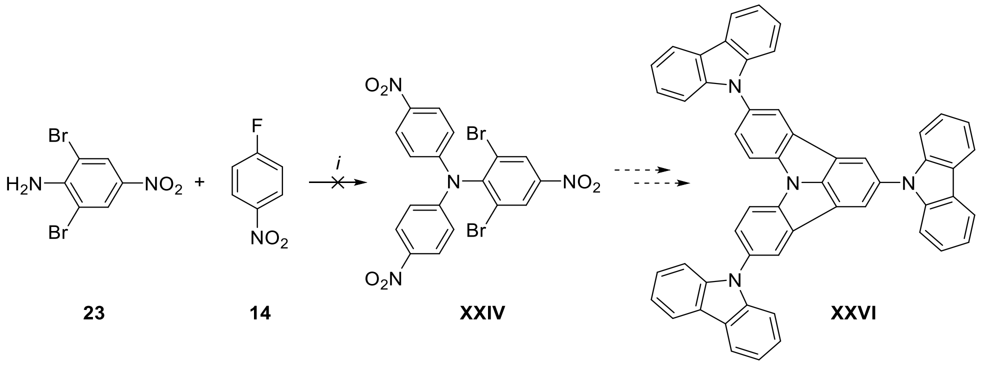

Scheme C.12: Strategy towards **Cz$_3$ICz** (**XXVI**) *via* the trinitro compound **XXIV**. *i*: DMSO, Cs_2CO_3, 130 °C.

The S_NAr reaction of 1-fluoro-4-nitrobenzene (**14**) and 2,6-dibromo-4-nitrobenzenamine (**23**) was carried out analogously to previous S_NAr reactions. **23** was heated to 130 °C with **14** and Cs_2CO_3 in DMSO overnight. Then the reaction mixture was poured on water and a soft, sticky precipitate formed, which was subsequently filtrated. After refluxing in EtOH, a glasslike solid remained stuck to the inside of the flask. The product could not be separated from the byproducts, primarily due to low solubility of the crude product in common solvents.

Due to the unavailability of a properly substituted ICz, a different strategy was investigated. A first screening reaction using a mixture of the brominated byproducts from the bromination of ICz showed that these byproducts could be brominated a second and third time with NBS when refluxed in AcOH:$CHCl_3$ (1:1). This reaction is rather slow, because increased substitution further decreases solubility and reactivity.

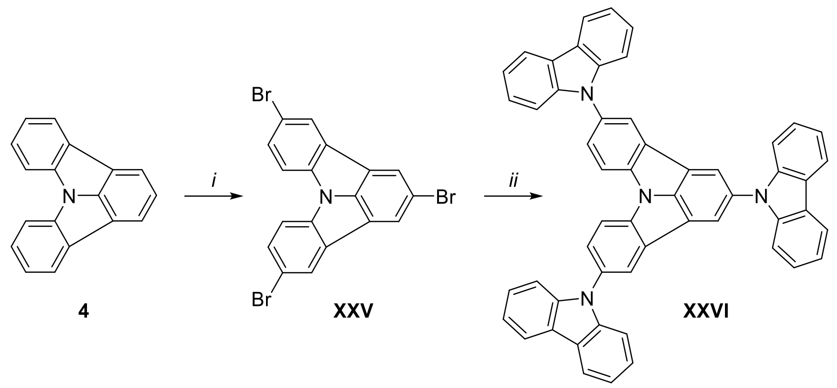

Scheme C.13: Strategy towards **Cz$_3$ICz** (**XXVI**) *via* the tribromo compound **XXV**. *i*: DCM, Br$_2$, 0 °C. *ii*: crude, CuSO$_4$·5H$_2$O, K$_2$CO$_3$, 9*H*-carbazole (**1**), 250 °C.

Subsequent experiments revealed, that ICz can be easily brominated up to three times using bromine in DCM (Scheme C.13). **4** was dissolved in DCM and cooled in an ice bath. Bromine (3.3 eq.) was also dissolved in DCM, cooled and then added dropwise. After 7 h, the formed precipitate was filtrated and subsequently refluxed in toluene, giving **XXV** as a beige solid in 73% yield. **XXV** was then used in an Ullmann condensation reaction with 9*H*-carbazole analogously to a protocol by Kautny *et al.*[14] **XXV**, 9*H*-carbazole (**1**), CuSO$_4$·5H$_2$O and K$_2$CO$_3$ were mixed and heated to 250 °C. After 72 h, the reaction mixture was cooled to rt and extracted with water and DCM. Most of the excess 9*H*-carbazole (**1**) was removed by sublimation and subsequent column chromatography gave **XXVI** in 76% yield.

C.3.4 Characterization

In order to investigate the molecular properties of the developed materials, measurements of the most important properties were conducted and are discussed in this chapter. Results are summarized at the end of this chapter.

C.3.4.1 Absorption and fluorescence

The absorption spectra of the three novel CzICz derivatives (Figure C.1) exhibit a general redshift of the absorption onset with an increased degree of substitution from **5CzICz** to **Cz₂ICz** to **Cz₃ICz** (located at 389, 402 and 411 nm, respectively). Furthermore, the local maximum at the long wavelength end of the absorption spectrum, attributed to the ICz motive, widens and its intensity decreases with additional carbazole units, probably due to the increased π-system.[14] All three spectra contain prominent absorption peaks below 300 nm with a maximum around 290 nm, which can be attributed to the π-π* transition of the carbazole and/or ICz moieties with a high contribution of the nitrogen electrons.[15,29]

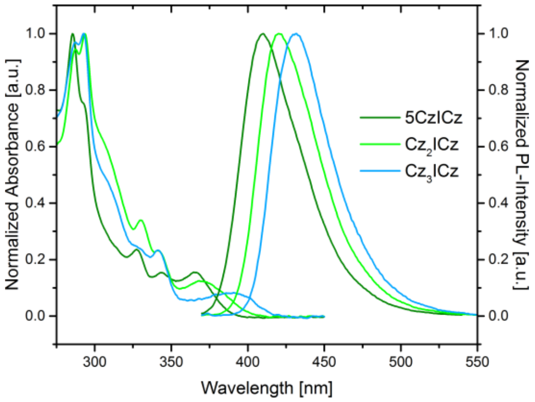

Figure C.1: Absorption and fluorescence spectra of **5CzICz**, **Cz₂ICz** and **Cz₃ICz**. All spectra were recorded in DCM at a concentration of 5 nmol/ml and are normalized to 1.

Photoluminescence spectra obtained from DCM solutions only show a single peak for each substance. The maxima also follow the trend of a general redshift with increased substitution and are located at 410, 420 and 432 nm for **5CzICz**, **Cz₂ICz** and **Cz₃ICz**, respectively. The differences in wavelength of the emission maxima are comparable to those of the absorption onset.

As shown in Figure C.2, intermolecular interactions leading to excimer formation are suppressed in all of these substances, as no additional low-energy emission bands can be observed. In both solid state and thin film measurements, **5CzICz** showed two slightly redshifted shoulders. In contrast, **Cz$_2$ICz** exhibits stronger interactions in the crystalline solid, leading to a significant redshift, whereas those interactions are suppressed in the thin film. Finally, **Cz$_3$ICz** showed very similar fluorescence in thin film and solid state with a generally low redshift. In summary, excimer formation could successfully be prevented by the employed molecular designs.

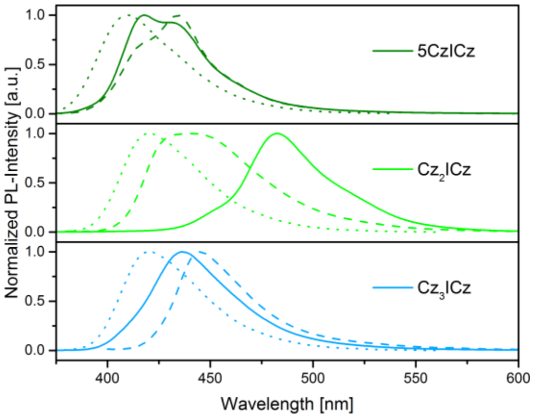

Figure C.2: Fluorescence spectra of **5CzICz**, **Cz$_2$ICz** and **Cz$_3$ICz** 5 nmol/ml in DCM (dotted lines), solid state (continuous lines) and thin film (dashed lines) normalized to 1.

C.3.4.2 Electrochemical analysis

The HOMO and LUMO energy levels of the CzICz compounds were determined by cyclic voltammetry. They were estimated from the onsets of the oxidation and reduction peaks, respectively, relative to ferrocene. HOMO levels are located at -5.57, -5.54 and -5.63 eV for **5CzICz**, **Cz$_2$ICz** and **Cz$_3$ICz**, respectively, while LUMO levels are located at -2.47, -2.47 and -2.59 eV. All compounds exhibit irreversible oxidation, as typically observed for carbazole and ICz materials.[14] Cyclic voltammograms are depicted in F.2.

C.3.4.3 Phosphorescence

The phosphorescence spectra of the three CzICz derivatives (Figure C.3) are well resolved and show the same trend as the absorption onsets: increased substitution leads to a redshift of the phosphorescent maxima. The high-energy maxima are located at 438, 440 and 444 nm for

5CzICz, **Cz_2ICz** and **Cz_3ICz**, respectively, corresponding to 2.83, 2.82 and 2.80 eV. These high E_Ts make the three CzICz derivatives well suited as host materials for blue PhOLEDs. Prototype devices were fabricated from these substances and are described in C.7.

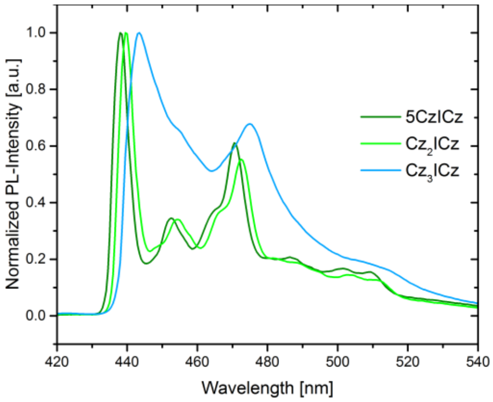

Figure C.3: Phosphorescence spectra of **5CzICz**, **Cz_2ICz** and **Cz_3ICz** recorded in toluene at 77 K normalized to 1.

C.3.4.4 Summary

All results of the characterizations are summarized in Table 1. Low driving voltage for prototype devices can be expected from the low bandgaps of 3.02-3.19 eV. Furthermore, good performances, even for blue devices, can be expected due to the high triplet energies of 2.80-2.83 eV and good thermal stabilities.

Table 1: Physical data of target substances **5CzICz**, **Cz_2ICz** and **Cz_3ICz**.

Substance	$T_g/T_{rc}/T_m$ [°C][a]	Opt. BG [eV][b,c]	$\lambda_{PL,max}$ [nm][c]	HOMO/LUMO [eV][d]	E_T [eV][e]	ΔE_{ST} [eV][f]
5CzICz	101/181/244	3.19	410	-5.57/-2.47	2.83	0.42
Cz_2ICz	171/n.o.[g]/308	3.08	420	-5.54/-2.47	2.82	0.33
Cz_3ICz	327/n.o.[g]/n.o.[g]	3.02	432	-5.63/-2.59	2.80	0.29

[a] Determined from DSC analysis; T_g: glass transition temperature; T_{rc}: recrystallization temperature; T_m: melting point.

[b] Determined from the absorption onset.

[c] Measured in DCM solutions (5 mM) at rt.

[d] Calculated from cyclic voltammetry measurements.

[e] Estimated from the highest energy vibronic transition in solid solutions DCM:toluene:MeOH (10:10:1) at 77 K.

[f] Calculated from the onset of fluorescence and the first phosphorescence maximum.

[g] Not observed.

C.4 Synthesis of ICzPCz and ICzICz

Another part of this thesis was the synthesis of the other two planarized CBP derivatives described by Kautny *et al*.[14] These substances already showed rather good performances in OLED devices. However, the formation of excimers was observed. To further study this undesired phenomenon and understand the structural features, which favor excimer formation, a new batch of these materials was prepared.

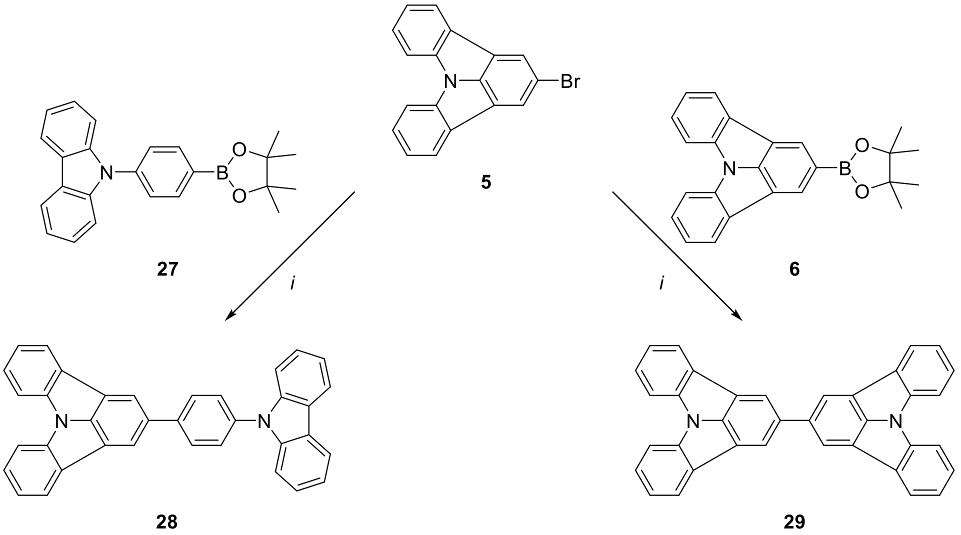

Scheme C.14: Synthesis of **28** and **29** *via* Suzuki cross coupling reaction. *i*: THF, aq. K_2CO_3, $Pd(PPh_3)_4$, rf.

The previously synthesized **5** was used in Suzuki cross coupling reactions with the boronic esters **27** and **6**, giving **ICzPCz** (**28**) and **ICzICz** (**29**), respectively (Scheme C.14). **5**, aqueous K_2CO_3 and **27** or **6** were suspended in dry THF under argon atmosphere. $Pd(PPh_3)_4$ was added under argon counterflow and the reaction mixtures were refluxed for 40 h. Column chromatography and subsequent crystallization from toluene gave **28** in 31% yield. **29** was isolated by filtration in 81% yield containing approximately 5-10% impurities.

28 showed rather good solubility. In contrast, **29** did not dissolve in reasonable amounts of boiling common solvents, therefore preventing further purification by conventional methods. Sublimation in high vacuum (300 °C, $1.0 \cdot 10^{-6}$ Torr) also did not significantly decrease the amount of impurities.

C.5 Synthesis of bipolar materials

The second part of this thesis aimed for the synthesis of novel bipolar materials as potential TADF emitters or host materials for blue OLEDs. One major challenge in the development of such materials for blue devices is the need for high E_Ts. Intramolecular charge transfer leads to a redshift and therefore lower E_Ts. In order to prevent this intramolecular charge transfer, we aimed to synthesize bipolar materials with the weak ICz donor in combination with different acceptor units, such as ketones or the 1,3,5-triazine, which have already been successfully used in TADF materials.[9,12,30]

C.5.1 Synthesis of the triazines

The general strategy to obtain the triazine derivatives started from 2,4,6-trichloro-1,3,5-triazine (**30**). Substitution reactions such as S_NAr or the Suzuki cross coupling reaction were employed to introduce substituents. Due to the more difficult preparation of the ICz derivatives, the phenyl rings were introduced to the triazine core first using different approaches. Initially, a Suzuki cross coupling reaction with phenylboronic acid (**31**) was investigated (Scheme C.15).

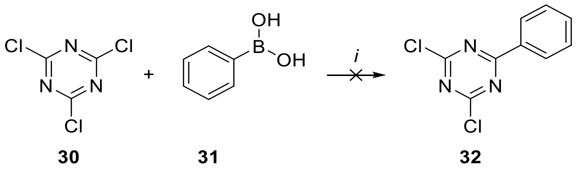

Scheme C.15: Possible synthesis of dichlorophenyltriazine **32** *via* Suzuki cross coupling reaction. *i*: THF, aq. K_2CO_3, $Pd(PPh_3)_4$, rf.

30, **31** and $Pd(PPh_3)_4$ were suspended in aqueous K_2CO_3 with THF under argon atmosphere and heated to reflux overnight. Extraction with DCM followed by column chromatography, however, did not give the desired product.

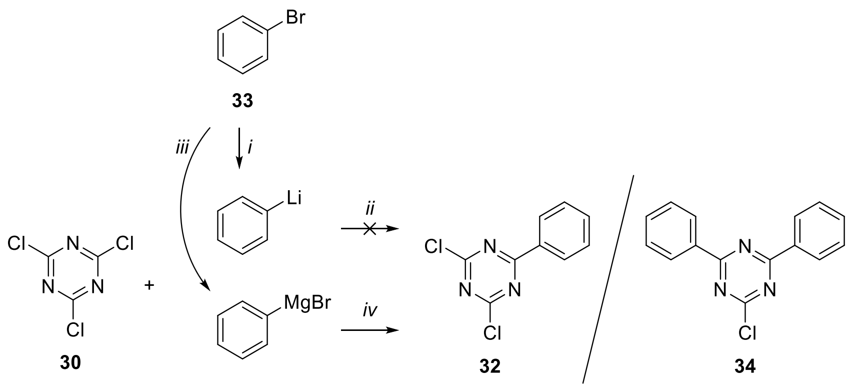

Scheme C.16: Synthetic strategies towards the triazines **32** and **34**. *i*: THF, -80 °C, *n*-BuLi *ii*: -80 °C → rt. *iii*: THF, Mg turnings, I_2, rf. *iv*: THF, 0 °C → rt.

Subsequently, a S_NAr reaction was carried out using freshly prepared phenyllithium (Scheme C.16). Bromobenzene **33** was cooled to -80 °C in dry THF under argon atmosphere. After addition of *n*-BuLi, the reaction mixture was stirred for 1 h. **30** was cooled to -80 °C in a separate flask in dry THF under argon atmosphere and the phenyllithium solution was slowly added using a syringe. The reaction mixture was then allowed to slowly warm to rt overnight. It was then poured on aqueous NH_4Cl (10%) and repeatedly extracted with Et_2O. The crude product was refluxed in EtOH, but the product did not crystallize and removal of the solvent gave an insoluble substance, probably due to hydrolysis. In ^1H NMR-spectra recorded in $CDCl_3$, no additional N-H or O-H signals were observed. However, crystals grown from pyridine were identified as solvate crystals of the hydrolyzed species (F.1).

The protocol described by An *et al*. made the chlorophenyltriazines **32** and **34** available using a freshly prepared Grignard reagent instead of phenyllithium (Scheme C.16).[31] For both syntheses, magnesium turnings and a catalytic amount of iodine were suspended in dry THF. Solutions of **33** in dry THF were added dropwise and the mixtures were carefully heated to start the reaction, as indicated by self-sustaining reflux. After complete addition of the solutions of **33**, external heating was used to reflux for 1 h. The Grignard reagents were cooled to rt and then added to cooled (0 °C) solutions of **30** in THF. In case of the reaction leading to **32**, 1.33 eq. of **30** were used while the other reaction employed 3.4 eq. of the Grignard reagent. The reaction mixtures were then allowed to warm to rt overnight. Extraction with

$CHCl_3$ followed by column chromatography gave **32** and **34** in 66% and 25% yield, respectively. Due to the low solubility of the brominated ICz **5**, the respective Grignard reagent could not be synthesized. Therefore, this pathway to introduce the ICz moiety to the triazine core was not feasible. Alternatively, the triazines **ICz$_2$Tz** (**XXXV**) and **ICzTz** (**XXXVI**) could be synthesized using a Suzuki cross coupling reaction with the boronic ester **6** staring from the phenyltriazines **32** and **34** (Scheme C.17).

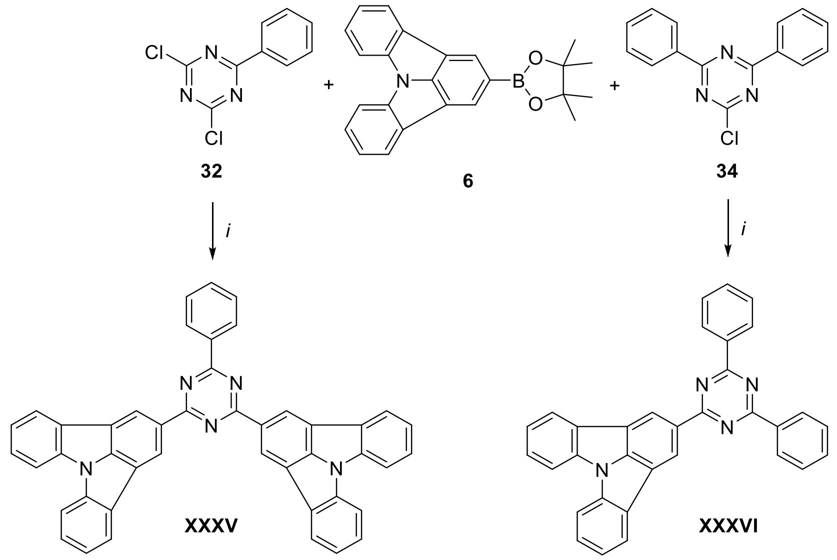

Scheme C.17: Synthesis of the ICz triazines **XXXV** and **XXXVI** using the Suzuki cross coupling reaction. *i*: THF, aq. K_2CO_3, $Pd(PPh_3)_4$, rf.

Phenyltriazine (**32** or **34**) and **6** were suspended in degassed THF and 2 M aqueous K_2CO_3 under argon atmosphere. $Pd(PPh_3)_4$ was then added under argon counterflow. The mixtures were refluxed for 48 h and then filtrated. **XXXV** was obtained in 23% yield as an off-white solid, which could not be further purified due to its insolubility in common solvents and high sublimation temperature. Crystallization from toluene gave **XXXVI** in 61% yield.

To obtain **ICz$_3$Tz** a threefold Suzuki cross coupling reaction of **30** and the boronic ester **6** was carried out analogously (Scheme C.18).

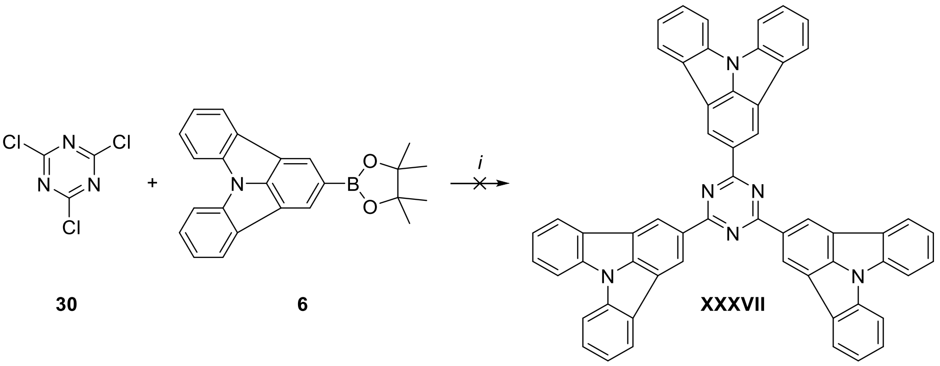

Scheme C.18: Synthesis strategy towards **ICz$_3$Tz** (**XXXVII**). *i*: THF, aq. K_2CO_3, $Pd(PPh_3)_4$, rf.

However, this reaction did not give the desired product even after reaction times of over one week. Alternatively, a stepwise approach was used. The S_NAr reaction of **30** and a lithiated ICz was investigated in order to obtain **XXXVIII** for subsequent cross coupling reactions with the boronic ester **6** (Scheme C.19).

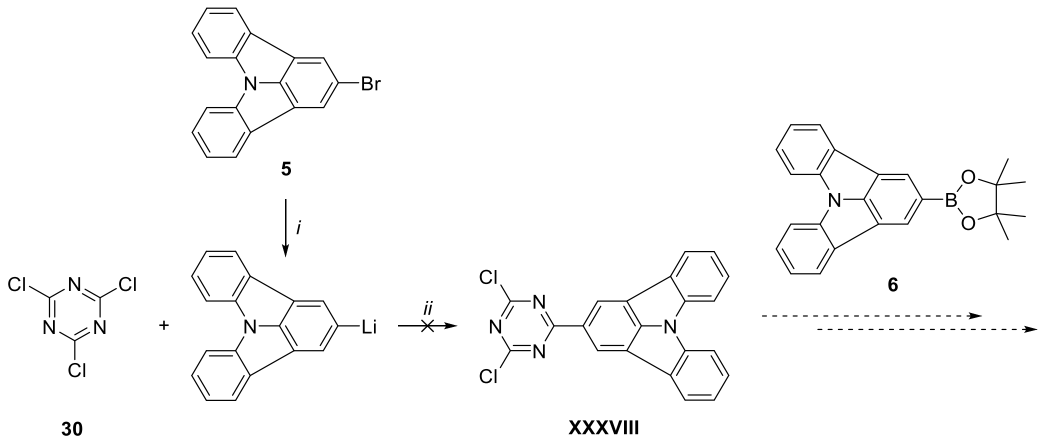

Scheme C.19: Synthesis of **XXXVIII** *via* lithiation of **5** and subsequent S_NAr. *i*: THF, -80 °C, *n*-BuLi *ii*: -80 °C → rt.

5 was cooled to -80 °C in dry THF under argon atmosphere. After addition of *n*-BuLi, the reaction mixture was stirred for 1 h giving a yellow slurry. The suspension was then transferred to a cooled solution of **30** in dry THF under argon using a syringe. The reaction mixture was then allowed to slowly warm to rt overnight. After workup, only **5** and dehalogenated ICz were obtained.

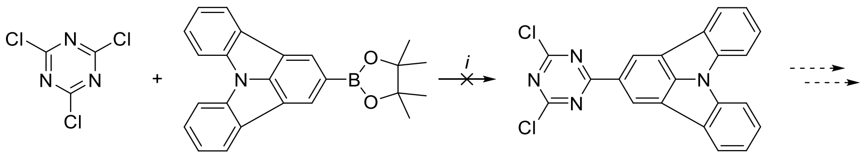

30 **6** **XXXVIII**

Scheme C.20: Synthesis of **XXXVIII** *via* Suzuki cross coupling reaction. *i*: THF, aq. K_2CO_3, $Pd(PPh_3)_4$, rf.

In the final approach a stepwise coupling reaction was investigated (Scheme C.20). **30** and **6** were suspended in degassed THF under argon atmosphere. $Pd(PPh_3)_4$ and aqueous K_2CO_3 were added under argon counterflow. The mixture was then refluxed overnight and the formed white precipitate was filtrated. However, ^{1}H NMR-spectroscopy revealed that the formed product was the hydrolyzed 1,3,5-triazine-2,4,6(1*H*,3*H*,5*H*)-trione.

Due to the decreasing solubility with increasing number of ICz units attached to the triazine core, the **ICz$_3$Tz** would probably be very difficult to purify. The accompanying high sublimation temperature would have further impeded purification. Therefore, further attempts to prepare **ICz$_3$Tz** were not investigated.

C.5.2 Characterization

In order to investigate the molecular properties of the developed materials, measurements of the most important properties were conducted and are discussed in this chapter. Results are summarized at the end of this chapter.

C.5.2.1 Absorption and fluorescence

Overall, the two synthesized ICz triazines show very similar absorption and emission spectra (Figure C.4). The absorption onsets can be observed at 385 and 390 nm for **ICzTz** and **ICz$_2$Tz**, respectively. Both spectra exhibit prominent absorption peaks below 300 nm, with maxima or shoulders around 290 nm, typical for the π-π* transition of the ICz moieties with a high contribution of the nitrogen electrons. Further redshifted, around 340 nm, the absorption bands for the ICz π-π* transition arising from the whole π-system can be observed.[15]

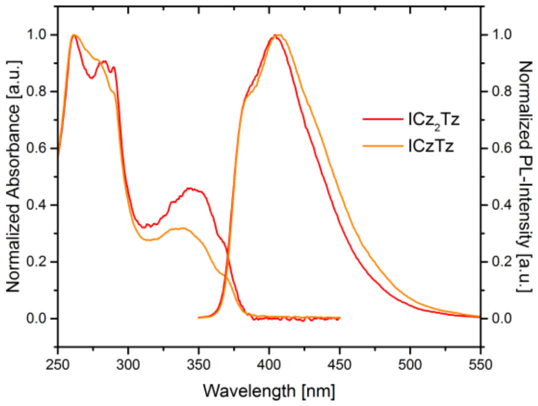

Figure C.4: Absorption and fluorescence spectra of **ICz$_2$Tz** and **ICzTz**. All spectra were recorded in DCM at a concentration of 5 nmol/ml and are normalized to 1.

The photoluminescence spectra obtained from DCM solutions show a prominent maximum at 409 (**ICzTz**) and 404 nm (**ICz$_2$Tz**). An additional shoulder can be observed around 380 nm.

C.5.2.2 Electrochemical analysis

The HOMO energy levels of the triazine based compounds were determined by cyclic voltammetry. They were estimated from the onsets of the oxidation peaks, relative to ferrocene and are located at -6.14 and -6.12 eV for **ICzTz** and **ICz$_2$Tz**, respectively. Both compounds exhibit irreversible oxidation, as typically observed for ICz materials.[14] Cyclic voltammograms are depicted in F.2.

C.5.2.3 Phosphorescence

The phosphorescence spectra of the two triazines look qualitatively the same (Figure C.5). Of the two most prominent peaks for each of the two substances, the first one is located at 435 nm, while the second one can be observed at 466 nm for both substances.

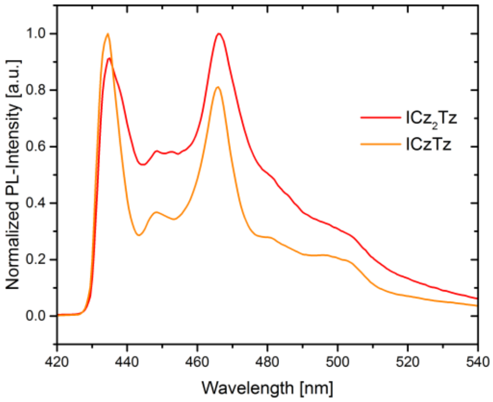

Figure C.5: Phosphorescence spectra of **ICz$_2$Tz** and **ICzTz** recorded in toluene at 77 K normalized to 1.

C.5.2.4 Summary

All results of the characterizations are summarized in Table 2. The rather high ΔE_{ST} values of around 0.55 eV make these two substances unsuited as TADF emitters. Nonetheless, the E_Ts of 2.85 eV make them good candidates for host materials for blue PhOLED devices. Also, the high thermal stability of these materials is superior compared to CBP.

Table 2: Physical data of target substances **ICzTz** and **ICz$_2$Tz**.

Substance	T_m [°C][a]	Opt. BG [eV][b,c]	$\lambda_{PL,max}$ [nm][c]	HOMO/LUMO [eV][d,e]	E_T [eV][f]	ΔE_{ST} [eV][g]
ICzTz	326	3.22	409	-6.14/-2.92	2.85	0.54
ICz$_2$Tz	409	3.18	404	-6.17/-2.99	2.85	0.55

[a] Determined from DSC analysis; T_m: melting point; no glass transition was observed.
[b] Determined from the absorption onset.
[c] Measured in DCM (5 mM) at rt.
[d] HOMO levels were calculated from cyclic voltammetry measurements.
[e] LUMO levels were calculated from HOMO levels and the optical bandgap.
[f] Estimated from the highest energy vibronic transition in solid solutions DCM:toluene:MeOH (10:10:1) at 77 K.
[g] Calculated from the onset of fluorescence and the first phosphorescence maximum.

C.5.3 Synthesis towards carbonyl compounds

The first approach to synthesize the symmetric ICz ketone aimed to form the secondary alcohol first followed by oxidation. To investigate the feasibility of those two reactions, they were initially carried out on the more readily available **33** (Scheme C.21).

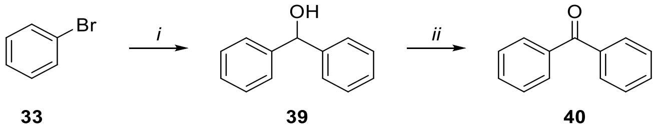

Scheme C.21: Synthesis of a symmetric aryl ketone from a brominated aromatic species. *i*: THF, -80 °C, 1. *n*-BuLi, 2. HCOOEt → rt. *ii*: toluene, MnO_2, rf.

33 in dry THF under argon atmosphere was cooled to -80 °C. After slow addition of *n*-BuLi, the reaction mixture was kept at -80 °C for 30 min and was then quenched with HCOOEt. Extraction with DCM followed by column chromatography gave **39** in 38% yield. The synthesis of **40** followed a modified protocol by Kamimura *et al.*[32] **39** and MnO_2 were suspended in 20 ml of toluene and heated to reflux. After complete conversion (GC-MS, 2.5 h), the reaction mixture was cooled to rt and filtrated over silica. The solvent was removed *in vacuo* giving **40** in 73% yield.

To synthesize the secondary alcohol **XLI**, an analogous reaction with the brominated ICz **5** was carried out (Scheme C.22). **5** was suspended in dry THF and cooled to -85 °C under argon atmosphere. After addition of *n*-BuLi, the reaction mixture was stirred at constant temperature for 45 min before being quenched with HCOOEt. It was then allowed to slowly warm to rt overnight. Extraction was carried out with aqueous NH_4Cl (10%) and DCM. The combined organic layers where then dried over anhydrous Na_2SO_4 and concentrated *in vacuo*. After column chromatography, only the starting material **5** and the unsubstituted ICz **4** could be identified by ^1H NMR spectroscopy. A possible explanation for the unsuccessful conversion might be the low solubilities of both the starting material **5** and the lithiated ICz, which forms a slurry in THF. It is therefore very difficult to stir the reaction mixture properly, especially when using small vessels. The fact that **5** could be isolated from the reaction mixture indicates incomplete lithiation.

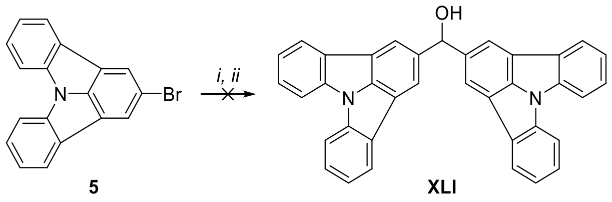

Scheme C.22: Synthesis strategy towards the secondary alcohol **XLI**. *i*: THF, -80 °C, 1. *n*-BuLi, 2. HCOOEt → rt. *ii*: 1. THF, Mg turnings, I_2, rf, 2. HCOOEt, rt.

As an alternative to the lithiated species, the Grignard reagent of ICz was considered as a possible nucleophile (Scheme C.22). Magnesium turnings and a catalytic amount of iodine were suspended in dry THF. **5** was also suspended in THF and added to the other suspension. Since no exothermal reaction was observed, the mixture was externally heated to reflux after complete addition. After some time, **5** completely dissolved leaving only suspended magnesium. After cooling to rt, HCOOEt was added and the reaction mixture was stirred overnight. Hot filtration and concentration *in vacuo* gave only **5** with no indication, that the Grignard reagent was formed under those conditions.

A different approach for the synthesis of **XLVI** used the acyl chloride **XLV** as an electrophile (Scheme C.23). This pathway also paved the way for further reactions employing **XLV**, such as the synthesis of the ICz-substituted oxadiazole as an interesting donor-acceptor molecule.

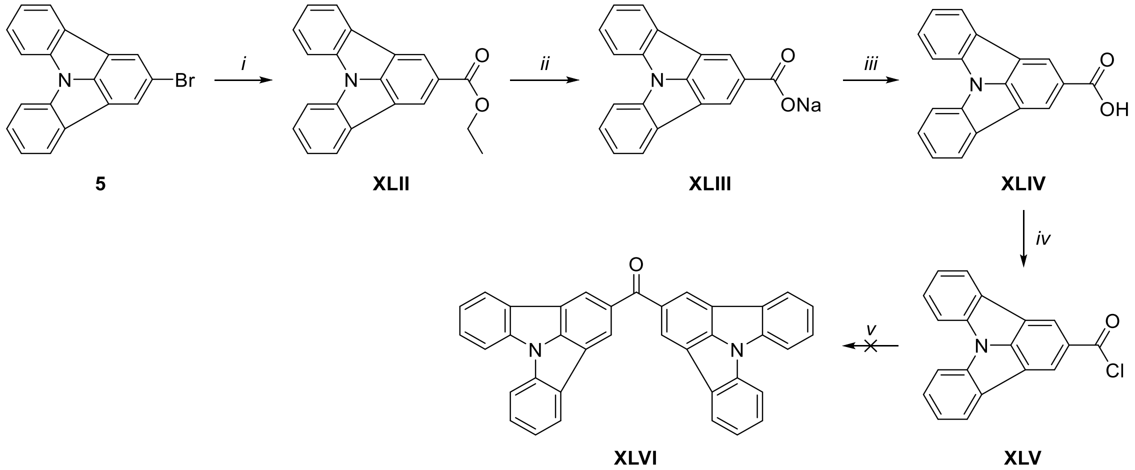

Scheme C.23: Synthesis towards the symmetric ICz ketone **XLVI**. *i*: THF, -80 °C, 1. *n*-BuLi, 2. ClCOOEt → rt. *ii*: THF:NaOH 2 M (1:1), rf. *iii*: THF:HCl 2 M (1:1), rf. *iv*: $SOCl_2$, rf. *v*: **5**, THF, -80 °C, 1. *n*-BuLi, 2. **XLV** → rt.

5 was suspended in dry THF under argon atmosphere and cooled to -80 °C. After addition of *n*-BuLi, the reaction mixture was stirred for 1 h. Excess ClCOOEt (3 eq.) was quickly added and the reaction mixture was allowed to slowly warm to rt over the weekend. THF and excess ClCOOEt were then removed *in vacuo*. After extraction with water and DCM, the crude product was crystallized from toluene yielding single crystals of **XLII** (F.1). The remaining toluene solution was concentrated *in vacuo* and further purified by column chromatography giving the ester **XLII** in 67% overall yield. For the hydrolysis **XLII** was refluxed in in THF:NaOH 2 M (1:1) under argon atmosphere. After full conversion (TLC, 96 h), the reaction mixture was allowed to slowly cool to rt, the aqueous layer was carefully removed and afterwards the crystallized product was filtrated. The THF filtrate was then concentrated *in vacuo* and crystallized from THF:NaOH, giving the sodium salt **XLIII** in 93% overall yield. Acidification was carried out by suspending **XLIII** in THF:HCl 2 M (1:1) and heating to reflux for 1 h. After cooling to rt, the suspension was filtrated giving the carboxylic acid **XLIV** in 82% yield. The synthesis of the acyl chloride **XLV** was carried out as a modification of the protocol by Kautny.[21] **XLIV** was suspended in $SOCl_2$ with a catalytic amount of DMF. After refluxing for 20 min, the solid completely dissolved. The solution was kept at reflux overnight and after cooling to rt was concentrated *in vacuo* giving **XLV** as a yellow solid in quantitative yield.

Since the acyl chloride **XLV** is a stronger electrophile than the ketone **XLVI**, the reaction with the lithiated ICz should give the ketone in a stoichiometric reaction. **5** was suspended in dry THF under argon atmosphere and cooled to -80 °C. After addition of *n*-BuLi, the reaction mixture was stirred for 1 h. Because **XLV** did not dissolve in reasonable amounts of THF, it was added as a suspension under argon counterflow. The mixture was allowed to slowly warm to rt over the weekend. The yellow suspension consisted mainly of an insoluble product, which could not be extracted with water and DCM. The filtrated solid also showed extremely low solubility in $CHCl_3$, DMSO, AcOH (solution turning dark violet), toluene and pyridine. The strong coloration of the suspension in AcOH and ^1H NMR of the crude product strongly indicated the formation of the tertiary alcohol instead of the ketone **XLVI**. Because of insufficient solubility of the acyl chloride, probably only the surface of the particles could react, which in turn had excess of the lithiated species available to react with giving the alcohol instead of the ketone.

Due to the solubility issues of the acyl chloride **XLV** the synthesis of the previously mentioned oxadiazole was not carried out.

Another approach to synthesize a ketone substituted ICz is the application of a carbonitrile as a precursor for the keto-functionality. Henry *et al*. already synthesized **49** *via* flash vacuum pyrolysis of the corresponding nitro-compound.[33] Due to the lack of an appropriate furnace and in order to further investigate the scope of the C-H activation reaction with NHC-lig., **49** was synthesized from the brominated substrate **XLVIII** (Scheme C.24).

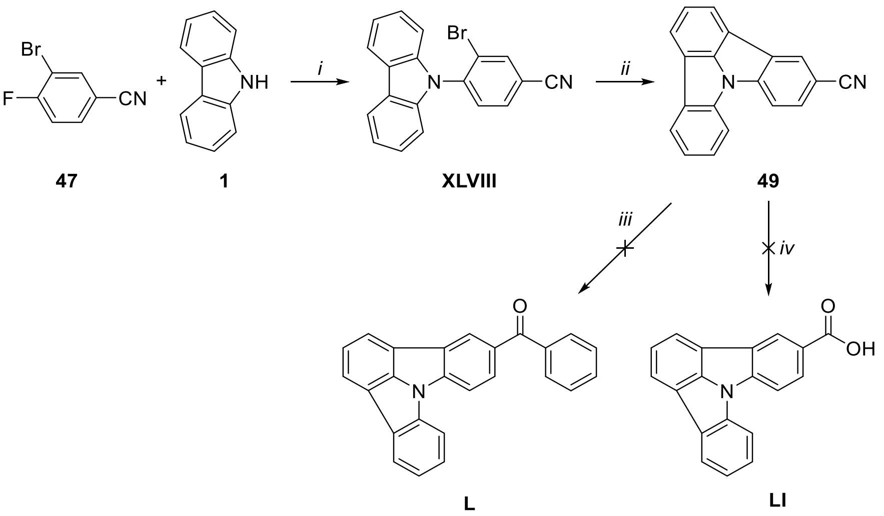

Scheme C.24: Syntheses of the ICz nitrile **49**. *i*: DMSO, Cs_2CO_3, 120 °C. *ii*: DMA, K_2CO_3, $Pd(OAc)_2$, NHC-lig., 130 °C. *iii*: bromobenzene, THF, -80 °C, 1. *n*-BuLi, 2. **49** → rt. *iv*: EtOH:NaOH 20% (1:3), 100 °C.

The synthesis of **XLVIII** was carried out analogously to previous S_NAr reactions as a modification of the protocol by Bintinger.[19] **1**, **47** and Cs_2CO_3 (1.1 eq.) were suspended in DMSO and heated to 120 °C until full conversion (TLC, 6 h). After cooling to rt, the reaction mixture was poured on water and the precipitating crude product was filtrated. Column chromatography and subsequent crystallization from EtOH gave **XLVIII** in 35% yield. In this reaction, the fluoroaryl is the limiting component. Fewer equivalents of **1** could have improved the yield percentage, but would have probably given a smaller absolute yield. Subsequent C-H activation using NHC-lig. and $Pd(OAc)_2$ in DMA with K_2CO_3 as a base gave **49** in 97% yield.

To explore the applicability of **49** as electrophile, the reaction of **49** with phenyllithium was investigated. For the synthesis of the ketone **L**, bromobenzene was dissolved in dry THF and cooled to -80 °C. After addition of *n*-BuLi, the reaction mixture was stirred for 1 h. **49** was then added under argon counterflow and the reaction was allowed to warm to rt overnight. After workup, only the nitrile **49** was isolated.

The next step was the hydrolysis of **49,** carried out as a modification of the protocol reported by Natera *et al*.[34] **49** was heated to 100 °C in a mixture of EtOH:NaOH 20% (1:3) and stirred for 72 h. A reddish-brown precipitate formed between the two liquid layers and was filtrated. Characterization by ^{1}H-NMR spectroscopy, however, could not confirm the formation of **LI**.

C.6 Synthesis of the highly annulated ring system LIV

Finally, the applicability of the C-H activation in the preparation of an extended planar π-system was investigated (Scheme C.25). With its large planar π-electron system, **BDPDCz** (**LIV**) could be an excellent hole transporting material for the use in OLEDs. As a matter of fact, **LIV** has already been isolated by Niebel *et al.* as a byproduct in the preparation of a similar substance.[35]

In the first step, **1** and **52** were suspended in DMSO and heated to 120 °C for 48 h. The mixture was then cooled to rt, poured on water and the crude product was filtrated. Refluxing in ACN followed by crystallization from toluene gave **LIII** as off-white crystals in 40% yield (F.1).[36] Subsequent C-H activation of **LIII** was carried out using NHC-lig. and Pd(OAc)$_2$ in DMA with K$_2$CO$_3$ as a base. The reaction mixture was heated to 130 °C overnight. The precipitated product was then filtrated and crystallized from nitrobenzene giving **LIV** as green crystals in 81% yield (F.1).

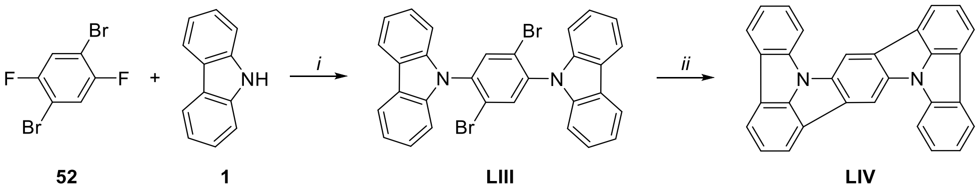

Scheme C.25: Two-step synthesis towards **LIV**. *i*: DMSO, Cs$_2$CO$_3$, 120 °C. *ii*: DMA, K$_2$CO$_3$, Pd(OAc)$_2$, NHC-lig., 130 °C.

Through two-sided C-H activation **LIV** could be obtained, forming a rather complex molecule in just two reaction steps with good yields. **LIV** is the only target molecule in this thesis not containing a substituted ICz. It can, however, be regarded as a fused ICz dimer with a shared benzene ring at the center. Indeed, the molecule is fully planar (F.1) and exhibits π-stacking, therefore potentially showing good charge carrier transport properties.

C.6.1 Characterization

In order to investigate the molecular properties of the developed materials, measurements of the most important properties were conducted and are discussed in this chapter. Results are summarized at the end of this chapter.

C.6.1.1 Absorption and fluorescence

The absorption spectrum of **BDPDCz** shows similar characteristics as 9*H*-carbazole and ICz moieties around 300 nm, which can be attributed to a π-π* transition of ICz with a high contribution of the nitrogen electrons (Figure C.6). Another prominent peak can be observed at 356 nm, characteristic for a π-π* transition of an ICz moiety incorporating a substantial portion of the π-system. Additionally, π-π* transitions are observed at longer wavelengths (380-430 nm), which can be attributed to contributions of orbitals which are located over the whole molecule. The absorption onset is located at 435 nm and thus shows the lowest optical bandgap of all target substances. The fluorescence spectrum obtained from a DCM solution only showed one rather narrow prominent peak with a maximum at 431 nm.

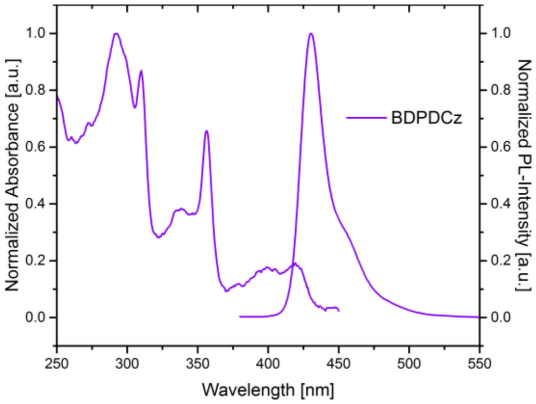

Figure C.6: Absorption and fluorescence spectra of **BDPDCz**. All spectra were recorded in DCM at a concentration of 5 nmol/ml and are normalized to 1.

Unexpectedly, the fluorescence spectrum of a prepared thin film (dried droplets from a saturated DCM solution) only featured very small additional peaks in the low-energy part of the spectrum, indicating only negligible intermolecular interactions (Figure C.7). When the substance was instead sublimated onto a glass slide, just one rather narrow peak with a maximum at 478 nm was observed, a sign of the formation of a very amorphous layer. This observation was rather unexpected due to the strong π-π stacking in the crystal. Due to this narrow emission, **BDPDCz** might be suited as a blue emitter in OLEDs.

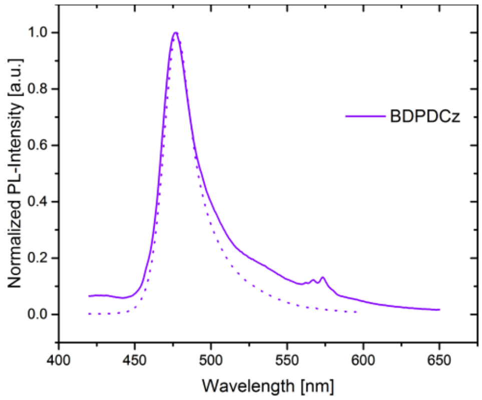

Figure C.7: Fluorescence spectra of **BDPDCz** from a drop casted thin film (continuous line) and a sublimated thin film (dotted line) normalized to 1.

C.6.1.2 Electrochemical analysis

The HOMO energy level of **BDPDCz** was determined by cyclic voltammetry. It was estimated from the onset of the oxidation peak, relative to ferrocene and is located at -5.42 eV. This compound also exhibits irreversible oxidation, as typically observed for carbazole and ICz materials.[14] The corresponding cyclic voltammogram is depicted in F.2.

C.6.1.3 Phosphorescence

The phosphorescence spectrum of **BDPDCz** is well-resolved and shows a prominent maximum at 483 nm (Figure C.8). The E_T determined from this highest vibronic transition was calculated to be 2.57 eV, which is rather high for such an extended π-system.

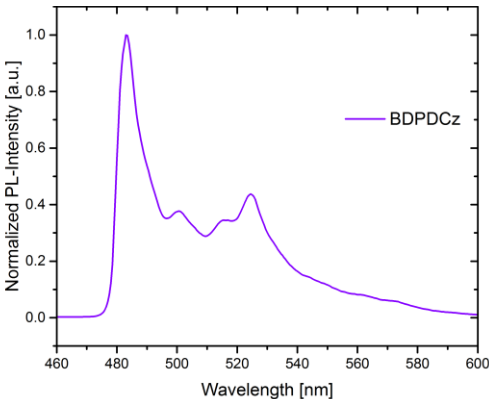

Figure C.8: Phosphorescence spectrum of **BDPDCz** recorded in toluene at 77 K normalized to 1.

C.6.1.4 Summary

All results of the characterizations are summarized in Table 2. The rather narrow emission around 478 nm makes this substance interesting as a possible blue emitter. Furthermore, the low bandgap could allow for low driving voltages and therefore high device efficiencies. Like the previous target materials, this substance shows high thermal stability compared to CBP.

Table 3: Physical data of the target substance **BDPDCz**.

Substance	T_m [°C][a]	Opt. BG [eV][b,c]	$\lambda_{PL,max}$ [nm][c]	HOMO/LUMO [eV][d,e]	E_T [eV][f]	ΔE_{ST} [eV][g]
BDPDCz	423	2.85	431	-5.42/2.57	2.57	0.43

[a] Determined from DSC analysis; T_m: melting point; no glass transition was observed.
[b] Determined from the absorption onset.
[c] Measured in DCM (5 mM) at rt.
[d] HOMO levels were calculated from cyclic voltammetry measurements.
[e] LUMO levels were calculated from HOMO levels and the optical bandgap.
[f] Estimated from the highest energy vibronic transition in solid solutions DCM:toluene:MeOH (10:10:1) at 77 K.
[g] Calculated from the onset of fluorescence and the first phosphorescence maximum.

C.7 Final purification and device fabrication

Final purification of the products prior to investigation in prototype devices was achieved by sublimation in a custom high vacuum setup described in Scheme C.26. It consisted of a Leybold Turbovac 50 turbomolecular pump (P_1) with a Turbotronic NT 10 frequency converter, a zeolite drying column, a rotary vane vacuum pump (P_2) and a Balzers Compact FullRange Gauge TPG 251 sensor (P) with a SingleGauge TPG 251 measurement unit. The different temperatures and pressures used for sublimation are summarized in Table 4.

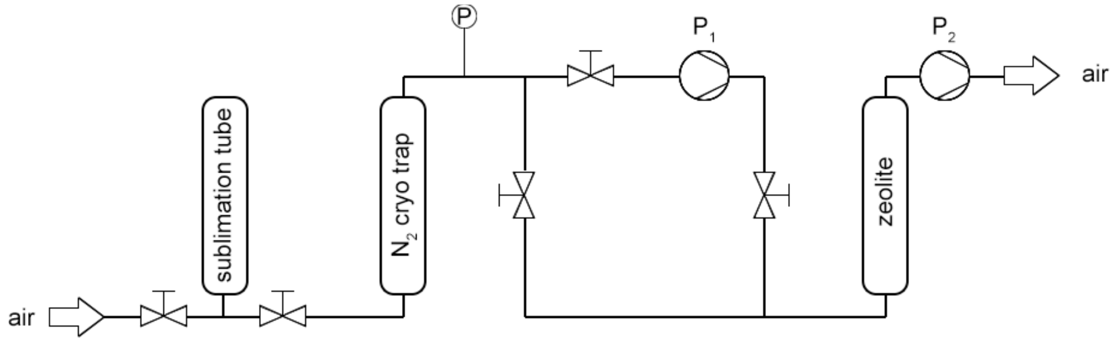

Scheme C.26: Setup for sublimation of the target substances. P: pressure sensor. P_1: turbomolecular pump. P_2: rotary vane vacuum pump.

Table 4: Summary of the sublimation temperatures and pressures of the final products.

Substance	Temperature [°C]	Pressure [Torr]
5CzICz	255	$4.0\cdot10^{-6}$
Cz$_2$ICz	n.d.[b]	n.d.[b]
Cz$_3$ICz[a]	300	$1.5\cdot10^{-6}$
ICzPCz	280	$6.0\cdot10^{-6}$
ICzICz	300	$1.0\cdot10^{-6}$
ICzTz	270	$6.0\cdot10^{-6}$
ICz$_2$Tz[a]	300	$2.6\cdot10^{-6}$
BDPDCz	300	$1.6\cdot10^{-6}$

[a] No sublimation observed. [b] Not determined.

Recorded pressures are of course specific for this particular setup due to the path length between recipient and pressure sensor. Not all substances could be sublimated due to high sublimation temperatures. It has to be noted though, that none of the substances showed thermal decomposition at these temperatures.

In order to characterize the viability of the synthesized substances as host materials, prototype OLED devices were fabricated and characterized by Chenyang Zhao in the Ma research group at the Changchun Institute of Applied Chemistry of the Chinese Academy of Sciences.

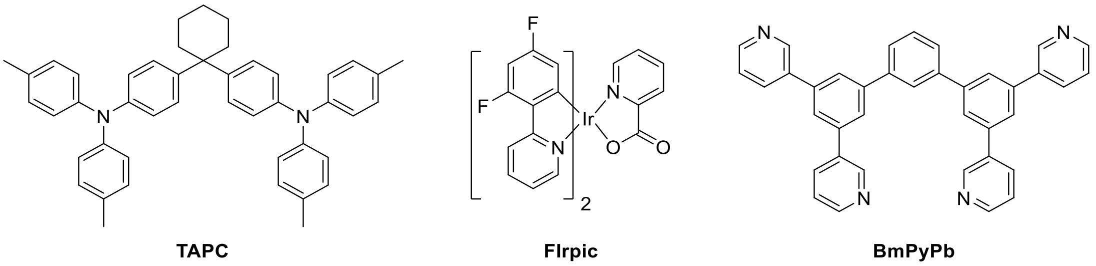

Scheme C.27: Molecular structures materials used for the first device series.

The first devices (**1B** series) used the blue phosphorescent emitter FIrpic. The architecture ITO / MoO_3 (8 nm) / TAPC:MoO_3 (50 nm, 20%) / TAPC (30 nm) / X:FIrpic (10 nm, 10%) / BmPyPb (10 nm) / BmPyPb:Li_2CO_3 (30 nm, 3%) / Li_2CO_3 / Al (200 nm) was used employing the three different CzICz derivatives as host materials: X = **5CzICz** (**1B1**), **Cz$_2$ICz** (**1B2**) and **Cz$_3$ICz** (**1B3**). Current density – voltage – brightness – efficiency characteristics of all devices are given in F.3, results are summarized in Table 5.

Devices **1B1**, **1B2** and **1B3** show similar performances with maximum current efficiencies of 29.8, 27.5 and 24.6 cd A^{-1}, maximum power efficiencies of 33.4, 32.4 and 27.6 lm W^{-1} and maximum external quantum efficiencies of 14.7, 13.4 and 12.0%, respectively. Furthermore, the turn-on voltage of 2.6 V for the three devices is rather low.

Table 5: Results from the first series of prototype devices measured at a brightness of 100 cd m^{-2} / 1000 cd m^{-2} / 5000 cd m^{-2} / max.

Device	V_{on} [V]^a	L_{max} [cd m^2]^b	CE [cd A^{-1}]^c	PE [lm W^{-1}]^d	EQE [%]
1B1	2.6	32112	28.5/22.7/18.4/29.8	30.7/20.2/12.2/33.4	14.0/11.1/9.1/14.7
1B2	2.6	17902	27.3/21.7/16.1/27.5	30.5/20.6/11.3/32.4	13.3/10.6/7.9/13.4
1B3	2.6	19556	24.4/22.4/18.0/24.6	27.4/20.9/13.2/27.6	11.9/10.9/8.8/12.0

^{a} Turn on voltage. ^{b} Maximum luminance. ^{c} Current efficiency. ^{d} Power efficiency.

After these promising results, a second series containing red (**2R**), green (**2G**) and blue (**2B**) devices was fabricated. The three slightly different architectures employed were: ITO / MoO_3 (8 nm) / TAPC (75 nm) / X:Ir(MDQ)$_2$(acac) (12 nm, 5%) / Bphen (70 nm) / LiF / Al for red devices, ITO / MoO$_3$ (8 nm) / TAPC (60 nm) / X:Ir(ppy)$_2$(acac) (12 nm, 8%) / Bphen (60 nm) / LiF / Al for green devices and ITO / MoO$_3$ (8 nm) / TAPC (50 nm) / X:FIrpic (15 nm, 10%) / Bphen (45 nm) / LiF / Al for blue devices. Again, the three CzICz derivatives were used as host materials in each of the devices: X = **5CzICz** (**2R1, 2G1, 2B1**), **Cz$_2$ICz** (**2R2, 2G2, 2B2**) and **Cz$_3$ICz** (**2R3, 2G3, 2B3**). Current density – voltage – brightness – efficiency characteristics of all devices are given in F.3, results are summarized in Table 6.

While the new blue devices **2B1**, **2B2** and **2B3** did not perform as well as previous ones (**1B** series) with maximum current efficiencies of 22.6, 24.2, 18.9 cd A^{-1} and maximum power efficiencies of 18.0, 21.5 and 20.6 lm W^{-1}, red and green devices showed particularly good results. Red devices **2R1**, **2R2** and **2R3** exhibited maximum current efficiencies of 32.7, 30.0 and 24.9 cd A^{-1}, maximum power efficiencies of 31.0, 29.3 and 25.2 lm W^{-1} and maximum external quantum efficiencies of 20.2, 20.4 and 17.6%, respectively. Furthermore, external quantum efficiencies at high luminosities (5000 cd m^{-2}) were significantly higher than for blue devices. Green devices **2G1**, **2G2** and **2G3** exhibited maximum current efficiencies of 78.0, 81.0 71.8 cd A^{-1}, maximum power efficiencies of 76.3, 87.4 and 62.2 lm W^{-1} and maximum external quantum efficiencies of 20.8, 21.5 and 19.2%, respectively. These devices exhibited consistently high efficiencies with no significant roll-off up to 5000 cd m^{-2}.

Table 6: Results from the second series of prototype devices measured at a brightness of 100 cd m^{-2} / 1000 cd m^{-2} / 5000 cd m^{-2} / max.

Device	V$_{on}$ [V][a]	L$_{max}$ [cd m^{2}][b]	CE [cd A^{-1}][c]	PE [lm W^{-1}][d]	EQE [%]
2R1	2.8	47220	32.5/30.8/27.1/32.7	25.0/15.9/10.1/31.0	20.1/18.7/16.1/20.2
2R2	2.8	47685	29.9/29.0/25.7/30.0	24.0/15.3/9.6/29.3	20.2/19.5/17.0/20.4
2R3	2.8	42324	24.8/23.2/20.4/24.9	19.1/11.7/7.5/25.2	17.5/16.3/14.2/17.6
2G1	2.6	48030	74.6/77.9/75.1/78.0	74.8/57.9/42.4/76.3	19.9/20.8/20.0/20.8
2G2	2.6	48023	79.9/79.4/75.6/81.0	82.5/59.3/42.4/87.4	21.2/21.1/20.1/21.5
2G3	2.6	48710	61.3/69.1/69.7/71.8	60.0/48.6/38.3/62.2	16.4/18.5/18.7/19.2
2B1	2.8	29987	19.6/22.1/18.9/22.6	16.9/13.5/8.5/18.0	n.d.[e]
2B2	2.8	24102	23.4/23.8/20.7/24.2	20.2/14.4/9.0/21.5	n.d.[e]
2B3	2.8	18170	17.9/15.1/11.9/18.9	15.2/8.6/4.7/20.6	n.d.[e]

[a] Turn on voltage. [b] Maximum luminance. [c] Current efficiency. [d] Power efficiency. [e] Not determined.

C.8 Summary and outlook

In the course of this thesis, novel aromatic substances based on the ICz scaffold were synthesized. All of them showed a high triplet energy of approximately 2.8 eV arising from a localized triplet state on the ICz unit, which makes them well-suited as host materials for blue phosphorescent emitters, such as FIrpic and Fir6.

The impact of different substitution patterns of carbazole-indolo[3,2,1-*jk*]carbazole derivatives was investigated with regard to the extent of excimer formation. The newly developed substances showed decreased intermolecular interactions compared to the parent compounds, as evidenced by the respective emission spectra of thin films of the materials. As a result, prototype red, green and blue PhOLED devices showed improved efficiencies due to the inhibited excimer formation. Furthermore, **ICzICz** and **ICzPCz** have been synthesized for future investigation of the excimer formation in OLED devices.

The preparation of bipolar materials, such as ICz substituted triazines and carbonyl compounds, proved to be challenging due to sensitivity against hydrolysis and low solubility of intermediates and precursors. Nonetheless, the two triazines **ICzTz** and **ICz$_2$Tz** could be synthesized. While their ΔE_{ST} is too large for TADF, the high E_Ts still make them promising candidates for host materials.

Furthermore, the scope of the C-H activation reaction employing NHC-lig. with $Pd(OAc)_2$ was extended to novel substrates. Ring closure occurred in the presence of nitro- and nitrile-groups and two sided reactions were performed on a dihalogenated triarylamine and a dibromo-benzene derivative. Furthermore, all precursors for the C-H activation could be reliably synthesized *via* S_NAr reactions. Additionally, the concept to synthesize large π-systems proved to be very feasible, paving the way for the preparation of novel highly annulated ring systems.

Future research will focus on the improvement of the solubility of bipolar materials, since sufficient solubility will greatly facilitate workup and enhance processability. One way to achieve this goal is the introduction of alky chains to the molecules. Furthermore, an increased solubility will allow for the investigation of a large variety of acceptor units, such as oxadiazole, in order to tune the electronic and physical properties.

D Experimental part

D.1 General remarks

Unless explicitly mentioned otherwise, all reagents from commercial suppliers were used without further purification. Anhydrous solvents like DCM and THF were absolutized by the PURESOLV-system from Innovative Technology Inc. Other anhydrous solvents were purchased from commercial suppliers. The commercially available lithiation reagent *n*-BuLi was used without additional quantitative analyses, using the declared value.

D.2 Chromatographic methods

D.2.1 Thin layer chromatography

Thin layer chromatography (TLC) was performed using TLC-aluminum foil (Merck, silica 60 F_{254}).

D.2.2 Column chromatography

Preparative column chromatography was performed using a BÜCHI Sepacore flash system which was equipped with the following components:

Pump system:	BÜCHI pump modules C-605 (2 units) BÜCHI pump manager C-615
Detector:	BÜCHI UV photometer C-635
Fraction collector:	BÜCHI fraction collector C-660

The appropriate PP-cartridges were packed with silica (Merck, 40-63 µm).

D.3 Analytical methods

D.3.1 GC-MS measurements

GC-MS measurements were conducted using a GC-MS interface from Thermo Scientific:

- TRACE 1300 Gas Chromatograph with a Restek Rxi-5Sil MS column (l=30 m, ID=0.25 mm, 0.25 µm film, achiral).
- ISQ LT Single Quadrupole Mass Spectrometer (electron ionization).

D.3.2 HR-MS measurements

HR-MS analysis was carried out (methanol solutions, 10 ppm) using a HTC PAL system autosampler (CTC Analytics AG, Zwingen, Switzerland), an Agilent 1100/1200 HPLC with binary pumps, a degasser and a column thermostat (Agilent Technologies, Waldbronn, Germany) and an Agilent 6230 AJS ESI–TOF mass spectrometer (Agilent Technologies, Palo Alto, United States).

D.3.3 NMR-Spectroscopy

NMR spectra were recorded using a Bruker Avance DPX-200 MHz (200 MHz for ^{1}H), DRX-400 MHz (400 MHz for ^{1}H; 100 MHz for ^{13}C) or DRX-600 MHz (600 MHz for ^{1}H; 150 MHz for ^{13}C) Fourier transform spectrometer. ^{1}H- and ^{13}C-spectra are given as stated: chemical shift in parts per million (ppm) referenced to the according solvent (^{1}H: $CDCl_3$ δ=7.26 ppm, CD_2Cl_2 δ=5.32 ppm, DMSO-d_6 δ=2.50 ppm; ^{13}C: $CDCl_3$ δ=77.0 ppm, CD_2Cl_2 δ=54.0 ppm, DMSO-d_6 δ=39.5 ppm) with tetramethylsilane (TMS) at δ=0 ppm. Multiplicities of the signals are given as: ^{1}H: s=singlet, d=doublet, t=triplet and m=multiplet.

D.3.4 Single crystal diffraction

Single crystal structures were determined in collaboration with Dr. Berthold Stöger and the Institute of Chemical Technologies and Analytics, Division of Structural Chemistry. All data were collected on an APEX II diffractometer with κ geometry, equipped with a CCD detector using Mo K_α irradiation at 100 K in a dry stream of nitrogen.

D.3.5 Cyclic voltammetry

Cyclic voltammetry was performed using a three-electrode configuration consisting of a Pt or ITO working electrode, a Pt counter electrode and a Ag/AgCl reference electrode and a PGSTAT128N potentiostat provided by Metrohm Autolab B.V. Measurements were carried out in a 0.5 mM or saturated (for poorly soluble substances) solution in anhydrous DCM (oxidation scan) or ACN (reduction scan) with Bu_4NBF_4 (0.1 M) as supporting electrolyte. The solutions were purged with nitrogen for 15 min prior to measurement. HOMO and LUMO energy levels were calculated from the onset of oxidation and reduction, respectively. The onset potential was determined by the intersection of two tangents drawn at the background and the rising of oxidation or reduction peaks. Ferrocene was used for potential calibration.

D.3.6 Absorption spectroscopy

Absorption spectra were recorded on a Thermo Scientific NanoDrop One^{c} Microvolume UV-Vis spectrophotometer in degassed DCM solution (5 µM).

D.3.7 Fluorescence and phosphorescence spectroscopy

Fluorescence and phosphorescence spectra were recorded on a PerkinElmer LS 55 Fluorescence spectrometer. For fluorescence measurements 5 µM degassed solutions in DCM were used. Phosphorescence spectra of 2.5 µM solutions in degassed DCM:toluene:MeOH (10:10:1) were recorded at 77 K.

D.4 Synthesis and characterization of the compounds

Detailed experimental procedures for the synthesis of each compound as well as their characterization are presented in the following chapter.

D.4.1 Synthesis of basic building blocks

9-(2-Bromophenyl)-9*H*-carbazole (3)

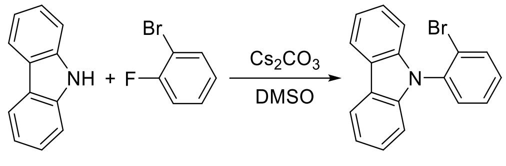

1	2	3
$C_{12}H_9N$	C_6H_4BrF	$C_{18}H_{12}BrN$
167.21	175.00	322.21

The synthesis of **3** followed a protocol by Bintinger.[19] **1** (30.10 g, 180 mmol, 1.0 eq.), **2** (31.50 g, 180 mmol, 1.0 eq.) and Cs_2CO_3 (70.38 g, 216 mmol, 1.2 eq.) were suspended in 250 ml of DMSO and heated to 130 °C for 48 h. Since no full conversion was reached, additional Cs_2CO_3 (5.87 g, 18 mmol, 0.1 eq.) was added. After a total of 72 h, the reaction mixture was cooled to rt, poured on 500 ml of water and the precipitating crude product was filtrated. **3** (50.19 g, 156 mmol, 87%) was obtained after crystallization from EtOH as pale yellow crystals. Colorless crystals for single crystal diffraction were obtained after a second crystallization step (F.1).

^{1}H NMR (400 MHz, $CDCl_3$, FID TSC118/10): δ=8.16 (d, J=7.7 Hz, 2H), 7.87 (dd, J=8.0, 1.4 Hz, 1H), 7.57-7.48 (m, 2H), 7.45-7.39 (m, 3H), 7.32-7.28 (m, 2H), 7.07 (d, J=8.2 Hz, 2H) ppm.

Indolo[3,2,1-*jk*]carbazole (4)

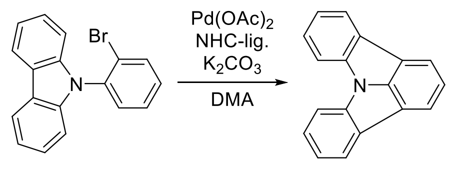

3	4
$C_{18}H_{12}BrN$	$C_{18}H_{11}N$
322.21	241.29

The synthesis of **4** followed a protocol by Bintinger.[19] **3** (49.9 g, 155 mmol, 1 eq.) and K_2CO_3 (42.8 g, 310 mmol, 2 eq.) were suspended in degassed DMA (500 ml, 1000 ppm water content) under argon atmosphere. Subsequently, NHC-lig. (1.32 g, 3.1 mmol, 0.02 eq.) and $Pd(OAc)_2$ (0.70 g, 3.1 mmol, 0.02 eq.) were added under argon counterflow. The reaction mixture was then heated to 130 °C until full conversion (TLC, GC-MS, 18 h) and cooled to rt. It was then poured on water and repeatedly extracted with DCM. The combined organic layers were dried over anhydrous Na_2SO_4 and further purified by flash filtration over silica. Removal of the solvent *in vacuo* gave **4** (37.5 g, 155 mmol, 100%) as a beige solid. ^1H NMR (400 MHz, $CDCl_3$, FID TSC134/20): δ=8.16 (ddd, J=7.8, 1.2, 0.8 Hz, 2H), 8.06 (d, J=7.4 Hz, 2H), 7.93 (d, J=8.2 Hz, 2H), 7.62-7.55 (m, 3H), 7.37 (td, J=7.6, 1.1 Hz, 2H) ppm.

2-Bromoindolo[3,2,1-*jk*]carbazole (5)

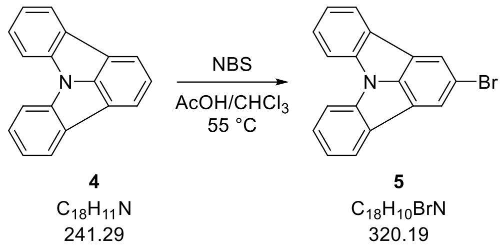

The synthesis of **5** followed a protocol by Kautny.[21] **4** (4.34 g, 18.0 mmol, 1.00 eq.) was suspended in 100 ml of AcOH:$CHCl_3$ (1:1) and heated to 55 °C. NBS (3.36 g, 18.9 mmol, 1.05 eq.) was added in small portions over 1 h. The reaction mixture was stirred at rt overnight and then filtrated. The solid crude product was refluxed in ACN and filtrated yielding **5** (2.40 g, 7.5 mmol, 42%) as a white solid. ^1H NMR (400 MHz, $CDCl_3$, FID TSC123/40): δ=8.12 (s, 2H), 8.04 (d, J=7.8 Hz, 2H), 7.85 (d, J=8.1 Hz, 2H), 7.56 (td, J=7.8, 1.2 Hz, 2H), 7.35 (td, J=7.6, 0.9 Hz, 2H) ppm.

2-(4,4,5,5-Tetramethyl-1,3,2-dioxaborolan-2-yl)indolo[3,2,1-*jk*]carbazole (6)

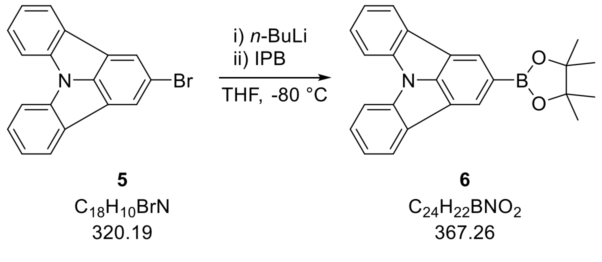

The synthesis of **4** followed a protocol by Bintinger.[19] **5** (11.21 g, 35 mmol, 1.0 eq.) was suspended in 200 ml of dry THF under argon atmosphere. After cooling to -80 °C, *n*-BuLi (15.6 ml, 2.5 M in hexanes, 39 mmol, 1.1 eq.) was added slowly giving an orange slurry. After 1 h, IPB (7.82 g, 42 mmol, 1.2 eq.) was added and the reaction mixture was allowed to slowly warm to rt overnight. After removal of the THF *in vacuo*, the crude yellow oil was distributed between aqueous NH_4Cl (10%) and DCM and the aqueous layer was repeatedly extracted. The combined organic layers were dried over anhydrous Na_2SO_4 and the solvent was removed *in vacuo*. The obtained beige solid was then refluxed in 250 ml of ACN, filtrated and dried yielding **6** (9.43 g, 26 mmol, 73%) as a white solid. Further purification was achieved by crystallization from toluene. ^1H NMR (400 MHz, $CDCl_3$, FID TSC125/40): δ=8.58 (s, 2H), 8.14 (d, J=7.7 Hz, 2H), 7.91 (d, J=8.0 Hz, 2H), 7.56 (td, J=7.8, 1.2 Hz, 2H), 7.37 (td, J=7.6, 0.8 Hz, 2H), 1.46 (s, 12H) ppm.

D.4.2 Synthesis of 5CzICz

9-(2,4-Dibromophenyl)-9*H*-carbazole (VIII)

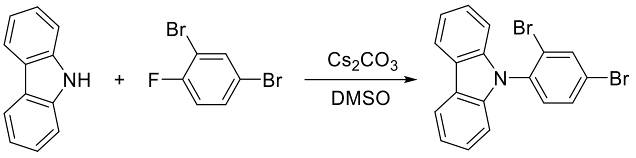

1 $C_{12}H_9N$ 167.21 **7** $C_6H_3Br_2F$ 253.90 **VIII** $C_{18}H_{11}Br_2N$ 401.10

The synthesis of **VIII** was carried out as a modification of the protocol by Bintinger.[19] **1** (0.84 g, 5.0 mmol, 1.0 eq.), **7** (1.27 g, 5.0 mmol, 1.0 eq.) and Cs_2CO_3 (1.79 g, 5.5 mmol, 1.1 eq.) were suspended in 25 ml of DMSO and heated to 120 °C until full conversion (TLC, 6 h). The reaction mixture was then poured on 100 ml of water and the precipitating crude product was filtrated. Column chromatography (light petroleum:DCM 92:8) yielded **VIII** (1.05 g, 2.6 mmol, 52%) as a colorless solid. Single crystals of **VIII** were obtained by crystallization from ACN (F.1). ^1H NMR (200 MHz, $CDCl_3$, FID TSC108/50): δ=8.15 (d, J=7.7 Hz, 2H), 8.03 (d, J=2.2 Hz, 1H), 7.67 (dd, J=8.4, 2.2 Hz, 1H), 7.46-7.26 (m, 5H), 7.06 (d, J=7.9 Hz, 2H) ppm.

9-(2-Bromo-4-9*H*-carbazol-9-ylphenyl)-9*H*-carbazole (XI)

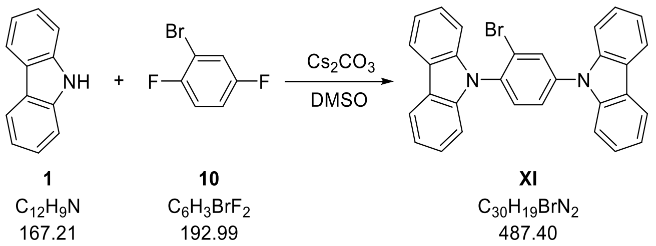

The synthesis of **XVII** was carried out as a modification of the protocol by Bintinger.[19] **1** (8.36 g, 50 mmol, 2.0 eq.), **10** (4.83 g, 25 mmol, 1.0 eq.) and Cs_2CO_3 (19.55 g, 60 mmol, 2.4 eq.) were suspended in 25 ml of DMSO and heated to 120 °C for 48 h (TLC, no further conversion). Since no full conversion was observed after 48 h, additional Cs_2CO_3 (1.63 g, 5 mmol, 0.2 eq.) was added. After 72 h, the reaction mixture was cooled to rt, poured on 200 ml of water and the precipitating crude product was filtrated. **XI** (5.58 g, 11 mmol, 46%) was obtained as a colorless solid after column chromatography (light petroleum:DCM 85:15 → 83:17). ^{1}H NMR (600 MHz, CD_2Cl_2, FID TSC111/40): δ=8.22-8.20 (m, 4H), 8.16 (d, J=2.3 Hz, 1H), 7.83 (dd, J=8.3, 2.3 Hz, 1H), 7.77 (d, J=8.2 Hz, 1H), 7.65 (d, J=8.2 Hz, 2H), 7.53-7.48 (m, 4H), 7.39-7.34 (m, 4H), 7.26 (d, J=8.2 Hz, 2H) ppm. ^{13}C NMR (150 MHz, CD_2Cl_2, FID TSC111/41): δ=141.4, 140.9, 139.7, 135.9, 132.7, 132.7, 127.8, 126.9, 126.7, 125.1, 124.3, 123.8, 121.2, 121.0, 120.9, 120.8, 110.6, 110.2 ppm. Calculated: *m/z* 486.0732 $[M]^+$. Found: MS (ESI): *m/z* 486.0723 $[M]^+$.

5-(9*H*-Carbazol-9-yl)indolo[3,2,1-*jk*]carbazole (XII)

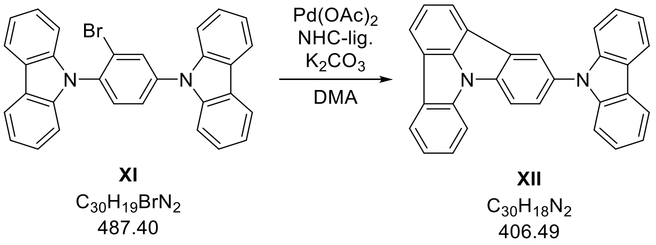

The synthesis of **XVII** was carried out as a modification of the protocol by Bintinger.[19] **XI** (3.41 g, 7 mmol, 1 eq.) and K_2CO_3 (1.94 g, 14 mmol, 2 eq.) were suspended in degassed DMA (30 ml, 1000 ppm water content) under argon atmosphere. Subsequently, NHC-lig. (60 mg, 0.14 mmol, 0.02 eq.) and $Pd(OAc)_2$ (31 mg, 0.14 mmol, 0.02 eq.) were added under argon counterflow. The reaction mixture was then heated to 130 °C until full conversion (TLC, 24 h) and cooled to rt. It was then distributed between water and DCM. The black residue was removed *via* filtration and the aqueous layer was repeatedly extracted with DCM. The combined organic layers were then dried over anhydrous Na_2SO_4 and concentrated *in vacuo*. **XII** (2.25 g, 6 mmol, 79%) was obtained as a colorless solid after column chromatography (light petroleum:DCM 85:15). Single crystals of **XII** were obtained after refluxing in ACN and crystallization from toluene (F.1). ^{1}H NMR (600 MHz, $CDCl_3$, FID TSC120/40): δ=8.31 (d, J=1.9 Hz, 1H), 8.21 (d, J=8.0 Hz, 2H), 8.20 (d, J=9.4 Hz, 1H), 8.12-8.11 (m, 2H), 8.04 (d, J=7.4 Hz, 1H), 7.99 (d, J=7.9 Hz, 1H), 7.74 (dd, J=8.3, 2.0 Hz, 1H), 7.64-7.61 (m, 2H), 7.47-7.42 (m, 5H), 7.35-7.32 (m, 2H) ppm. ^{13}C NMR (150 MHz, $CDCl_3$, FID TSC120/41): δ=144.4, 141.6, 138.6, 137.6, 131.5, 131.3, 130.0, 127.0, 126.0, 125.9, 123.3, 123.2, 122.4, 122.1, 120.3, 120.1, 119.8, 119.8, 118.8, 118.0, 112.9, 112.2, 109.7 ppm.[1] Calculated: *m/z* 406.1470 $[M]^+$. Found: MS (ESI): *m/z* 406.1468 $[M]^+$.

D.4.3 Synthesis of Cz_2ICz

2,6-Dibromo-*N*,*N*-bis(4-nitrophenyl)benzenamine (15)

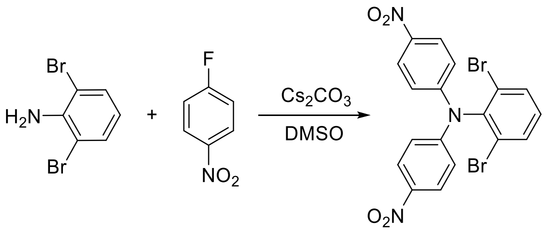

13 $C_6H_5Br_2N$ 250.92

14 $C_6H_4FNO_2$ 141.10

15 $C_{18}H_{11}Br_2N_3O_4$ 493.11

The synthesis of **15** was carried out as a modification of the protocol by Kautny *et al.*[23] **13** (3.67 g, 15 mmol, 1.0 eq.), **14** (4.66 g, 33 mmol, 2.2 eq.) and Cs_2CO_3 (10.75 g, 33 mmol, 2.2 eq.) were suspended in 75 ml of DMSO and heated to 130 °C overnight. After cooling to rt, the reaction mixture was poured on 300 ml of water and the precipitating crude product was filtrated. **15** (5.64 g, 11 mmol, 76%) was obtained as yellow solid after two iterations of refluxing in EtOH and subsequent filtration. ^{1}H NMR (400 MHz, CD_2Cl_2, FID TSC145/30): δ=8.17 (d, J=10.2 Hz, 4H), 7.76 (d, J=8.1 Hz, 2H), 7.27 (t, J=8.0 Hz, 1H), 7.12 (d, J=10.2 Hz, 4H) ppm.

---

[1] One carbon was not detected.

5,11-Dinitroindolo[3,2,1-*jk*]carbazole (XVII)

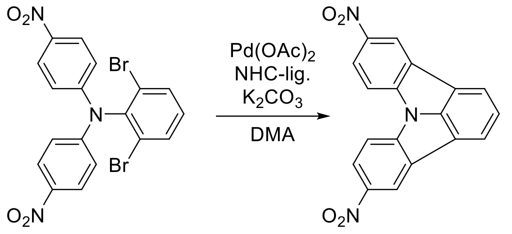

15
$C_{18}H_{11}Br_2N_3O_4$
493.11

XVI
$C_{18}H_9N_3O_4$
331.29

The synthesis of **XVI** was carried out as a modification of the protocol by Bintinger.[19] **15** (12.33 g, 25 mmol, 1 eq.) and K_2CO_3 (13.82 g, 100 mmol, 4 eq.) were suspended in degassed DMA (100 ml, 1000 ppm water content) under argon atmosphere. NHC-lig. (213 mg, 0.5 mmol, 0.02 eq.) and $Pd(OAc)_2$ (112 mg, 0.5 mmol, 0.02 eq.) were then added under argon counterflow. The reaction mixture was heated to 130 °C until full conversion (TLC, 48 h) and then cooled to rt. The precipitated product was filtrated and dried *in vacuo* yielding **XVI** (7.68 g, 23 mmol, 93%) as greenish solid. ^{1}H NMR (600 MHz, DMSO-d$_6$, FID TSC090/30): δ=9.36 (d, J=2.3 Hz, 2H), 8.67 (d, J=8.9 Hz, 2H), 8.57 (dd, J=8.9, 2.3 Hz, 2H), 8.51 (d, J=7.4 Hz, 2H), 7.82 (t, J=7.4 Hz, 1H) ppm. ^{13}C NMR (150 MHz, DMSO-d$_6$, FID TSC090/31): δ=145.5, 143.3, 140.8, 130.1, 125.2, 123.1, 122.8, 119.9, 117.9, 113.8 ppm.

Indolo[3,2,1-*jk*]carbazole-5,11-diamine (XVII)

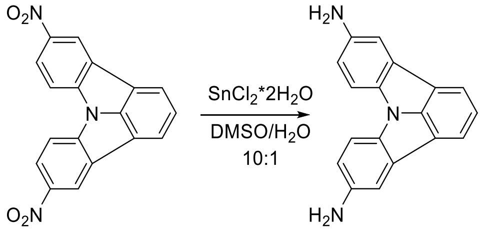

XVI
$C_{18}H_9N_3O_4$
331.29

XVII
$C_{18}H_{13}N_3$
271.32

XVI (1.32 g, 4 mmol, 1 eq.) and $SnCl_2 \cdot 2H_2O$ (9.04 g, 40 mmol, 10 eq.) were suspended in 22 ml of DMSO/H_2O (10:1) under argon atmosphere and heated to 80 °C overnight. Then the reaction mixture was basified with 2 M NaOH and repeatedly extracted with $CHCl_3$. The combined organic layers were dried over anhydrous Na_2SO_4 and concentrated *in vacuo*.

Column chromatography (light petroleum:EA 1:3 → EA) yielded **XVII** (643 mg, 2 mmol, 59%) as a yellow-green solid. ^{1}H NMR (600 MHz, CD_2Cl_2, FID TSC110/20): δ=7.96 (d, J=7.3 Hz, 2H), 7.65 (d, J=8.5 Hz, 2H), 7.49 (t, J=7.4 Hz, 1H), 7.47 (d, J=2.3 Hz, 2H), 6.93 (dd, J=8.5, 2.3 Hz, 2H), 3.78 (s, 4H) ppm. ^{13}C NMR (150 MHz, CD_2Cl_2, FID TSC110/21): δ=145.0, 142.0, 133.1, 131.0, 122.2, 119.7, 118.8, 115.2, 112.6, 109.7 ppm. Calculated: *m/z* 271.1109 $[M]^+$. Found: MS (ESI): *m/z* 271.1109 $[M]^+$.

5,11-Di(9*H*-carbazol-9-yl)indolo[3,2,1-*jk*]carbazole (XIX)

Procedure a:

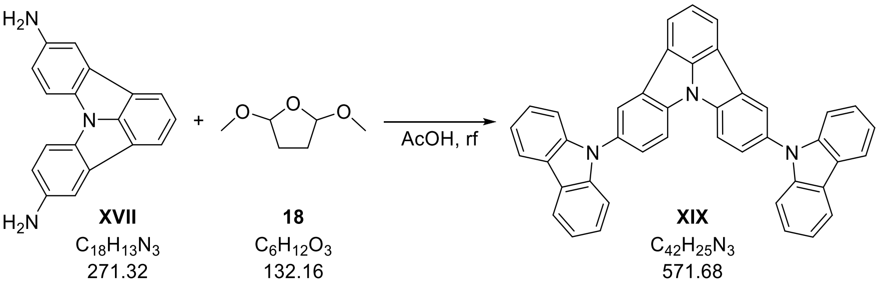

The synthesis of **XIX** followed a modified protocol by Lv *et al.*[18] **XVII** (244 mg, 0.9 mmol, 1 eq.) and **18** (357 mg, 2.7 mmol, 3 eq.) were dissolved in AcOH (130 ml) under argon atmosphere and heated to reflux. After 5 h, additional **18** (357 mg, 2.7 mmol, 3 eq.) was added. Two more eq. of **18** (238 mg, 1.8 mmol, 2 eq.) were added after 18 h and the reaction mixture was refluxed for another 7 h. After cooling to rt, the reaction mixture was poured on 100 ml of cooled 2 N HCl and repeatedly extracted with DCM. The combined organic layers were then washed with 2 M NaOH, dried over anhydrous Na_2SO_4 and concentrated *in vacuo*. **XIX** (20 mg, 0.03 mmol, 4%) was obtained after column chromatography (light petroleum:DCM 92:8 → 75:25).

Procedure b:

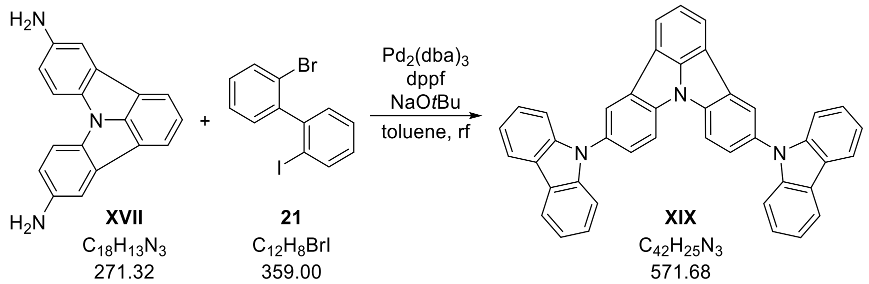

The synthesis of **XIX** followed a modified protocol by Iwaki *et al.*[37] **XVII** (0.76 g, 2.8 mmol, 1.0 eq.), **21** (2.21 g, 6.2 mmol, 2.2 eq.), $Pd_2(dba)_3$ (513 mg, 0.56 mmol, 0.2 eq.), dppf (621 mg, 1.12 mmol, 0.4 eq.) and NaO*t*Bu (2.15 g, 22.4 mmol, 8 eq.) were suspended in degassed toluene under argon atmosphere and heated to reflux. After full conversion (TLC, 18 h), the reaction mixture was poured on water and repeatedly extracted with DCM. The combined organic layers were dried over anhydrous Na_2SO_4 and concentrated *in vacuo*. **XIX** (1.25 g, 2.2 mmol, 78%) was obtained as a bright yellow solid after column chromatography (light petroleum:DCM 85:15 → 33:67). Further purification was achieved by crystallization from toluene. ^{1}H NMR (600 MHz, $CDCl_3$, FID TSC122/120): δ=8.37 (d, J=1.9 Hz, 2H), 8.22 (d, J=7.8 Hz, 4H), 8.20 (d, J=8.3 Hz, 2H), 8.12 (d, J=7.4 Hz, 2H), 7.80 (dd, J=8.3, 2.1 Hz, 2H), 7.67 (t, J=7.4 Hz, 1H), 7.49-7.45 (m, 8H), 7.36-7.33 (m, 4H) ppm. ^{13}C NMR (150 MHz, $CDCl_3$, FID TSC122/121): δ=145.1, 141.5, 137.6, 131.9, 131.4, 126.3, 126.0, 123.6, 123.3, 122.6, 120.5, 120.4, 119.9, 118.4, 113.0, 109.7 ppm. Calculated: *m/z* 571.2048 $[M]^+$. Found: MS (ESI): *m/z* 571.2053 $[M]^+$.

2-Bromo-2'-iodo-1,1'-biphenyl (21)

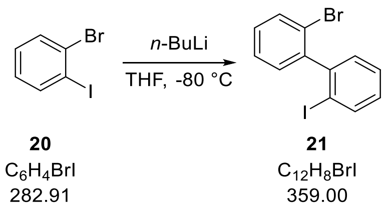

The synthesis of **21** followed the procedure described by Leroux and Schlosser.[26] To 300 ml of dry THF **20** (22.1 g, 78 mmol, 1.00 eq.) was added under argon atmosphere. After cooling to -80 °C, *n*-BuLi (17 ml, 2.5 M in hexanes, 43 mmol, 0.55 eq.) was added dropwise. The reaction mixture was kept at -75 °C for 30 min before being allowed to slowly warm to rt overnight. After removing the solvent *in vacuo*, the crude product was dissolved in Et_2O and washed with water. The washing solution was extracted with Et_2O and the combined organic layers were dried with brine and over anhydrous Na_2SO_4. The solvent was subsequently removed *in vacuo*. After crystallization from EtOH, **21** (14.0 g, 39 mmol, 100%) was obtained as white crystalline solid. ^1H NMR (200 MHz, $CDCl_3$, FID TSC115/10): δ=7.95 (dd, J=7.9, 1.1 Hz, 1H), 7.67 (dd, J=7.8, 1.3 Hz, 1H), 7.46-7.35 (m, 2H), 7.31-7.18 (m, 3H), 7.07 (td, J=11.5, 1.7 Hz, 1H) ppm.

D.4.4 Synthesis of Cz$_3$ICz

2,5,11-Tribromoindolo[3,2,1-*jk*]carbazole (XXV)

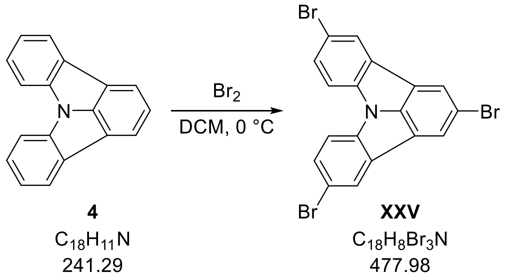

4 (483 mg, 2 mmol, 1 eq.) was dissolved in 10 ml of DCM and cooled to 0 °C. Br_2 (1.05 g, 6.6 mmol, 3.3 eq.) was separately dissolved in 10 ml of DCM, cooled and then added to the solution of **4** immediately forming a precipitate. After 7 h, the precipitate was filtrated, washed with DCM and aqueous Na_2SO_3 solution. After refluxing in toluene and subsequent filtration, **XXV** (700 mg, 1.5 mmol, 73%) was obtained as beige solid. ^1H NMR (600 MHz, DMSO-d_6, FID TSC135/40): δ=8.59 (d, J=2.0 Hz, 2H), 8.51 (s, 2H), 8.32 (d, J=8.58 Hz, 2H), 7.82 (dd, J=8.6, 2.0 Hz, 2H) ppm. ^{13}C NMR (150 MHz, DMSO-d_6, FID TSC135/41): δ=141.9, 137.1, 130.5, 130.2, 126.8, 124.1, 118.5, 115.7, 114.9 ppm.[1]

---

[1] One carbon was not detected.

2,5,11-Tri(9*H*-carbazol-9-yl)indolo[3,2,1-*jk*]carbazole (XXVI)

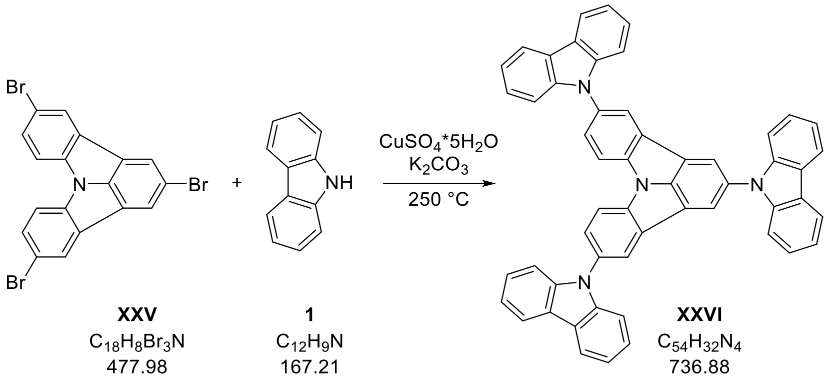

The synthesis of **XXVI** followed an Ullmann condensation protocol by Kautny *et al.*[14] **XXV** (1.91 g, 4 mmol, 1 eq.), **1** (3.01 g, 18 mmol, 4.5 eq.), $CuSO_4\cdot5H_2O$ (0.15 g, 0.6 mmol, 0.15 eq.) and K_2CO_3 (2.49 g, 18 mmol, 4.5 eq.) were thoroughly mixed and heated to 250 °C in a vial. Due to constant sublimation of **1**, the reaction mixture was repeatedly cooled to around 100 °C in order to be manually homogenized again. After 72 h, the reaction mixture was cooled to rt. The solidified mixture was dissolved in DCM and water and repeatedly extracted with DCM. The combined organic layers were dried over anhydrous Na_2SO_4 and concentrated *in vacuo*. Most of the excess **1** was then removed from the crude product by sublimation. Column chromatography (light petroleum:DCM 70:30) yielded **XXVI** (2.25 g, 3.1 mmol, 76%) as beige solid. Further purification was achieved by crystallization from toluene. ^{1}H NMR (600 MHz, $CDCl_3$, FID TSC136/130): δ=8.34 (d, J=2.0 Hz, 2H), 8.24-8.23 (m, 4H), 8.21-8.19 (m, 6H), 7.86 (dd, J=8.5, 2.1 Hz, 2H), 7.49 (d, J=7.9 Hz, 4H), 7.47-7.45 (m, 4H), 7.43-7.41 (m, 2H), 7.38 (d, J=8.5 Hz, 2H), 7.35-7.30 (m, 6H). ^{13}C NMR (150 MHz, $CDCl_3$, FID TSC136/131): δ=144.0, 142.2, 141.4, 138.1, 133.6, 132.4, 131.1, 127.0, 126.0, 126.0, 123.3, 123.1, 122.9, 120.9, 120.4, 120.3, 120.0, 119.9, 119.1, 113.3, 109.6, 109.6 ppm. Calculated: *m/z* 736.2627 $[M]^+$. Found: MS (ESI): *m/z* 736.2624 $[M]^+$.

D.4.5 Synthesis of ICzPCz and ICzICz

Tetrakis(triphenylphosphine)palladium(0)

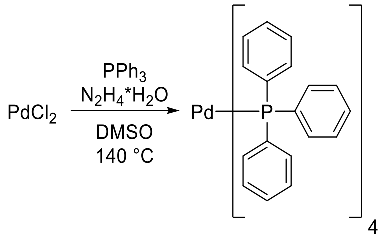

$PdCl_2$
Cl_2Pd
177.32

$Pd(PPh_3)_4$
$C_{72}H_{60}P_4Pd$
1155.59

The synthesis of $Pd(PPh_3)_4$ was carried out using a modification of the protocol by Coulson *et al.*[38] $PdCl_2$ (277 mg, 1.6 mmol, 1 eq.) and PPh_3 (1.97 g, 7.5 mmol, 4.8 eq.) were suspended in 25 ml of DMSO under argon atmosphere and heated to 140 °C giving a clear solution. $N_2H_4 \cdot H_2O$ (0.30 g, 6 mmol, 3.8 eq.) was then added dropwise and the solution cooled to rt. The product was then filtrated using a Schlenk-frit and washed with dry EtOH and Et_2O under argon atmosphere giving $Pd(PPh_3)_4$ (1.74 g, 1.5 mmol, 96%) as a bright yellow powder.

2-[4-(9*H*-Carbazol-9-yl)phenyl]indolo[3,2,1-*jk*]carbazole (28)

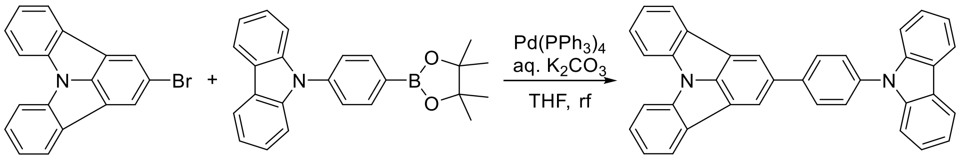

5
$C_{18}H_{10}BrN$
320.19

27
$C_{24}H_{24}BNO_2$
369.27

28
$C_{36}H_{22}N_2$
482.59

The synthesis of **28** was carried out according to Kautny *et al.*[14] **5** (1.92 g, 6 mmol, 1 eq.), **27** (2.77 g, 7.5 mmol, 1.25 eq.) and K_2CO_3 (7.5 ml, 2 M aq. solution, 15 mmol, 2.5 eq.) were suspended in 110 ml of dry, degassed THF under argon atmosphere. Subsequently, $Pd(PPh_3)_4$ (347 mg, 0.3 mmol, 0.05 eq.) was added under argon counterflow. The reaction mixture was then refluxed (40 h, TLC), cooled to rt, poured on water and repeatedly extracted with DCM. The combined organic layers were dried over anhydrous Na_2SO_4 and concentrated *in vacuo*. Column chromatography (light petroleum:DCM 80:20 → 50:50) and subsequent crystallization from toluene yielded **28** (898 mg, 1.9 mmol, 31%) as a bright rose crystalline solid. ^1H NMR

(400 MHz, $CDCl_3$, FID TSC127/160): δ=8.36 (s, 2H), 8.23-8.18 (m, 4H), 8.00 (dt, J=8.6, 2.0 Hz, 2H), 7.97 (d, J=7.8 Hz, 2H), 7.72 (dt, J=8.6, 2.0 Hz, 2H), 7.61 (td, J=7.8, 1.2 Hz, 2H), 7.55 (d, J=8.2 Hz, 2H), 7.47 (ddd, J=8.2, 7.0, 1.2 Hz, 2H), 7.42 (td, J=7.6, 1.2 Hz, 2H), 7.33 (ddd, J=7.8, 7.0, 1.2 Hz, 2H) ppm.

2,2'-Biindolo[3,2,1-*jk*]carbazole (29)

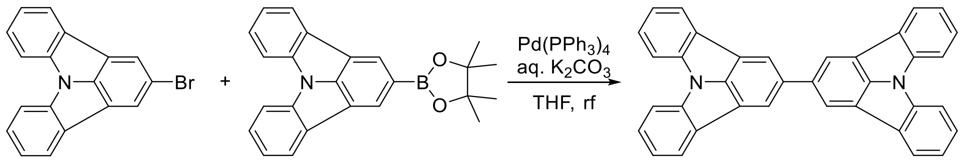

5 $C_{18}H_{10}BrN$ 320.19

6 $C_{24}H_{22}BNO_2$ 367.26

29 $C_{36}H_{20}N_2$ 480.57

The synthesis of **29** was carried out according to Kautny *et al.*[14] **5** (2.30 g, 7.2 mmol, 1 eq.), **6** (3.31 g, 9 mmol, 1.25 eq.) and K_2CO_3 (9 ml, 2 M aq. solution, 18 mmol, 2.5 eq.) were suspended in 135 ml of dry, degassed THF under argon atmosphere. Subsequently, $Pd(PPh_3)_4$ (416 mg, 0.36 mmol, 0.05 eq.) was added under argon counterflow. The reaction mixture was then refluxed (40 h, TLC), cooled to rt and filtrated yielding **29** (2.81 g, 5.8 mmol, 81%) as a yellowish solid containing approximately 5-10% impurities. ^1H NMR (400 MHz, $CDCl_3$, FID TSC128/120): δ=8.43 (s, 4H), 8.24 (d, J=7.8 Hz, 4H), 7.98 (d, J=8.2 Hz, 4H), 7.61 (td, J=7.6, 1.2 Hz, 4H), 7.41 (td, J=7.6, 1.2 Hz, 4H) ppm.

D.4.6 Synthesis of the triazines

2,4-Dichloro-6-phenyl-1,3,5-triazine (32)

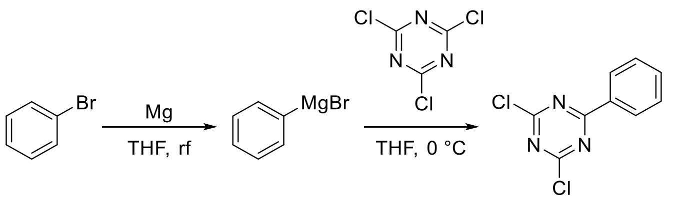

33 C_6H_5Br 157.01

30 $C_3Cl_3N_3$ 184.40

32 $C_9H_5Cl_2N_3$ 226.06

The synthesis of **32** was carried out using a modified protocol by An *et al.*[31] Mg turnings (486 mg, 20 mmol, 1.1 eq.) and a small I_2 crystal were suspended in 5 ml of dry THF under argon atmosphere. **33** (2.83 g, 18 mmol, 1 eq.) was filled in a dropping funnel and diluted with 5 ml of THF. Approximately 2 ml of the solution were added to the suspension and short heating started the reaction as indicated by decoloration and self-sustaining reflux. The remaining solution of **33** was further diluted with 20 ml of THF and slowly added. After the reaction mixture stopped refluxing, it was externally heated to rf for 1 h and then cooled to rt. A solution of **30** (4.43 g, 24 mmol, 1.3 eq.) in 60 ml of dry THF under argon atmosphere was prepared separately and cooled in an ice/NaCl cooling bath. The PhMgBr solution was then transferred to a dropping funnel using a syringe and slowly added to the solution of **30** at 0 °C. The reaction mixture was then allowed to slowly warm to rt overnight and was subsequently concentrated *in vacuo*. The crude product was distributed between water and $CHCl_3$. After repeated extraction with $CHCl_3$, the combined organic layers were dried over anhydrous Na_2SO_4 and concentrated *in vacuo*. Purification by column chromatography (light petroleum:DCM 80:20) yielded **32** (2.70 g, 11.9 mmol, 66%) as a white solid. ^1H NMR (400 MHz, $CDCl_3$, FID TSC172/20): δ=8.53-8.50 (m, 2H), 7.69-7.64 (m, 1H), 7.56-7.52 (m, 2H) ppm.

2-Chloro-4,6-diphenyl-1,3,5-triazine (34)

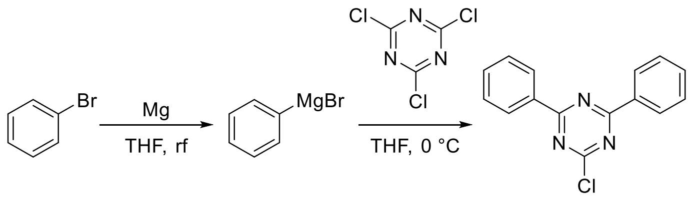

33 C_6H_5Br 157.01

30 $C_3Cl_3N_3$ 184.40

34 $C_{15}H_{10}ClN_3$ 267.72

The synthesis of **34** followed the procedure described by An *et al.*[31] Mg turnings (1.40 g, 57.5 mmol, 3.6 eq.) and a small I_2 crystal were suspended in 5 ml of dry THF under argon atmosphere. **33** (8.70 g, 55.4 mmol, 3.4 eq.) was filled in a dropping funnel with 40 ml of THF. About 10 ml were added to the suspension and short heating started the reaction as indicated by decoloration and self-sustaining reflux. The remainder of the solution was then added under reflux. After the reaction mixture stopped refluxing, it was externally heated to reflux for 1 h and then cooled to rt. A solution of **30** (2.99 g, 16.2 mmol, 1 eq.) in 25 ml of dry THF under argon atmosphere was prepared separately and cooled in an ice/NaCl cooling bath. The PhMgBr solution was then transferred to a dropping funnel using a syringe and slowly added to the solution of **30** at 0 °C. After heating the reaction mixture to 35 °C, it was stirred overnight. The reaction mixture was poured on aqueous NH_4Cl (10%) and repeatedly extracted with $CHCl_3$. The combined organic layers were then dried over anhydrous Na_2SO_4 and concentrated *in vacuo*. Purification by column chromatography (light petroleum:DCM 20:1 → DCM) yielded **34** (1.09 g, 4.1 mmol, 25%) as a white solid. ^1H NMR (200 MHz, $CDCl_3$, FID TSC105/10): δ=8.63 (d, J=7.0 Hz, 2H), 7.68-7.51 (m, 3H) ppm.

2,2'-(6-Phenyl-1,3,5-triazine-2,4-diyl)bis[indolo[3,2,1-*jk*]carbazole] (XXXV)

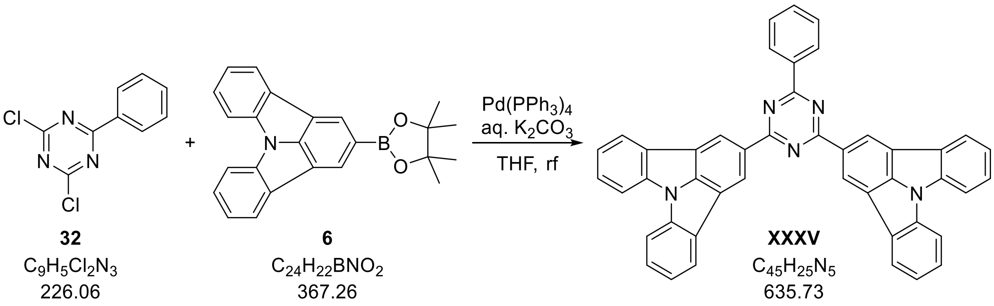

The synthesis of **XXXV** was carried out as a modification of the protocol by Kautny *et al.*[14] **32** (113 mg, 0.5 mmol, 1 eq.), **6** (404 mg, 1.1 mmol, 2.2 eq.) and K_2CO_3 (2.5 ml, 2 M aq. solution, 5 mmol, 2.5 eq.) were suspended in 10 ml of dry, degassed THF under argon atmosphere. Subsequently, $Pd(PPh_3)_4$ (29 mg, 0.025 mmol, 0.05 eq.) was added under argon counterflow. The reaction mixture was then refluxed (48 h, TLC), cooled to rt and filtrated yielding **XXXV** (72 mg, 0.11 mmol, 23%) as an off-white solid. ^1H NMR (600 MHz, DMSO-d_6, FID TSC099/40): δ=9.92 (s, 4H), 9.07-9.05 (m, 2H), 8.66 (d, J=7.6 Hz, 4H), 8.42 (d, J=8.2 Hz, 4H), 7.82-7.77 (m, 3H), 7.74 (t, J=7.5 Hz, 4H), 7.58 (t, J=7.5 Hz, 4H) ppm.[1] Calculated: *m/z* 636.2183 $[M+H]^+$. Found: MS (ESI): *m/z* 636.2162 $[M+H]^+$.

---

[1] Due to low solubility, a ^{13}C spectrum could not be obtained.

2-(4,6-Diphenyl-1,3,5-triazin-2-yl)indolo[3,2,1-*jk*]carbazole (XXXVI)

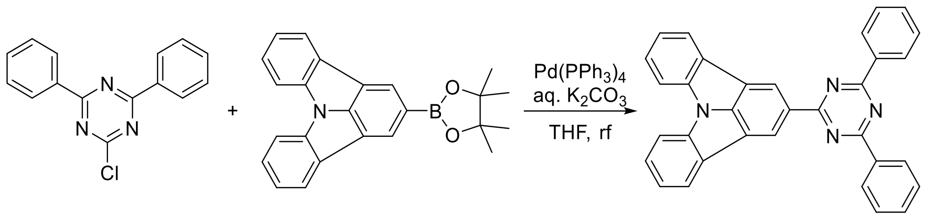

34 $C_{15}H_{10}ClN_3$ 267.72

6 $C_{24}H_{22}BNO_2$ 367.26

XXXVI $C_{33}H_{20}N_4$ 472.55

The synthesis of **XXXVI** was carried out as a modification of the protocol by Kautny *et al.*[14] Starting from **34** (1.07 g, 4 mmol, 1 eq.), **6** (1.62 g, 4.4 mmol, 1.1 eq.), K_2CO_3 (5 ml, 2 M aq. solution, 10 mmol, 2.5 eq.), $Pd(PPh_3)_4$ (231 mg, 0.2 mmol, 0.05) and dry THF (60 ml) the reaction mixture was refluxed for 48 h. After cooling to rt, the reaction mixture was filtrated and the residue was washed with water. The crude product was then recrystallized from toluene yielding **XXXVI** (1.16 g, 2.5 mmol, 61%) as a light grey powder. Further purification was achieved by recrystallization from pyridine. ^1H NMR (600 MHz, DMSO-d_6, FID TSC116/70): δ=9.75 (s, 2H), 8.92-8.90 (m, 4H), 8.58 (d, J=7.7 Hz, 2H), 8.39 (d, J=8.0 Hz, 2H), 7.79-7.76 (m, 2H), 7.74-7.71 (m, 6H), 7.53 (t, J=7.5 Hz, 2H) ppm.[1] Calculated: *m/z* 472.1688 $[M]^+$. Found: MS (ESI): *m/z* 472.1676 $[M]^+$.

D.4.7 Synthesis towards carbonyl compounds

α-Phenylbenzenemethanol (39)

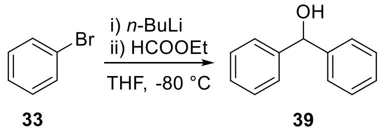

33 C_6H_5Br 157.01

39 $C_{13}H_{12}O$ 184.24

A solution of **33** (1.57 g, 10 mmol, 2 eq.) in 50 ml of dry THF was prepared under argon atmosphere. After cooling to -80 °C, *n*-BuLi (4.0 ml, 2.5 M in hexanes, 10 mmol, 2 eq.) was added dropwise. The reaction mixture was kept at -80 °C for 30 min and then quenched with

---

[1] Due to low solubility, a ^{13}C spectrum could not be obtained.

HCOOEt (0.37 g, 5 mmol, 1 eq.). The mixture was allowed to slowly warm to rt overnight, poured on aqueous NH_4Cl (10%) and repeatedly extracted with DCM. The combined organic layers were dried over anhydrous Na_2SO_4 and concentrated *in vacuo*. Column chromatography (light petroleum:DCM) yielded **39** (350 mg, 1.9 mmol, 38%) as yellow oil, which crystallized at rt. ^1H NMR (200 MHz, $CDCl_3$, FID TSC080/10): δ=7.42-7.25 (m, 10H), 5.86 (s, 1H) ppm.

Diphenylmethanone (40)

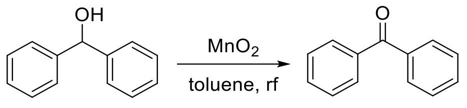

39 $C_{13}H_{12}O$ 184.24 **40** $C_{13}H_{10}O$ 182.22

The synthesis of **40** followed a modified protocol by Kamimura *et al.*[32] **39** (138 mg, 0.75 mmol, 1 eq.) and MnO_2 (76 mg, 0.87 mmol, 1.2 eq.) were suspended in 20 ml of toluene and heated to reflux. After complete conversion (GC-MS, 2.5 h), the reaction mixture was cooled to rt and then filtrated over silica. The solvent was removed *in vacuo* yielding **40** (100 mg, 0.55 mmol, 73%) as a yellow oil. ^1H NMR (200 MHz, $CDCl_3$, FID TSC082/10): δ=7.81 (d, J=7.1 Hz, 4H), 7.63-7.55 (m, 2H), 7.51-7.44 (m, 4H) ppm.

Ethyl indolo[3,2,1-*jk*]carbazole-2-carboxylate (XLII)

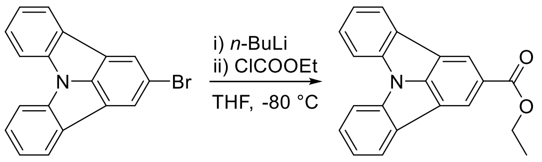

5 $C_{18}H_{10}BrN$ 320.19 **XLII** $C_{21}H_{15}NO_2$ 313.36

5 (8.43 g, 26.3 mmol, 1 eq.) was suspended in 500 ml of dry THF under argon atmosphere. After cooling to -80 °C, *n*-BuLi (12.8 ml, 2.5 M in hexanes, 32 mmol, 1.2 eq.) was added slowly giving an orange slurry. After 1 h, excess ClCOOEt (8.57 g, 79 mmol, 3 eq.) was quickly added. The reaction mixture was then allowed to slowly warm to rt over the weekend. THF and excess ClCOOEt were then removed *in vacuo*. The crude product was distributed between water and DCM and repeatedly extracted. The combined organic layers were dried over anhydrous

Na_2SO_4 and the solvent removed *in vacuo*. The crude product was dissolved in 220 ml of boiling toluene, filtrated, concentrated *in vacuo* and finally crystallized from 30 ml of toluene yielding single crystals (F.1). The remaining toluene solution was concentrated *in vacuo* and then further purified by column chromatography (light petroleum:DCM 80:20 → 50:50). **XLII** (5.49 g, 17.5 mmol, 67%) was obtained as white solid/crystals. ^{1}H NMR (400 MHz, $CDCl_3$, FID TSC159/70): δ=8.84 (s, 2H), 8.18 (d, J=7.7 Hz, 2H), 7.92 (d, J=8.0 Hz, 2H), 7.60 (td, J=7.7, 1.2 Hz, 2H), 7.41 (td, J=7.7, 1.0 Hz, 2H), 4.52 (q, J=7.2 Hz, 2H), 1.52 (t, J=7.2 Hz, 3H) ppm.

Sodium indolo[3,2,1-*jk*]carbazole-2-carboxylate (XLIII)

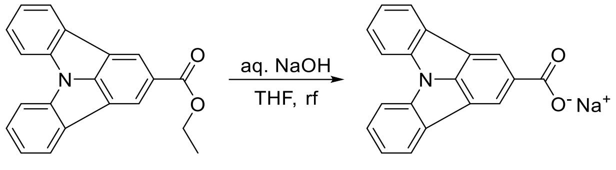

XLII
$C_{21}H_{15}NO_2$
313.36

XLIII
$C_{19}H_{10}NNaO_2$
307.28

XLII (2.19 g, 7 mmol, 1 eq.) was suspended in 120 ml of THF and 120 ml of 2 M NaOH under argon atmosphere and heated to reflux. After full conversion (TLC, 96 h), the reaction mixture was cooled to rt and the product crystallized from the organic layer. The aqueous layer was carefully removed with a syringe and the organic layer was filtrated. The THF filtrate was then concentrated *in vacuo* and refluxed in THF:NaOH. More product crystallized after evaporation of the THF at ambient conditions and was also filtrated. **XLIII** (2.01 g, 6.5 mmol, 93%) was obtained as white crystals. ^{1}H NMR (400 MHz, DMSO-d_6, FID TSC160/10): δ=8.81 (s, 2H), 8.30-8.25 (m, 4H), 7.59 (td, J=7.8, 1.2 Hz, 2H), 7.40 (td, J=7.5, 0.9 Hz, 2H) ppm.

Indolo[3,2,1-*jk*]carbazole-2-carboxylic acid (XLIV)

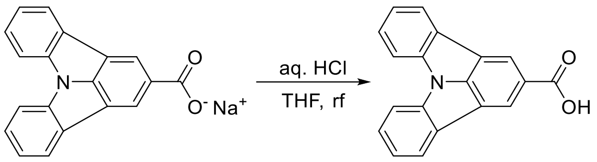

XLIII $C_{19}H_{10}NNaO_2$ 307.28 → **XLIV** $C_{19}H_{11}NO_2$ 285.30

XLIII (4.15 g, 13.5 mmol, 1 eq.) was suspended in a mixture of 100 ml of THF and 100 ml of 2 M HCl and heated to reflux for 1 h. After cooling to rt, the suspension was filtrated yielding **XLIV** (3.17 g, 11.1 mmol, 82%) as a white powder. ^{1}H NMR (400 MHz, DMSO-d$_6$, FID TSC168/10): δ=12.95 (s, 1H), 8.89 (s, 2H), 8.40 (d, J=7.6 Hz, 2H), 8.33 (d, J=8.1 Hz, 2H), 7.67 (td, J=7.9, 1.2 Hz, 2H), 7.46 (td, J=7.6, 0.8 Hz, 2H) ppm.

Indolo[3,2,1-*jk*]carbazole-2-carbonyl chloride (XLV)

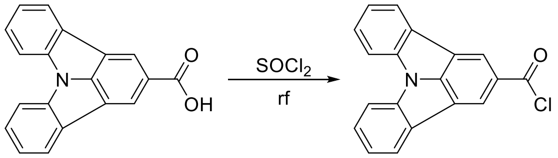

XLIV $C_{19}H_{11}NO_2$ 285.30 → **XLV** $C_{19}H_{10}ClNO$ 303.75

The synthesis of **XLV** was carried out as a modification of the protocol by Kautny.[21] **XLIV** (1.14 g, 4 mmol, 1 eq.) was suspended in 10 ml of SOCl$_2$ with a catalytic amount of DMF and refluxed. After 20 min, the solid completely dissolved. The solution was kept at reflux overnight and after cooling to rt was concentrated *in vacuo* giving **XLV** as a yellow solid in quantitative yield. ^{1}H NMR (400 MHz, CDCl$_6$, FID TSC169/10): δ=8.70 (s, 2H), 8.06 (d, J=7.8 Hz, 2H), 7.79 (d, J=8.2 Hz, 2H), 7.59 (td, J=7.8, 1.2 Hz, 2H), 7.40 (td, J=7.6, 1.0 Hz, 2H) ppm.

3-Bromo-4-(9*H*-carbazol-9-yl)benzonitrile (XLVIII)

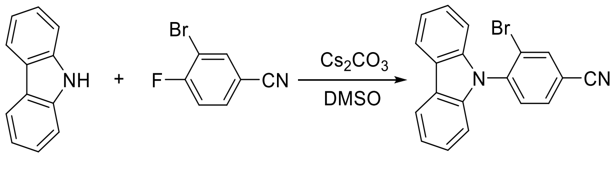

1 $C_{12}H_9N$ 167.21 + **47** C_7H_3BrFN 200.01 → **XLVIII** $C_{19}H_{11}BrN_2$ 347.22

The synthesis of **XLVIII** was carried out as a modification of the protocol by Bintinger.[19] **1** (0.84 g, 5 mmol, 1 eq.), **47** (1.00 g, 5 mmol, 1 eq.) and Cs_2CO_3 (1.79 g, 5.5 mmol, 1.1 eq.) were suspended in 25 ml of DMSO and heated to 120 °C until full conversion (TLC, 6 h). After cooling to rt, the reaction mixture was poured on 100 ml of water and the precipitating crude product was filtrated. Column chromatography (light petroleum:DCM 75:25) and subsequent crystallization from EtOH yielded **XLVIII** (599 mg, 1.7 mmol, 35%) as colorless crystals (F.1). ^{1}H NMR (400 MHz, $CDCl_3$, FID TSC166/90): δ=8.18 (d, J=1.9 Hz, 1H), 8.15 (dt, J=7.8, 0.8 Hz, 2H), 7.83 (dd, J=8.2, 1.9 Hz, 1 H), 7.63 (d, J=8.2 Hz, 1H), 7.42 (ddd, J=8.2, 7.1, 1.2 Hz, 2 H), 7.35-7.31 (m, 2H), 7.05 (dt, J=8.2, 0.8 Hz, 2H) ppm.

Indolo[3,2,1-*jk*]carbazole-5-carbonitrile (49)

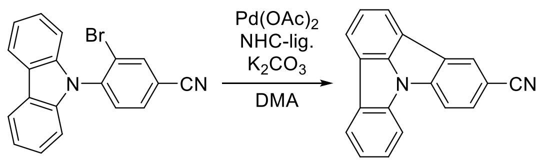

XLVIII
$C_{19}H_{11}BrN_2$
347.22

49
$C_{19}H_{10}N_2$
266.30

The synthesis of **49** was carried out as a modification of the protocol by Bintinger.[19] **XLVIII** (512 mg, 1.5 mmol, 1 eq.) and K_2CO_3 (415 mg, 3 mmol, 2 eq.) were suspended in degassed DMA (20 ml, 1000 ppm water content) under argon atmosphere. Subsequently, NHC-lig. (13 mg, 0.03 mmol, 0.02 eq.) and $Pd(OAc)_2$ (7 mg, 0.03 mmol, 0.02 eq.) were added under argon counterflow. The reaction mixture was heated to 130 °C until full conversion (TLC, 24 h) and then cooled to rt. Subsequently, it was poured on water and repeatedly extracted with DCM. The combined organic layers were dried over anhydrous Na_2SO_4 and concentrated *in* vacuo yielding **49** (387 mg, 1.5 mmol, 97%) as a light brown solid. Single crystals of **49** were obtained by crystallization from ACN (F.1). ^{1}H NMR (400 MHz, DMSO-d_6, FID TSC113/40): δ=8.78 (d, J=1.4 Hz, 1H), 8.42 (d, J=8.2 Hz, 1H), 8.34 (d, J=8.3 Hz, 1H), 8.27 (d, J=7.6 Hz, 1H), 8.24-8.21 (m, 2H), 8.01 (dd, J=8.5, 1.7 Hz, 1H), 7.70-7.62 (m, 2H), 7.46 (td, J=7.6, 1.2 Hz, 1H) ppm. ^{13}C NMR (100 MHz, DMSO-d_6, FID TSC113/31): δ=143.4, 139.5, 137.7, 130.7, 129.5, 129.4, 127.8, 127.6, 124.1, 123.5, 123.2, 121.1, 120.7, 119.7, 118.3, 116.6, 113.6, 113.5, 103.9 ppm.

D.4.8 Synthesis of the highly annulated ring system LIV

9,9’-(2,5-Dibromo-1,4-phenylene)bis[9*H*-carbazole] (LIII)

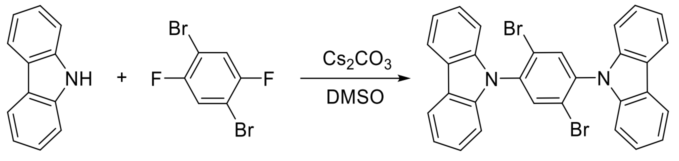

1 $C_{12}H_9N$ 167.21 **52** $C_6H_2Br_2F_2$ 271.89 **LIII** $C_{30}H_{18}Br_2N_2$ 566.30

The synthesis of **LIII** was carried out as a modification of the protocol by Bintinger.[19] **1** (1.34 g, 8 mmol, 2 eq.), **52** (1.09 g, 4 mmol, 1 eq.) and Cs_2CO_3 (2.87 g, 8.8 mmol, 2.2 eq.) were suspended in 25 ml of DMSO and heated to 120 °C for 48 h (TLC, no further conversion). After cooling to rt, the reaction mixture was poured on 450 ml of water and the precipitating crude product was filtrated. It was then refluxed in ACN, filtrated and crystallized from toluene yielding **LIII** (900 mg, 1.6 mmol, 40%) as off-white crystals (F.1).[36] ^1H NMR (600 MHz, CD_2Cl_2, FID TSC112/50): δ=8.20 (d, J=7.7 Hz, 4H), 8.05 (s, 2H), 7.51 (t, J=7.6 Hz, 4H), 7.37 (t, J=7.4 Hz, 4H), 7.28 (d, J=8.1 Hz, 4H) ppm. ^{13}C NMR (150 MHz, CD_2Cl_2, FID TSC112/51): δ=141.1, 138.8, 136.6, 126.8, 124.0, 123.8, 121.2, 121.1, 110.6 ppm. Calculated: *m/z* 563.9837 $[M]^+$. Found: MS (ESI): *m/z* 563.9850 $[M]^+$.

Benzo[1”,2”:4,5;5”,4”:4’,5’]dipyrrolo[3,2,1-*jk*:3’,2’,1’-*j’k’*]dicarbazole (LIV)

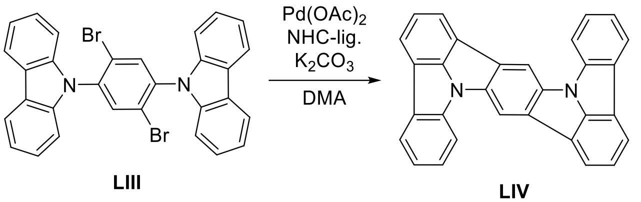

LIII $C_{30}H_{18}Br_2N_2$ 566.30 **LIV** $C_{30}H_{16}N_2$ 404.47

The synthesis of **LIV** was carried out as a modification of the protocol by Bintinger.[19] **LIII** (1.70 g, 3 mmol, 1 eq.) and K_2CO_3 (1.66 g, 12 mmol, 4 eq.) were suspended in degassed DMA (60 ml, 1000 ppm water content) under argon atmosphere. NHC-lig. (26 mg, 0.06 mmol, 0.02 eq.) and $Pd(OAc)_2$ (13 mg, 0.06 mmol, 0.02 eq.) were added under argon counterflow. The reaction mixture was heated to 130 °C overnight and then cooled to rt. The precipitated product was filtrated and washed with toluene. Crystallization from nitrobenzene yielded **LIV** (978 mg, 2.4 mmol, 81%) as green crystals (F.1). ^{1}H NMR (600 MHz, DMSO-d_6, FID TSC153/30): δ=9.30 (s, 2H), 8.52 (d, J=8.0 Hz, 2H), 8.36-8.34 (m, 4H), 8.27 (d, J=7.3 Hz, 2H), 7.75-7.71 (m, 4H), 7.47 (td, J=7.5, 0.8 Hz, 2H) ppm.[1] Calculated: *m/z* 404.1313 $[M]^+$. Found: MS (ESI): *m/z* 404.1316 $[M]^+$.

---

[1] Due to low solubility, a ^{13}C spectrum could not be obtained.

E Bibliography

1. Forrest, S. R. The path to ubiquitous and low-cost organic electronic appliances on plastic. *Nature* **428**, 911–918 (2004).
2. Pope, M., Kallmann, H. P. & Magnante, P. Electroluminescence in Organic Crystals. *J. Chem. Phys.* **38**, 2042–2043 (1963).
3. Jou, J.-H., Kumar, S., Agrawal, A., Li, T.-H. & Sahoo, S. Approaches for fabricating high efficiency organic light emitting diodes. *J. Mater. Chem. C* **3**, 2974–3002 (2015).
4. Uoyama, H., Goushi, K., Shizu, K., Nomura, H. & Adachi, C. Highly efficient organic light-emitting diodes from delayed fluorescence. *Nature* **492**, 234–238 (2012).
5. Tao, Y., Yang, C. & Qin, J. Organic host materials for phosphorescent organic light-emitting diodes. *Chem. Soc. Rev.* **40**, 2943–2970 (2011).
6. Zhang, Q. *et al.* Efficient blue organic light-emitting diodes employing thermally activated delayed fluorescence. *Nat. Photonics* **8**, 326–332 (2014).
7. Adachi, C., Baldo, M. A., Thompson, M. E. & Forrest, S. R. Nearly 100% internal phosphorescence efficiency in an organic light-emitting device. *J. Appl. Phys.* **90**, 5048–5051 (2001).
8. Tsai, W.-L. *et al.* A versatile thermally activated delayed fluorescence emitter for both highly efficient doped and non-doped organic light emitting devices. *Chem. Commun.* **51**, 13662–13665 (2015).
9. Endo, A. *et al.* Efficient up-conversion of triplet excitons into a singlet state and its application for organic light emitting diodes. *Appl. Phys. Lett.* **98**, 83302 (2011).
10. Fan, C. *et al.* Using an Organic Molecule with Low Triplet Energy as a Host in a Highly Efficient Blue Electrophosphorescent Device. *Angew. Chemie Int. Ed.* **53**, 2147–2151 (2014).
11. Adachi, C. *et al.* Endothermic energy transfer: A mechanism for generating very efficient high-energy phosphorescent emission in organic materials. *Appl. Phys. Lett.* **79**, 2082–2084 (2001).

12. Kim, M., Jeon, S. K., Hwang, S.-H. & Lee, J. Y. Stable Blue Thermally Activated Delayed Fluorescent Organic Light-Emitting Diodes with Three Times Longer Lifetime than Phosphorescent Organic Light-Emitting Diodes. *Adv. Mater.* **27**, 2515–2520 (2015).

13. Tsai, M.-H. *et al.* 3-(9-Carbazolyl)carbazoles and 3,6-Di(9-carbazolyl)carbazoles as Effective Host Materials for Efficient Blue Organic Electrophosphorescence. *Adv. Mater.* **19**, 862–866 (2007).

14. Kautny, P. *et al.* Indolo[3,2,1-*jk*]carbazole based planarized CBP derivatives as host materials for PhOLEDs with low efficiency roll-off. *Org. Electron.* **34**, 237–245 (2016).

15. Kautny, P. *et al.* Oxadiazole based bipolar host materials employing planarized triarylamine donors for RGB PHOLEDs with low efficiency roll-off. *J. Mater. Chem. C* **2**, 2069–2081 (2014).

16. Dunlop, H. G. & Tucker, S. H. Attempts to prepare optically active tervalent nitrogen compounds. Part I. Syntheses of 1 : 9-phenylenecarbazole and derivatives. *J. Chem. Soc.* 1945–1956 (1939).

17. Wharton, S. I., Henry, J. B., McNab, H. & Mount, A. R. The Production and Characterisation of Novel Conducting Redox-Active Oligomeric Thin Films From Electrooxidised Indolo[3,2,1-*jk*]carbazole. *Chem. Eur. J.* **15**, 5482–5490 (2009).

18. Lv, J., Liu, Q., Tang, J., Perdih, F. & Kranjc, K. A facile synthesis of indolo[3,2,1-*jk*]carbazoles via palladium-catalyzed intramolecular cyclization. *Tetrahedron Lett.* **53**, 5248–5252 (2012).

19. Bintinger, J. Sterically tuned triarylamines and oligothiophene derivatives as building blocks for novel organic electronic materials: synthesis and characterization. (TU Wien, 2011).

20. Jones, A. W., Louillat-Habermeyer, M.-L. & Patureau, F. W. Strained Dehydrogenative Ring Closure of Phenylcarbazoles. *Adv. Synth. Catal.* **357**, 945–949 (2015).

21. Kautny, P. Synthesis of Novel Bipolar Heterocyclic Systems as Host Materials for Phosphorescent Organic Light Emitting Diodes. (TU Wien, 2013).

22. Cakmak, O., Demirtas, I. & Balaydin, H. T. Selective bromination of 1-bromonaphthalene: efficient synthesis of bromonaphthalene derivatives. *Tetrahedron* **58**, 5603–5609 (2002).

23. Kautny, P., Fröhlich, J., Stöger, B. & Weil, M. Isotypic crystal structures of 2,6-dibromo-*N*,*N*-bis(4-nitrophenyl)aniline and 2,6-dichloro-*N*,*N*-bis(4-nitrophenyl)aniline. *Acta Cryst.* **E70**, 65–67 (2014).

24. Khan, F. A., Dash, J., Sudheer, C. & Gupta, R. K. Chemoselective reduction of aromatic nitro and azo compounds in ionic liquids using zinc and ammonium salts. *Tetrahedron Lett.* **44**, 7783–7787 (2003).

25. Rai, G. *et al.* Ionic liquid mediated efficient reduction of nitroarenes using stannous chloride under sonication. *Tetrahedron Lett.* **46**, 3987–3990 (2005).

26. Leroux, F. & Schlosser, M. The 'Aryne' Route to Biaryls Featuring Uncommon Substituent Patterns. *Angew. Chemie Int. Ed.* **41**, 4272–4274 (2002).

27. Huang, S.-T. *et al.* Synthesis and electroluminescent properties of polyfluorene-based conjugated polymers containing bipolar groups. *J. Polym. Sci. Part A Polym. Chem.* **47**, 6231–6245 (2009).

28. Wu, X., Dube, M. A. & Fry, A. J. Electrophilic nitration of triphenylamines as a route to high oxidation potential electrocatalysts. Polynitration, nitrodebromination, and bromine dance. *Tetrahedron Lett.* **47**, 7667–7669 (2006).

29. Ge, Z. *et al.* Novel Bipolar Bathophenanthroline Containing Hosts for Highly Efficient Phosphorescent OLEDs. *Org. Lett.* **10**, 421–424 (2008).

30. Tanaka, H., Shizu, K., Miyazaki, H. & Adachi, C. Efficient green thermally activated delayed fluorescence (TADF) from a phenoxazine–triphenyltriazine (PXZ–TRZ) derivative. *Chem. Commun.* **48**, 11392–11394 (2012).

31. An, Z.-F. *et al.* Conjugated Asymmetric Donor-Substituted 1,3,5-Triazines: New Host Materials for Blue Phosphorescent Organic Light-Emitting Diodes. *Chem. Eur. J.* **17**, 10871–10878 (2011).

32. Kamimura, A., Komatsu, H., Moriyama, T. & Nozaki, Y. Sub-stoichiometric oxidation of benzylic alcohols with commercially available activated MnO_2 under oxygen atmosphere: a green modification of the benzylic oxidation. *Tetrahedron* **69**, 5968–5972 (2013).

33. Henry, J. B., Wharton, S. I., Wood, E. R., McNab, H. & Mount, A. R. Specific Indolo[3,2,1-*jk*]carbazole Conducting Thin-Film Materials Production by Selective Substitution. *J. Phys. Chem. A* **115**, 5435–5442 (2011).

34. Natera, J. *et al.* A Novel Electrochromic Polymer Synthesized through Electropolymerization of a New Donor−Acceptor Bipolar System. *Macromolecules* **40**, 4456–4463 (2007).

35. Niebel, C. *et al.* Dibenzo[2,3:5,6]pyrrolizino[1,7-*bc*]indolo[1,2,3-*lm*]carbazole: a new electron donor. *New J. Chem.* **34**, 1243–1246 (2010).

36. Kautny, P., Schwartz, T., Stöger, B. & Fröhlich, J. An unusual case of OD-allotwinning: 9,9’(2,5- dibromo-1,4-phenylene)bis[9*H*-carbazole]. *Acta Cryst.* **B73**, 65–73 (2017).

37. Iwaki, T., Yasuhara, A. & Sakamoto, T. Novel synthetic strategy of carbolines *via* palladium-catalyzed amination and arylation reaction. *J. Chem. Soc. Perkin Trans. 1* 1505–1510 (1999).

38. Coulson, D. R., Satek, L. C. & Grim, S. O. in *Inorganic Syntheses* **13**, 121–124 (1972).

F Appendix

F.1 Single crystal structures

9-(2-Bromophenyl)-9*H*-carbazole (3)

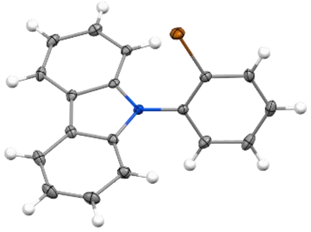

Figure F.1: Molecular structure of **3**. Br, C and N atoms are represented by brown, grey and blue ellipsoids drawn at 50% probability levels. Hydrogens are depicted as fixed size white spheres (radius: 0.2 Å).

9-(2,4-Dibromophenyl)-9*H*-carbazole (VIII)

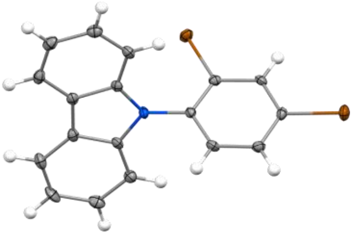

Figure F.2: Molecular structure of **VIII**. Br, C and N atoms are represented by brown, grey and blue ellipsoids drawn at 70% probability levels. Hydrogens are depicted as fixed size white spheres (radius: 0.2 Å).

5-(9*H*-Carbazol-9-yl)indolo[3,2,1-*jk*]carbazole (XII)

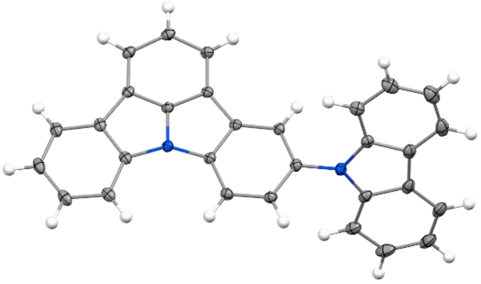

Figure F.3: Molecular structure of **XII**. C and N atoms are represented by grey and blue ellipsoids drawn at 20% probability levels. Hydrogens are depicted as fixed size white spheres (radius: 0.2 Å).

6-Phenyl-1,3,5-triazine-2,4(1*H*,3*H*)-dione· pyridine

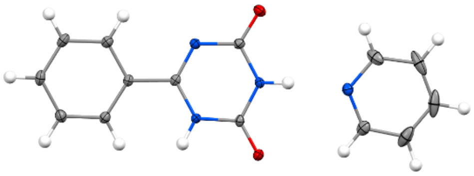

Figure F.4: Molecular structure of the hydrolyzed triazine. C, N and O atoms are represented by grey, blue and red ellipsoids drawn at 40% probability levels. Hydrogens are depicted as fixed size white spheres (radius: 0.2 Å).

Ethyl indolo[3,2,1-*jk*]carbazole-2-carboxylate (XLII)

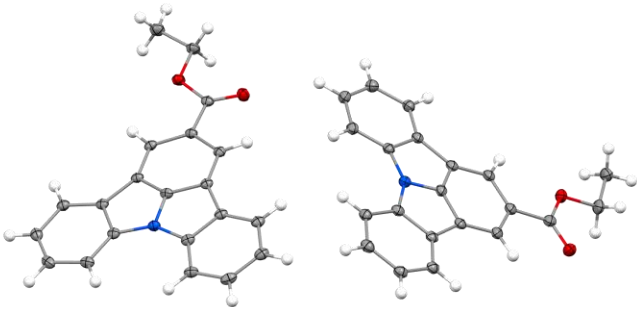

Figure F.5: Molecular structure of **XLII**. C, N and O atoms are represented by grey, blue and red ellipsoids drawn at 30% probability levels. Hydrogens are depicted as fixed size white spheres (radius: 0.2 Å).

3-Bromo-4-(9*H*-carbazol-9-yl)benzonitrile (XLVIII)

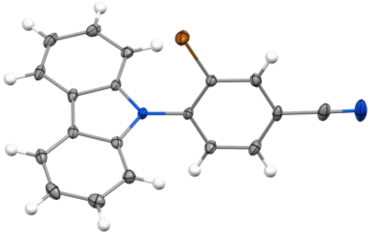

Figure F.6: Molecular structure of **XLVIII**. Br, C and N atoms are represented by brown, grey and blue ellipsoids drawn at 50% probability levels. Hydrogens are depicted as fixed size white spheres (radius: 0.2 Å).

Indolo[3,2,1-*jk*]carbazole-5-carbonitrile (49)

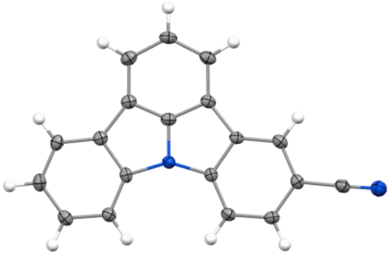

Figure F.7: Molecular structure of **49**. C and N atoms are represented by grey and blue ellipsoids drawn at 50% probability levels. Hydrogens are depicted as fixed size white spheres (radius: 0.2 Å).

9,9’-(2,5-Dibromo-1,4-phenylene)bis[9*H*-carbazole] (LIII)

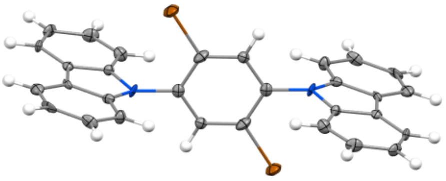

Figure F.8: Molecular structure of **LIII**. Br, C and N atoms are represented by brown, grey and blue ellipsoids drawn at 50% probability levels. Hydrogens are depicted as fixed size white spheres (radius: 0.2 Å).

Benzo[1”,2”:4,5;5”,4”:4’,5’]dipyrrolo[3,2,1-*jk*:3’,2’,1’-*j’k’*]dicarbazole (LIV)

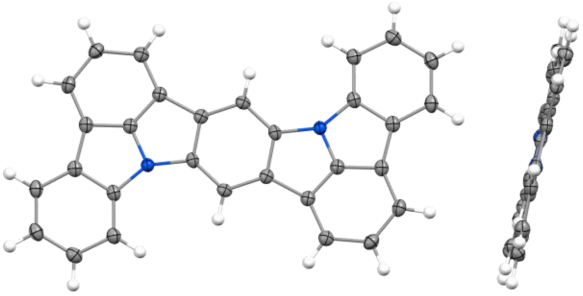

Figure F.9: Molecular structure of **LIV**. C and N atoms are represented by grey and blue ellipsoids drawn at 50% probability levels. Hydrogens are depicted as fixed size white spheres (radius: 0.2 Å).

F.2 Cyclic voltammograms

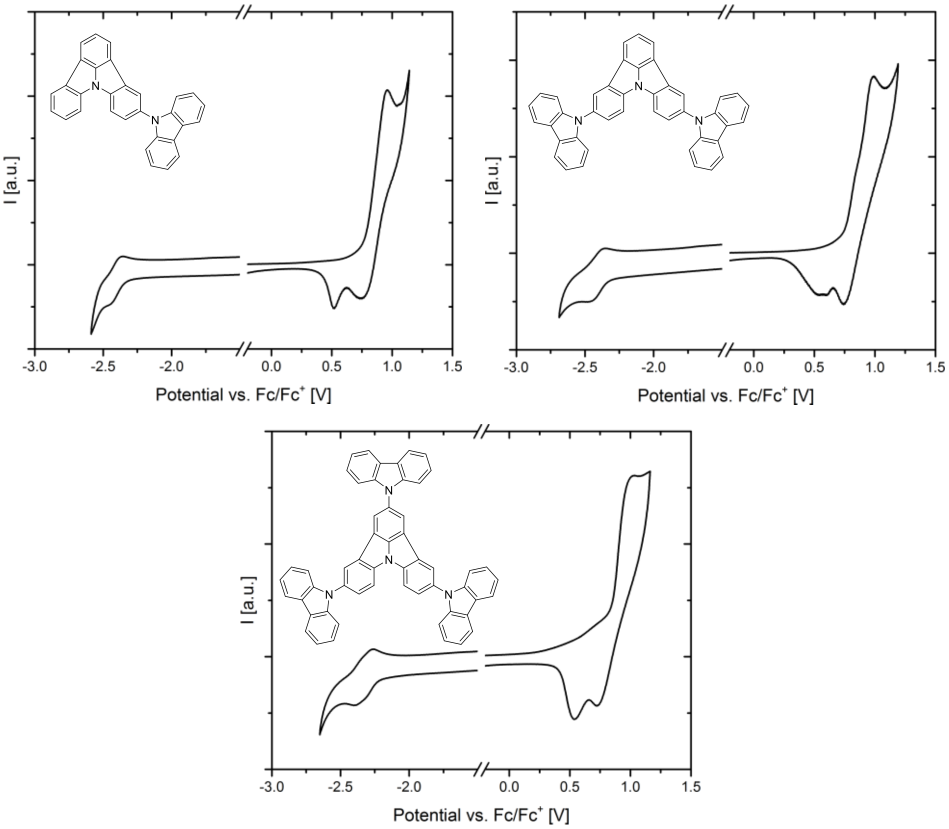

Figure F.10: Cyclic voltammograms of **5CzICz** (top left), **Cz$_2$ICz** (top right) and **Cz$_3$ICz** (bottom). Oxidation and reduction scans were recorded in DCM and ACN, respectively.

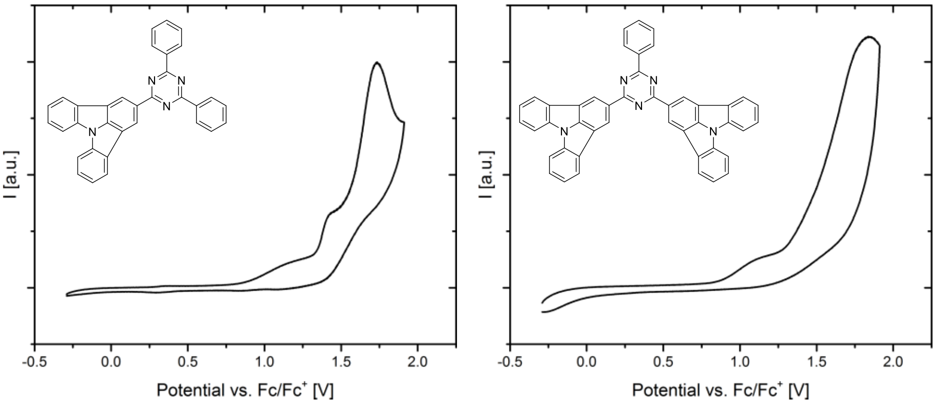

Figure F.11: Cyclic voltammograms of **ICzTz** (left) and **ICz$_2$Tz** (right) recorded in DCM.

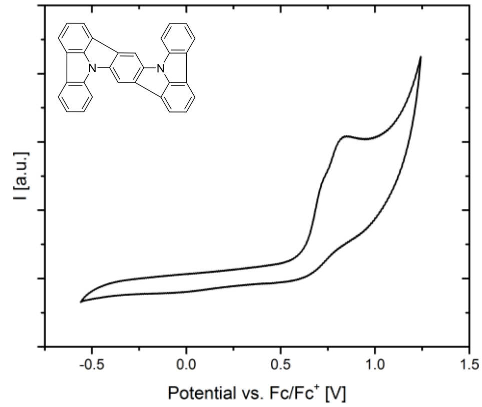

Figure F.12: Cyclic voltammogram of **BDPDCz** recorded in DCM.

F.3 Electroluminescent data

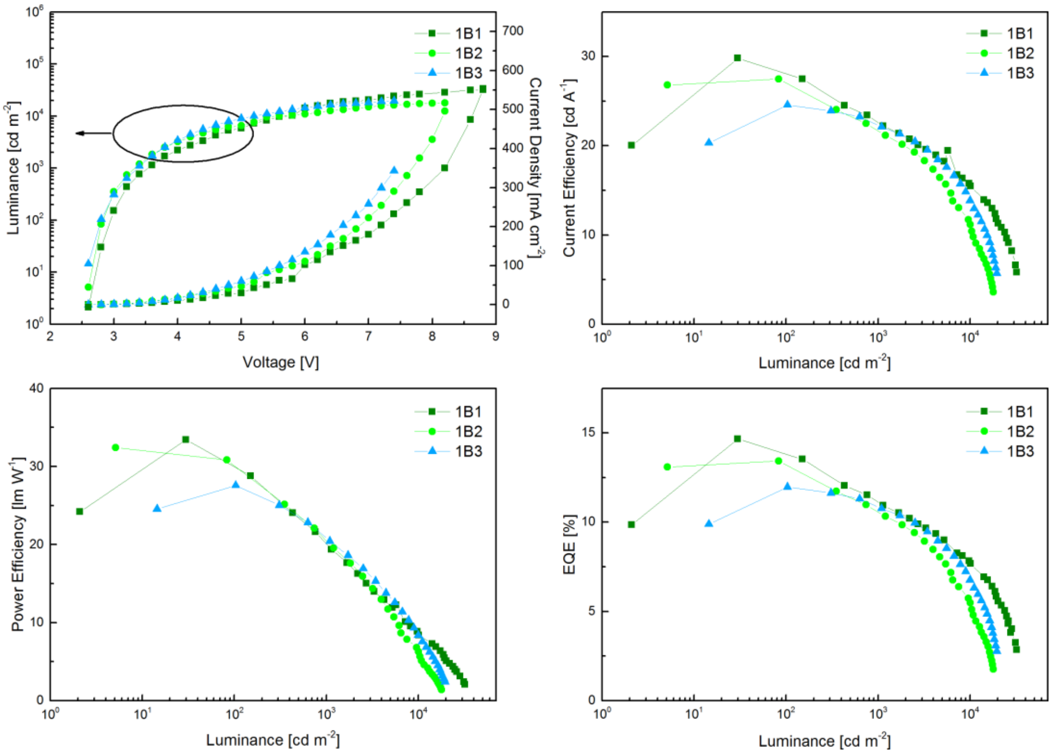

Figure F.13: Device characteristics of devices **1B1**, **1B2** and **1B3**.

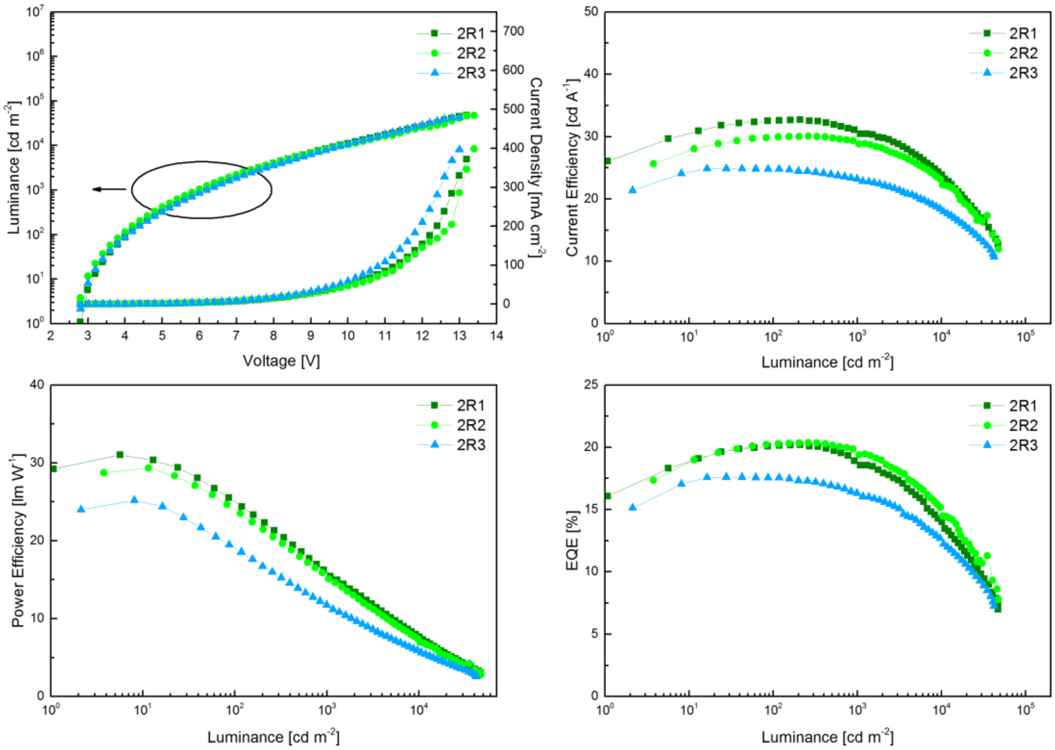

Figure F.14: Device characteristics of devices **2R1**, **2R2** and **2R3**.

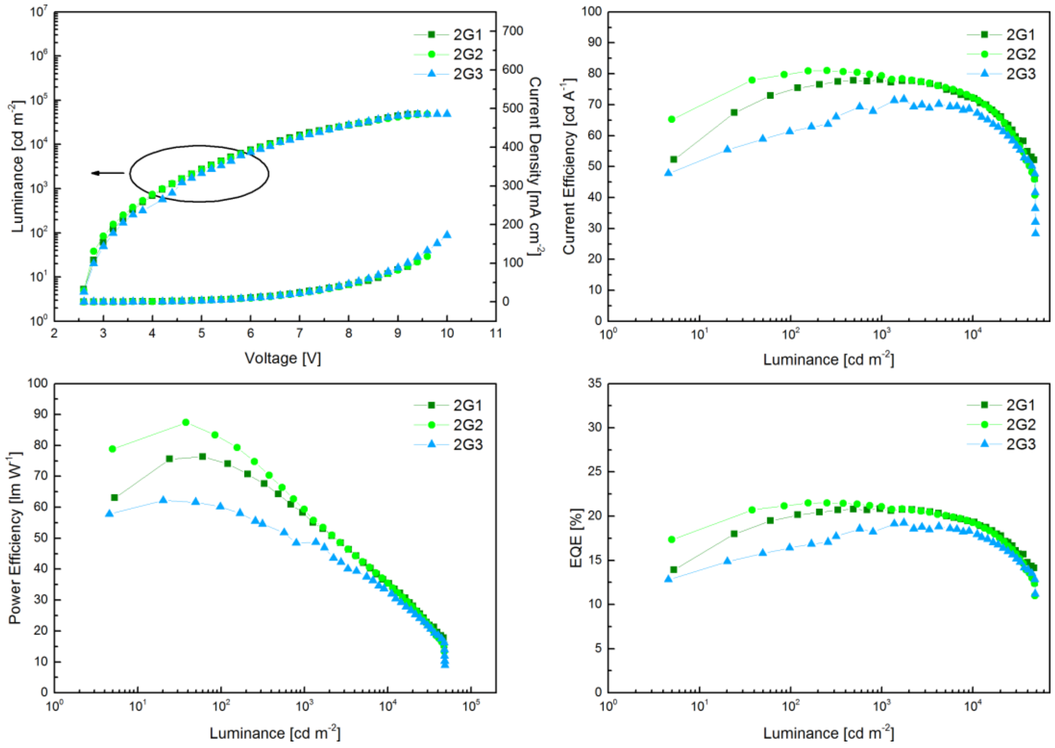

Figure F.15: Device characteristics of devices **2G1**, **2G2** and **2G3**.

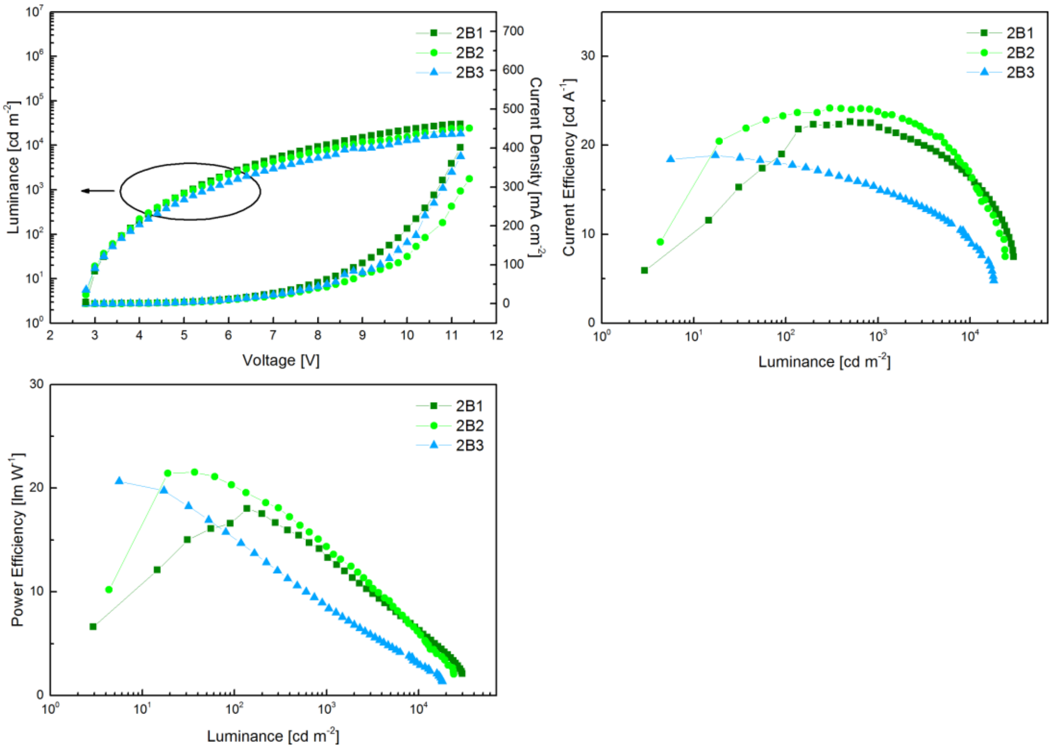

Figure F.16: Device characteristics of devices **2B1**, **2B2** and **2B3**.